ASSESSING THE CYTOPROTECTIVE PROPERTIES AND CENTRAL NERVOUS SYSTEM EXPRESSION PROFILE OF MAMMALIAN SIRTUIN SIRT3

by

Elena Sidorova

A thesis submitted in conformity with the requirements
for the degree of Master of Science

Graduate Department of Physiology
University of Toronto

Your file Votre référence
ISBN: 978-0-494-76649-1

Our file Notre référence
ISBN: 978-0-494-76649-1

ASSESSING THE CYTOPROTECTIVE PROPERTIES AND CENTRAL NERVOUS SYSTEM EXPRESSION PROFILE OF MAMMALIAN SIRTUIN SIRT3

Elena Sidorova
Master of Science

Graduate Department of Physiology
University of Toronto
2011

Abstract

Sirtuins are a family of nicotinamide adenine dinucleotide - dependent enzymes, which have gained recent interest due to their ability to directly or indirectly regulate cell metabolism, oxidative response mechanisms and cellular senescence. A mitochondrial sirtuin SIRT3, although still relatively under-investigated, regulates mitochondrial processes through deacetylation of metabolic enzymes and components of electron transport chain. We hypothesized that SIRT3 is a mitochondrial cytoprotective factor that exerts its function by decreasing reactive oxygen species levels, and protecting cells from oxidative stress. HEK-293 cells over-expressing SIRT3 exhibit reduced mitochondrial membrane potential and reactive oxygen species levels under basal conditions. In addition, cells over-expressing SIRT3 are less sensitive to hydrogen peroxide and glucose deprivation/glucose reperfusion induced-cell death. Since SIRT3 expression in the brain has not yet been investigated, its expression pattern in the rodent brain was characterized. Our results showed that SIRT3 mRNA and protein levels are robustly expressed in different regions of the adult rodent brain and their expression increases with age. Furthermore, SIRT3 is expressed predominantly in astrocytes in cultures derived from rat primary E18 cortical cells. These results suggest that SIRT3 possesses cytoprotective potential, and that its actions in the brain regulate astrocyte physiology.

ACKNOWLEDGEMENTS

First and foremost, I would like to thank my supervisor, Dr. James Eubanks, your dedication to science, your laboratory, your family and your easy going nature, truly is inspiring. Thank you for the countless hours of revisions, guidance and advice with my Thesis. You have been very helpful every step of the way.

Thank you to my committee members: Dr. Linda Mills, Dr. Philippe Monnier and Dr. Joanne Nash. I am very grateful for you taking the time to give me advice throughout my journey as a Graduate Student. In addition, I would like to thank my examination committee: Dr. Les Buck, Dr. Peter Carlen, and Dr. Linda Mills. I appreciate the time you took to read my thesis and be present at my defense.

The process of Graduate school would not be complete if it wasn't for the few people who make you smile when an experiment does not proceed as expected after living in the lab day in and day out. Thank you Joe Hayek, you have been the biggest rock to lean on at Toronto Western Hospital.

In addition I would like to thank my amazing family, I am blessed to be surrounded by such amazing people who support me every step of the way. To my friends – thank you for your patience, encouragement and laughter.

Lastly, I would like to thank my lovely fiancée and best friend, Peter Darmos. I cannot put in words how much you have helped me throughout this process. You took interest in every little detail of my Thesis project, from my experiments to the minute details of this document.

TABLE OF CONTENTS

LIST OF TABLES

LIST OF FIGURES

LIST OF ABBREVIATIONS

2DG	2-deoxy-D-glucose
3′UTR	3′ untranslated region
3HB	3-beta-hydroxybutyrate
AcAc	Acetoacetate
AceCS1	Acetyl coenzyme A synthetase type 1
AceCS2	Acetyl coenzyme A synthetase type 2
AIF	Apoptosis inducing factor
AMPK	AMP-activated protein kinase
ANOVA	Analysis of variance
ATP	Adenosine triphosphate
BSA	Bovine serum albumin
CCCP	Carbonyl cyanide m-chloro phenyl hydrazone
CNS	Central nervous system
CPS1	Carbamoyl phosphate synthetase 1
CR	Caloric restriction
CREB	cAMP-response element binding protein
CT	Threshold cycle
CypD	Cyclophilin D
DCF	5-(and-6)chloromethyl-2',7'dichlorohydrofluoresceindiacetate
DMEM	Dulbecco modified eagle medium
DNA	Deoxyribonucleic acid
ERC	Extrachromosomal rDNA circle
ETC	Electron transport chain
$FADH_2$	Reduced form of flavin adenine dinucleotide
FBS	Fetal bovine serum
FITC	Fluorescein isothiocyanate
FOXO	Forkhead transcription factor-O
GAPDH	Glyceraldehyde-3-phosphate dehydrogenase

GD	Glucose deprivation
GDH	Glutamate dehydrogenase
GFP	Green fluorescent protein
GFAP	Glial fibrillary acidic protein
GR	Glucose reperfusion
GSH	Reduced glutathione
GSSG	Glutathione disulfide
H^+	Proton
H_2O	Water
H_2O_2	Hydrogen peroxide
HDAC	Histone deacetylase
HEK-293	Human embryonic kidney-293 cells
HIF1α	Hypoxia-inducible factor-1α
HMGCS2	3-hydroxy-3-methylglutaryl-CoA synthase
HPRT	Hypoxanthine-guanine phosphoribosyltransferase
hSIRT3	Human SIRT3
IDH2	Isocitrate dehydrogenase 2
IMM	Inner mitochondrial membrane
IMS	Intermembrane space
kDa	Kilo-Dalton
LCAD	Long-chain acyl coenzyme A dehydrogenase
MAP2	Microtubule associated protein 2
MEF	Mouse embryonic fibroblasts
MLS	Mitochondrial localization sequence
miRNA	Micro RNA
mRNA	Messenger RNA
MPP	Mitochondrial processing peptidase
MnSOD	Mitochondrial superoxide dismutase
mSIRT3	Mouse SIRT3
Mt-GFP	Mitochondrial targeted GFP
mPTP	Mitochondrial permeability transition pore

NAD^+	Nicotinamide adenine dinucleotide
NADH	Reduced form of nicotinamide adenine dinucleotide
NADPH	Nicotinamide adenine dinucleotide phosphate
NDUFA9	NADH dehydrogenase (ubiquinone) 1 α subcomplex 9
NMDA	N-methyl-D-aspartate
NRF1	Nuclear respiratory factor 1
O_2	Molecular oxygen
$\cdot O_2^-$	Superoxide radical
OAADPr	2'3'-O-acetyl-ADP-ribose
OH^-	Hydroxyl radical
OMM	Outer mitochondrial membrane
P	Probability value
P53	Protein 53
PBS	Phosphate buffered saline
PGC-1α	Peroxisome proliferator-activated receptor γ coactivator 1-α
PI	Propidium iodide
PLO	Poly-L-ornithine
PMT	Photomultiplier tube
qRT-PCR	Quantitative real time polymerase chain reaction
rDNA	Ribosomal DNA
RNA	Ribonucleic acid
ROS	Reactive oxygen species
RFU	Relative fluorescence units
RT	Room temperature
SDS-PAGE	Sodium dodecyl sulphate polyacrylamide gel electrophoresis
SEM	Standard error of means
SIR	Silent information regulator
SDHA	Succinate dehydrogenase flavoprotein
TCA cycle	Tricarboxylic acid cycle
TIM	Translocase inner membrane
TOM	Translocase outer membrane

TS	Tumour supressor gene
UCP	Uncoupling protein
VNTR	Variable number of tandem repeats
$\Delta\Psi_m$	Mitochondrial membrane potential

INTRODUCTION

1.1 Background on SIR2

Studies in yeast (*Saccaromyces cerevisiae*) have led to the identification of a class of regulators collectively referred to as the family of SIR (silent information regulator) genes. SIR1-4 genes have been implicated in transcriptional silencing on different locations of the genome (Ivy et al., 1986). Silencing refers to a compact chromatin structure known as heterochromatin, which is attained by removal of the acetyl group from the lysine residues on histone tails. This process is known as deacetylation. Therefore, transcriptional machinery would not have access to the DNA due to the compact chromatin structure. On the other hand, acetylated chromatin is active, and is referred to as euchromatin; thus, it is able to be transcribed (Delcuve et al., 2009). There are sequences on the DNA which are involved in the silencing mechanism through recruitment of the SIR complex (Fox & McConnell, 2004). This complex has the ability to bind to the chromatin, specifically to histones H3 and H4. Once the complex has bound, it further blocks other proteins from binding and therefore induces transcriptional regulation through silencing.

However, silencing of the transcriptional activity does not necessary involve the entire SIR complex. SIR2 regulates yeast ribosomal DNA (rDNA) through silencing, a mechanism that has been suggested to slow the aging process (Gottlieb & Esposito, 1989). During yeast replication rDNA circles are generated through homologous recombination. These are known as extrachromosomal rDNA circles (ERCs), which accumulate in the cell with each cell division. Once the ERCs reach a certain number in the mother cell, cell senescence occurs and the cells can no longer replicate. Therefore, SIR2-induced heterochromatin state in the rDNA may slow down the progressive accumulation of the ERCs, and further extend lifespan (Kaeberlein et al., 1999). Furthermore, Braunsten et al. (1993) observed that an over-expression of the SIR2 gene alone induced global hypoacetylation in yeast histones. SIR2-mediated deacetylation of histones

was shown to be necessary to create a docking site for the entire SIR complex to bind to the nucleosome structures (Braunsten et al., 1996). Therefore, the deacetylase activity of SIR2, allows the remaining SIR proteins to have access to these histone residues. Taken together, these studies suggest that SIR2 regulates transcriptional silencing as well as the aging process.

1.2 Mammalian sirtuins

Unlike its family members, SIR2 expression is found to be present in all eukaryotes (Brachmann et al., 1995). Seven mammalian SIR2 homologues have been identified, named sirtuins. Mammalian sirtuins are classified as SIRT1-7 (Finkel et al., 2009). SIRT1 holds the closest evolutionary homology to yeast SIR2 (Frye, 2000), and it is also the most extensively studied sirtuin. All seven sirtuin homologues hold a conserved NAD^+- dependent catalytic domain of approximately 260 amino acids with variable amino- and carboxyl-terminals (Marmostein, 2004; Min et al., 2001). Thus, the enzymatic activity of sirtuins is dependent on the presence of NAD^+ as a cofactor (Guarente et al., 2000). Sirtuins are a class of enzymes, which are NAD^+-dependent deacetylases and/or ADP-ribosylases (see Figure 1) (Borra et al., 2004; Du et al., 2009; Haigis & Sinclair, 2010). Changing the acetylation/deacetylation state of a protein is a significant post-translational modification. Removing an acetyl group from a substrate can modify a protein's activity level, and therefore regulate fundamental pathways involved in metabolism, cell survival, and overall functioning of the cell (Glozak et al., 2005). ADP-ribosylation plays a role in signaling pathways within the cell as well as DNA repair mechanisms (Hassa et al., 2006). However, little is known about the physiological relevance of sirtuin-mediated ADP-ribosylation (discussed by Du et al., 2009).

During deacetylation, sirtuins hydrolyse NAD^+ by cleaving the glycosidic bond, which forms a nicotinamide and an ADP-ribose intermediate (Haigis & Guarente, 2006). This NAD^+ hydrolysis

is then followed by the removal of the acetyl group from a lysine residue of an acetylated protein. The acetyl group is then transferred to the 2′-OH position of ADP-ribose intermediate, which forms 2′-O-acetyl-ADP-ribose. The final products of the deacetylation reaction are a deacetylated protein, nicotamide and 2'-O-acetyl-ADP-ribose. During ADP-ribosylation, sirtuins also hydrolyze NAD^+ to produce ADP-ribose molecule and nicotamide. However, the ADP-ribose moiety is then transferred directly to the protein substrate. Thus, the two final products of the ADP-ribosylation reaction are an ADP-ribose-substrate and nicotamide. Details of which of the seven sirtuins are classified as deacetylases and/or ADP-ribosylases will be discussed in later sections.

Mammalian sirtuins reside in distinct subcellular compartments within the cell (Haigis & Guarente, 2006; Yu & Auwerks, 2009), and can be broken down into 3 broad classes of nuclear, cytoplasmic and mitochondrial enzymes. Nevertheless, there are controversies regarding the localization of some of the sirtuins, which will be discussed below. Sirtuins target a variety of substrates from their respective subcellular localizations, which are involved in diverse cellular processes (Shoba et al., 2009; North & Verdin, 2004) (see Table 1).

Fig. 1

A)

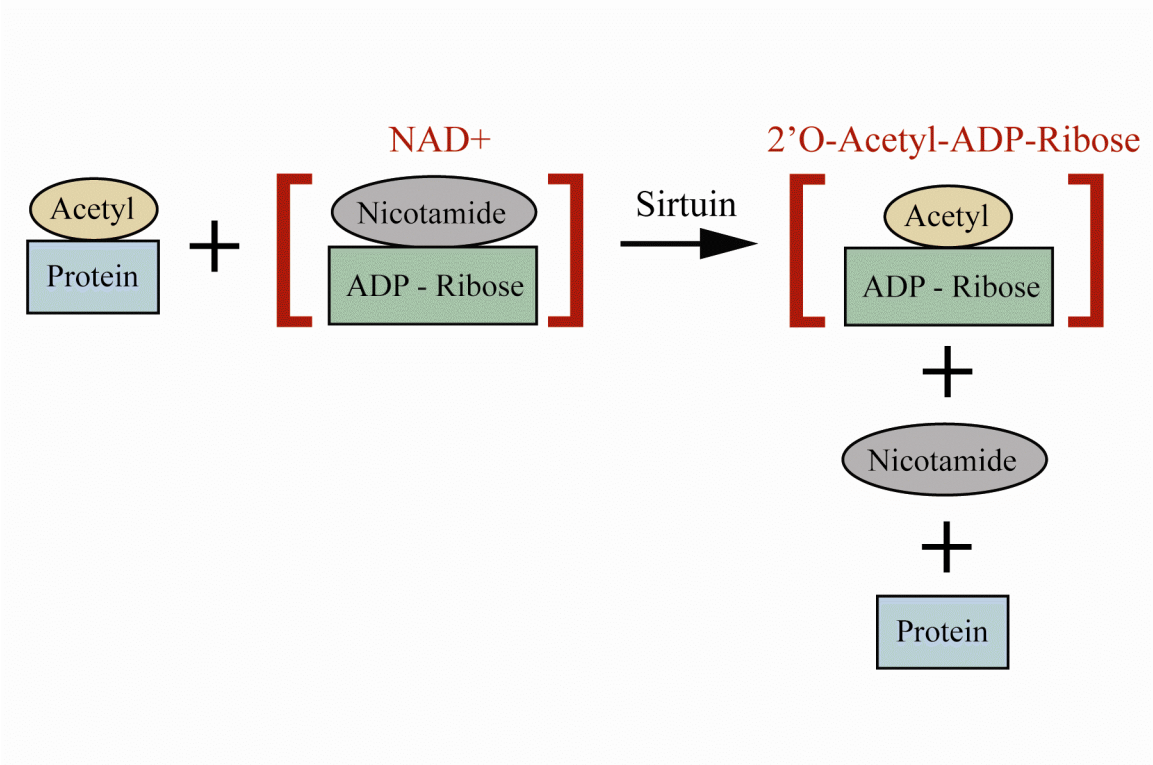
NAD+
2'O-Acetyl-ADP-Ribose
Acetyl
Protein
Nicotamide
ADP - Ribose
Sirtuin
Acetyl
ADP - Ribose
Nicotamide
Protein

B)

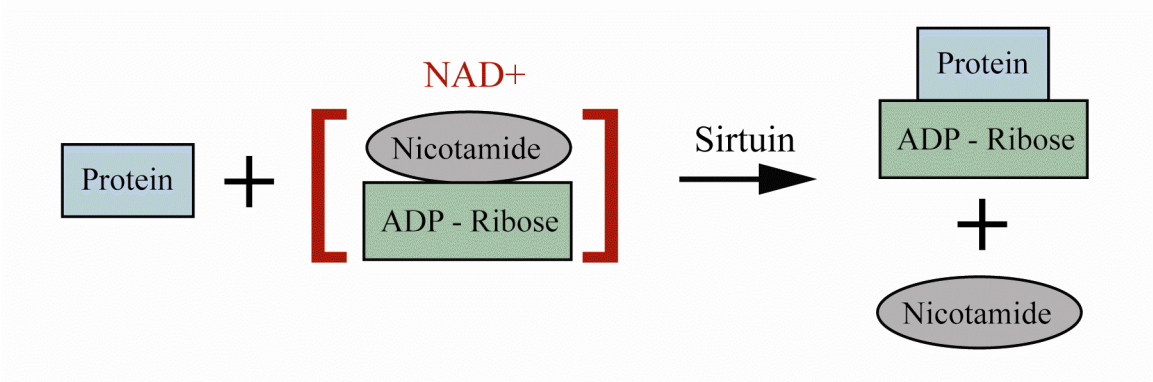
NAD+
Protein
Nicotamide
ADP - Ribose
Sirtuin
Protein
ADP - Ribose
Nicotamide

Figure 1: Sirtuin deacetylation and ADP-ribosylation mechanisms

A) Sirtuin-mediated deacetylation. The components necessary for the deacetylation reaction are an acetylated substrate and NAD^+. Sirtuins hydrolyze one molecule of NAD^+, and remove an acetyl group from a lysine residue of the target substrate. NAD^+ is cleaved to nicotamide and ADP-ribose. The acetyl group is then transferred to the ADP-ribose, which forms 2′-O-acetyl-ADP-ribose. The final products of the reaction are a deacetylated substrate, nicotamide and 2'-O-acetyl-ADP-ribose.

B) Sirtuin-mediated ADP-ribosylation. Sirtuins hydrolyze NAD^+ to produce an ADP-ribose molecule and nicotamide. The ADP-ribose moiety is then transferred directly to the substrate. The final products of the reaction are an ADP-ribose-substrate molecule and nicotamide.

Table 1: Enzymatic function, predominant subcellular localization and target proteins of mammalian sirtuins

Sirtuin	Enzymatic Function	Predominant Subcellular Localization	Targets Of Enzymatic Activity	References
SIRT1	NAD^+ dependent deacetylation	Nucleus, Cytoplasm	p53, AceCS1, FOXO, PGC1α, UCP2	Bordone et al., 2006; Brunet et al., 2004; Hallows et al., 2006; Nemoto et al., 2005
SIRT2	NAD^+ dependent deacetylation	Cytoplasm	Histone 4, FOXO, α - tubulin	North et al., 2003; Vaquero et al., 2006; Wang et al., 2007
SIRT3	NAD^+ dependent deacetylation	Mitochondrial Matrix	ATPase, AceCS2, LCAD, GDH, Complex I NDUFA9, mPTP	Ahn et al., 2008; Li et al., 2010; Schlicker et al., 2008; Schwer et al., 2006; Shi et al., 2006
SIRT4	ADP-ribosylation	Mitochondrial Matrix	GDH	Haigis et al., 2006
SIRT5	NAD^+ dependent deacetylation	Mitochondrial Intermembrane Space	Cytochrome c, CPS1	Nakawa et al., 2008; Schlicker et al., 2008
SIRT6	NAD^+ dependent deacetylation, ADP ribosylation	Nucleus	Histone 3 (telomeres)	Michishita et al., 2008
SIRT7	NAD^+ dependent deacetylation	Nucleus	RNA pol I p53	Forde et al., 2008; Vakhrusheva et al., 2008

1.2.1 Nuclear sirtuins

Converging evidence suggests that three sirtuins are predominately nuclear (SIRT1, -6, -7), and hold subcellular locations in nucleoplasm, heterochromatin and nucleoli, respectively (Haigis & Guarente, 2006; Haigis & Sinclair, 2010). Nuclear sirtuins execute their functions through regulating oxidative stress, senescence and metabolic processes of the nucleus (Hiroyasu et al., 2007; Shoba et al., 2009).

1.2.1.1 SIRT1

SIRT1 is a NAD^+ dependent deacetylase, which was originally recognized as a nuclear enzyme in HeLa cells (Mischishita et al, 2005); however, studies have indicated that it also resides throughout the cytoplasm (Jin et al., 2007; Mischishita et al., 2005). Although it is not fully understood under what conditions SIRT1 is shuttled between the subcellular compartments, it has been demonstrated that this sirtuin contains two nuclear localization and two nuclear export sequences (Tanno et al., 2007). SIRT1 is able to deacetylate histone and non-histone proteins in the nucleus, as well as other regulatory proteins in the cytoplasm (North & Verdin, 2004). SIRT1 regulates cell growth, senescence and stress-induced apoptosis (Schwer & Verdin, 2007).

1.2.1.2 SIRT6

Sirtuin 6 is a NAD^+ dependent deacetylase, which resides in the nucleus (Michishita et al., 2008). Recent studies showed SIRT6 to have strong auto-ADP-ribosylation activity in mouse tissue; however, the implication of this modification is unknown (Liszt et al., 2005). SIRT6 negatively regulates cell replicative senescence by associating with and stabilizing telomeric chromatin (Michishita et al., 2008). A telomere is a region of repetitive sequences of DNA located at the end of chromosomes (Wai, 2004). Telomeres get shortened with each DNA

replication cycle. The presence of telomeres protects the ends of the chromosome from degradation; thus their dysfunction is associated with early senescence. Accordingly, it has been demonstrated that SIRT6-deficient mice show evidence of telomeric dysfunction and early senescence (Kawahara et al., 2008). Taken together, these studies implicate SIRT6 in an active role in regulating the aging process.

1.2.1.3 SIRT7

SIRT7 resides in the nucleus (Michishita et al., 2005). Vakhrusheva et al (2008) suggested that SIRT7 holds robust NAD^+ dependent deacetylase activity, as SIRT7 knockout mice display higher levels of acetylated protein 53 (p53). P53 is a tumour suppressor protein, which plays an important role in DNA repair, growth arrest, and the initiation of apoptosis. This study showed that abolishing SIRT7 levels in cardiomyocytes also increases apoptosis. Taken together, SIRT7 plays a role in negatively regulating cell apoptosis, by deacetylating and therefore inactivating p53. Additionally, SIRT7 activates RNA polymerase I transcription activity by deacetylation (Ford et al., 2006). Overall, these studies suggest that SIRT7 is an anti-apoptotic factor and a regulator of RNA transcription machinery.

1.2.2 Cytoplasmic sirtuin

1.2.2.1 SIRT2

SIRT2 is a NAD^+ dependent deacetylase, which is predominately localized in the cytoplasm. In the cytoplasm, it deacetylates α-tubulin, and therefore plays a role in cell motility and cell division (North et al., 2003). SIRT2 has also been implicated in oxidative stress. Wang et al (2007) demonstrated that over-expression of SIRT2 in HEK-293 cells decreased reactive oxygen species (ROS) levels. This decrease was attributed to the deacetylation of FOXO3a, a member of the forkhead box O (FOXO) family of transcription factors. FOXOs regulate cell stress

resistance by activating antioxidant genes. Therefore, SIRT2 is linked to oxidative stress resistance and to regulation of cell division.

1.2.3 Mitochondrial sirtuins

Three mammalian sirtuins (SIRT3-5) are targeted to the matrix of the mitochondria. SIRT5 is also localized to the inner mitochondrial membrane (IMM). These mitochondrial sirtuins have been implicated in the regulation of metabolic processes. In addition, SIRT3 and SIRT5 are also involved in stress-resistance pathways (Huang et al., 2009; Shoba et al., 2009).

1.2.3.1 SIRT3

SIRT3 is initially synthesized as an enzymatically inert precursor protein. This sirtuin contains a mitochondrial localization sequence (MLS) on its amino-terminus, targeting it to the mitochondrial matrix (Onyango et al., 2002). Upon entering the mitochondrial matrix, the targeting sequence on the amino-terminus is cleaved by a mitochondrial processing peptidase (MPP). Once SIRT3 is cleaved, it becomes an enzymatically active NAD^+ dependent deacetylase (Schwer et al., 2002). However, several studies have argued that SIRT3 may reside and regulate substrates in the cytosol and nucleus (Nakamura et al., 2007; Scher et al., 2007). Despite the current controversies regarding its subcellular localization, SIRT3 is a regulator of global mitochondrial acetylation levels in rodents (Lombard et al., 2007). SIRT3 deacetylates and physically associates with complex I of the electron transport chain in mitochondria, specifically NADH dehydrogenase (ubiquinone) 1 α subcomplex 9 (NDUFA9) (Ahn et al., 2008). SIRT3 targets a number of substrates, which are linked to pathways involved in metabolism and anti-oxidative mechanisms (Huang et al., 2010; Schwer & Verdin 2008; Shoba et al., 2009). Although the subcellular localization of SIRT3 is still under ongoing debate, SIRT3 regulates a

plethora of mitochondrial processes - the details of which will be discussed in later sections of this thesis.

1.2.3.2 SIRT4

SIRT4 is also targeted to the mitochondrial matrix, where it is proteolytically processed at its amino-terminus (Ahuja et al., 2007). SIRT4 negatively regulates insulin secretion by ADP-ribosylating, and thus inactivating glutamate dehydrogenase (GDH) in pancreatic β-cells (Haigis et al., 2006). GDH is an enzyme within the mitochondrion which converts glutamate to α-ketoglutarate to fuel the TCA cycle, and ultimately adenosine triphosphate (ATP). By inactivating GDH, SIRT4 regulates blood glucose levels through controlling insulin secretion. This is because GDH increases the ATP/ADP ratio, which induces secretion of insulin (Haigis, 2006). Thereby inactivation of GDH reduces blood glucose levels, but at the expense of ATP. On the other hand, SIRT3 activates GDH activity through direct deacetylation (Lombard et al., 2007). This suggests that although both SIRT3 and SIRT4 reside in the same compartment, they induce opposing results.

1.2.3.3 SIRT5

SIRT5, similar to SIRT3 and SIRT4, is imported into the mitochondrial matrix, where it is cleaved at its amino-terminus by MPP (Nakawaga et al., 2009). However, confounding reports state that SIRT5 also localizes to the mitochondrial intermembrane space *in vitro* (Schlicker et al., 2008; Nakamura, 2008). SIRT5 induces its enzymatic function through NAD^+ dependent deacetylation. Although, SIRT5-deficient hepatic mice show no significant differences in global mitochondrial acetylation levels compared to that in SIRT3-deficient tissues (Lombard et al., 2007). SIRT5 has been speculated to play a role in apoptosis by deacetylating, and therefore activating an intermembrane localized factor, cytochrome c (Schlicker et al., 2008). Furthermore,

SIRT5 activates carbamoyl phosphate synthetase 1 (CPS1), a matrix enzyme which is important in energy metabolism by catalyzing the urea cycle (Nakawaga et al., 2009). Overall, these data suggest that SIRT5 regulates energy metabolism and apoptosis.

1.3 Sirtuins and mitochondria

Mitochondria are dynamic intracellular organelles that play a central role in metabolic processes, ROS genesis, as well as in regulating apoptosis in response to DNA damage or oxidative stress (Andreyev et al., 2005; Wei et al., 2009). Impaired mitochondrial processes play a critical role in disease pathogenesis and contribute to age-related metabolic defects (DiMaro & Schon, 2008). Converging experimental studies have implicated mitochondrial dysfunction in the pathogenesis of Alzheimer's, Parkinson's, stroke, cardiovascular and other neurodegenerative diseases (Chaturvedi & Beal, 2008). Thus, therapies targeting mitochondrial processes which regulate free radical generation or energy metabolism may reverse or prevent concomitant mitochondrial dysfunction in disease pathogenesis.

To date, several mitochondrial processes have been proposed as putative therapeutic targets. A proteomics survey conducted by Kim et al. (2006) reported that over 20% of mitochondrial proteins and enzymes of the liver are acetylated. The process of reversible acetylation, has increasingly become viewed as an important post-translational modification to number of mitochondrial proteins. Acetylation/deacetylation may affect the stability of a protein, its physical and/or chemical properties, as well as how it functions within mitochondria (Bao & Sack, 2010; Spange et al., 2009). Reversible mitochondrial acetylation is also implicated in mechanisms of metabolic processes, cell growth and overall cellular stress responses.

Importantly, the recognition that sirtuins can function as deacetylases has generated immense interest in their possible role in regulating mitochondrial function. Intriguingly, SIRT3-5 are localized exclusively in the mitochondrion. These mitochondrial enzymes have been demonstrated to influence a plethora of cellular processes that are involved in aging, stress resistance and metabolic regulation, while remaining within the organelle (Huang et al., 2009). By generating SIRT3-5 knockout mouse models, Lombard et al (2007) demonstrated that only mice deficient in SIRT3 display global hyperacetylation of mitochondrial proteins. However, there were no significant differences in the acetylation levels in mice lacking either SIRT4 or SIRT5. This study suggested that unlike the restricted roles of SIRT4 and SIRT5, SIRT3 is the primary regulator of global acetylation levels within mitochondria.

Although SIRT1 is not a mitochondrial resident, and therefore does not induce its deacetylation effects within the mitochondrion, it is an indirect regulator of mitochondrial functioning. SIRT1 is recognized to deacetylate peroxisome proliferator-activated receptor γ coactivator 1-α (PGC-1α)**,** a transcriptional co-activator that can activate genes involved in mitochondrial biogenesis as well as antioxidant defense processes (Haigis & Guarente, 2006). Less is known about SIRT2 and SIRT6, and whether the functions of these sirtuins have an effect on mitochondrial function remains elusive

In summary, current evidence suggests that the sirtuin family represents a possible target for 'mitochondrial medicine'; their precise roles, however, in influencing mitochondrial function remain to be clearly defined. Elucidating the cellular mechanisms by which sirtuins influence mitochondrial function is crucial if they are to be employed as therapeutic targets in human disease. From the seven mammalian sirtuins, SIRT1 is the most closely related to SIR2 (Frye, 2000), and to date the vast majority of studies have focused on this sirtuin. Although, SIRT1 has

shown much therapeutic potential, the remaining sirtuins have been relatively under-investigated. The regulatory role of global mitochondrial acetylation levels, implicates SIRT3 as a bona-fide target for mitochondrial medicine. Thus, for the remainder of this thesis, only SIRT3 will be discussed in further detail in the context of mitochondrial functions and cellular cytopreservation.

1.4 ROS, oxidative stress and apoptosis

ROS are metabolic products derived through a univalent reduction of molecular oxygen (O_2) to superoxide radical ($\cdot O_2^-$), which then has the capacity to be further metabolized into other ROS species (Auten & Davis, 2009; Kregel et al., 2006). This partial univalent reduction yields a formation of ROS species such as hydroxyl radical ($OH\cdot$) and hydrogen peroxide (H_2O_2). These species are formed by different mechanisms, and are innately produced as a by-products of cellular respiration in mitochondria (Halliwell et al., 2007), by NADPH oxidase (a membrane-bound enzyme in phagocytic cells), and by peroxisomes as well as lysosomes in the cytosol (Moldovan & Moldovan, 2004). Although many cellular organelles are involved in ROS production, mitochondria play a large role in continuous ROS genesis under basal conditions, and during oxidative stress (Kowaltovski et al., 2009).

Oxidative stress increases with aging, as well as during severe pathological processes of the body. It is defined as a disproportion between ROS formation and anti-oxidative defense mechanisms (Andreeyev et al., 2005). ROS can react with cellular macromolecules through oxidation reactions, which could lead to apoptotic processes. Apoptosis is a form of programmed cell death, which consists of controlled molecular cascades. A number of pathways are implicated in cell death, however mitochondrial ROS is a major player in all cell death cascades. Oxidative damage to mitochondria promotes outer mitochondrial membrane permeabilization.

Permeabilization of the mitochondrial membrane releases pro-apoptotic factors such as cytochrome c, AIF and Smac/Diablo towards the cytosol, which results in an initiation of specific caspase cascades (Kroemer et al., 2007). These cascades lead to cleavage of cellular proteins, DNA fragmentation and ultimately cell death. An important factor in mitochondrial membrane permeabilization is the mitochondrial permeability transition pore (mPTP), which is a large pore contained in the inner and outer mitochondrial membranes. Mitochondrial ROS can oxidize and open the mPTP, which leads to cellular death due to a decrease of ATP synthesis, release of pro-apoptotic factors and influx of Ca^{2+} (Crompton 1999). For a more complete review of cell death cascades the reader is directed to Cai et al. (1998), Crompton (1999), Elmore (2007), and Kroemer et al (2007).

1.5 Mitochondria and ROS

The mitochondrion is a double membrane organelle consisting of an outer mitochondrial membrane (OMM) and an inner mitochondrial membrane (IMM). The space between the two membranes referred to as the intermembrane space (IMS). The innermost compartment is known as the matrix and it contains enzymes that are responsible for the tricarboxylic acid cycle (TCA) reactions (reviewed in Turrens, 2003). Mitochondria produce the majority of cellular ATP through oxidative phosphorylation, which takes place in IMM where the electron transport chain (ETC) is located. The ETC is composed of five multisubunit complexes (I – V). These subunits are responsible for moving electrons from donors such as NADH and $FADH_2$. In the ETC, electrons are passed through the protein complexes via a series of oxidation-reduction reactions. The energy released by electron transport is utilized by complexes I, III, and IV to pump protons (H^+) out of the matrix into IMS, resulting in an electrochemical gradient across IMM known as inner mitochondrial membrane potential ($\Delta\Psi_m$) (Kowaltovski et al, 2009). The $\Delta\Psi_m$ provides

the driving force for phosphorylation of ADP to produce ATP by the ATP synthase (complex V). Thus, oxidative phosphorylation is the process of using derived energy from oxidation of substrates to produce ATP. In addition, molecular oxygen (O_2) is reduced at complex IV to produce water (H_2O), and therefore acts as a terminal electron acceptor.

However, throughout the ETC there is a premature leak of electrons, which leads to an incomplete reduction of O_2 generating $\cdot O_2^-$ as a by-product (Turrens, 2003; Andreyev et al., 2005). This electron leakage mainly occurs at complex I (NADH-dehydrogenase) and at complex III (cytochrome c reductase) (Andreyev et al., 2005). Complex I is an inner membrane multi-protein complex which oxidizes NADH to produce NAD^+ and transfers electrons for further reduction down the ETC. The exact mechanism for ROS formation at this site is not fully understood, however functional modifications of the enzyme plays a role in ROS genesis (Dawson & Dawson, 2003) and neurodegenerative diseases such as Parkinson's (Schapira, 1998). In addition, the enzymatic dysfunction in complex III has also been reported to play a role in $\cdot O_2^-$ formation.

1.5.1 Antioxidant defenses in mitochondria

Mitochondria contain multidimensional network of enzymatic and non-enzymatic defense systems. Major players of the antioxidant systems consist of manganese superoxide dismutase (MnSOD), catalase and glutathione (reviewed in Andreyev et al., 2005; Lin & Beal, 2006). MnSOD is solely localized to the matrix of the mitochondria, and its main function is to assist in dismutation of the harmful $\cdot O_2^-$ to H_2O_2 and O_2. Because its primary target is $\cdot O_2^-$, MnSOD is important for dismutation of ROS produced by complex I as well as complex III. Catalase is also an enzyme which is present within the mitochondrial matrix, in addition to its localization in the cytoplasm and in the peroxisomes. It has the ability to regulate ROS levels by catalyzing the

decomposition of H_2O_2, converting it to O_2 and H_2O. Glutathione is another important antioxidant, which also resides in the mitochondrial matrix as well as the cytoplasm. It has the capacity to reduce ROS products through the donation of electrons. Glutathione exists in two forms – reduced glutathione (GSH) and in its oxidized state known as glutathione disulfide (GSSG). Once GSH reduces H_2O_2 to form H_2O, GSH reacts with another oxidized GSH resulting in GSSG. GSSG can then be readily converted to GSH via the glutathione reductase enzyme. GSH levels also depend on nicotinamide adenine dinucleotide phosphate (NADPH), which is a by-product of the pentose phosphate pathway. NADPH is able to protect the cell against ROS by providing electrons to GSSG in order to regenerate reduced GSH.

The 'uncoupling to survive' hypothesis suggests another mechanism within mitochondria, which decreases ROS genesis (Andrews et al., 2005). This hypothesis supports the notion that endogenous uncoupling agents allow H^+ to leak back into the matrix, resulting in uncoupling of oxidative phosphorylation from ATP synthesis. This results in a reduction of $\Delta\Psi_m$ due to the change in the proton gradient between IMM and the matrix. Since there is a lower H^+ concentration in the IMS, there is a reduction in the number of H^+ flowing through the ATP synthase, resulting in a slower rate of oxidation phosphorylation. The attenuated rate in oxidation phosphorylation results in a more controlled flow of the electrons through the ETC. Therefore, the electrons do not stall and/or accumulate at the ETC complexes, and do not prematurely leak through the complexes to form ROS.

1.6 Functions of SIRT3

1.6.1 SIRT3 and mitochondrial processes

As previously discussed reversible acetylation is an important post-translational modification affecting proteins within mitochondria. The interchange between acetylated and deacetylated

states of mitochondrial proteins ensures that they can promptly respond to changes in their environment. Given that SIRT3 is a primary NAD^+-dependent deacetylase in mitochondria (Lombard et al., 2007), it relies on the consistent availability of mitochondrial NAD^+. As discussed in section 1.2.3.1, SIRT3 physically associates with complex I of the ETC (Ahn et al., 2008). Complex I catalyzes the oxidation of NADH derived from energy sources to produce NAD+. Thus, SIRT3 is able to utilize NAD^+ produced by complex I. However, during times of cellular stress and nutrient starvation the NAD^+/NADH ratio decreases. Fortunately, mitochondria harbor their own NAD^+ biosynthesis pathways (Yang et al., 2007). As sirtuins consume NAD^+ during their enzymatic actions, one molecule of nicotamide is produced. NAD^+ levels can then be replenished from nicotamide through a series of enzymatic steps called the 'salvage pathway' (for review see Kelly, 2010). Taken together, the abundance of NAD^+ within the mitochondrion and the large number of acetylated substrates provide an ideal environment for SIRT3 to exert its enzymatic actions.

SIRT3 targets mitochondrial substrates, which are responsible for the production of metabolites needed for the functioning of the TCA cycle, such as acetyl coenzyme A synthetase type 2 (AceCS2) (Hallows et al, 2006), glutamate dehydrogenase (GDH) and isocitrate dehydrogenase 2 (IDH2) (Schlicker et al., 2008). AceCS2 is a mitochondrial matrix enzyme that catalyzes the ligation of acetate with coenzyme A (CoA), therefore creating acetyl-CoA. Acetyl-CoA has an important role in regulating whether acetate groups will be used for energy production by the TCA cycle, or will be targeted for fat synthesis. Indeed, acetyl-CoA generated through the enzymatic actions of AceCS2 is targeted to the TCA cycle, and is utilized as an energy source (Fujino et al., 2001). Therefore, by deacetylating and activating AceCS2, SIRT3 allows for the utilization of acetate for energy production. SIRT1 has the ability to deacetylate acetyl coenzyme

A synthetase type 1 (AceCS1), which is the cytoplasmic homologue of AceCS2 (Hallows et al., 2006). However unlike AceCs2, acetyl-CoA generated by AceCS1 is used for fatty acid and cholesterol synthesis (Luong et al., 2000).

In addition, SIRT3 activates GDH as well as IDH2 through deacetylation (Schlicker et al., 2008). When GDH is in its active state, it metabolizes glutamate, producing α-ketoglutarate which is shunted to the TCA as an energy substrate. Similarly, SIRT3 is able to deacetylate and activate IDH2, which is another enzyme involved in the TCA cycle flux. IDH2 catalyzes a step within the TCA cycle by decarboxylating isocitrate, which also results in α-ketoglutarate production to be used further in the cycle (Schlicker et al., 2008).

SIRT3 has also been implicated in mitochondrial biogenesis, which is a process through which new mitochondria are generated. While the mechanisms are unknown, SIRT3 activates cAMP-response element binding protein (CREB) in adipocytes (Shi et al., 2005) and AMP-activated protein kinase (AMPK) in murine skeletal muscle (Palacios et al., 2009), which in turn increase the expression of PGC-1α. Increased transcriptional PGC-1α activity elevates expression of genes regulating mitochondrial biogenesis and genes encoding proteins involved in oxidative phosphorylation (Puigserver & Spiegelman, 2003). Overall these studies show that SIRT3 plays a role in mitochondrial metabolism by targeting and activating enzymes involved in the TCA cycle, as well as through possible activation of pathways involved in mitochondrial biogenesis.

1.6.2 Role of SIRT3 in mitochondrial oxidative stress

Oxidative damage to mitochondria contributes to its dysfunction, which further contributes to a wide range of diseases (Chaturvedi & Beal, 2008). Therefore, the balance between ROS formation and the antioxidant defence system needs to be restored. Ultimately, increasing mitochondrial antioxidant capacity would prove to be beneficial during conditions of oxidative

stress. Converging studies have suggested that SIRT3 may hold cytoprotective properties during such conditions.

SIRT3 is able to deacetylate cyclophilin D (CypD), which is a component of the mPTP that regulates the opening of the pore (Hafner et al., 2011). The authors suggested that by keeping CypD in a deacetylated state, SIRT3 is able to prevent the opening of the mPTP. Indeed, $SIRT3^{-/-}$ mice had augmented levels of fibrosis and increased mortality in response to cardiac stress caused by a transverse aortic constriction, a procedure which induces cardiac hypertrophy. However this phenotype was reversed by a pharmacological inhibitor of mPTP, cyclosporine A. Therefore authors concluded that SIRT3 may prevent opening of the mPTP during oxidative-type insults, whereas loss of SIRT3 would lead to permeabilization of the mitochondrial membrane, ROS elevation and cell death.

A recent study demonstrated that cardiomyocytes derived from $SIRT3^{-/-}$ mice, displayed elevated ROS levels following a stress-induced cardiac hypertrophy (Sundaresan et al., 2009). The authors demonstrated that MnSOD and catalase levels were up-regulated in cardiomyocytes over-expressing SIRT3. It was hypothesized that the increased levels of these antioxidant genes is due to the interaction between SIRT3 and FOXO3a. This study showed that SIRT3 was able to deacetylate, and therefore, activate FOXO3a. Sundaresan et al. (2009) hypothesized that the SIRT3/FOXO3a interaction takes place in the nucleus, given that FOXO3a shuttles between the nucleus and the cytoplasm. However, it is important to keep in mind that the murine form of SIRT3 was used in these over-expression experiments, and this form lacks the mitochondrial localization sequence (Scher et al., 2007). This truncated form of SIRT3 would not be targeted to mitochondria, and thereby have its enzymatic functions restricted to the cytoplasm and nucleus. Therefore, the observation that SIRT3 deacetylates FOXO3a in the nucleus may be artifactual. However, Jacobs et al (2008) showed that FOXO3a resides in the mitochondrion and SIRT3 is

able to directly interact with it. This study suggests that SIRT3 deacetylates FOXO3a directly in the mitochondrion, which promotes the nuclear localization of FOXO3a to induce expression of antioxidative genes.

Furthermore, HEK-293 cells ectopically over-expressing SIRT3 displayed elevated GSH levels, which protected cells from H_2O_2-induced insult (Someya et al., 2010). As discussed in earlier sections, SIRT3 is able to deacetylate IDH2 directly within mitochondria. Activated IDH2 then is able to decarboxylate isocitrate; the products of isocitrate decarboxylation are α-ketoglutarate as well as NADPH. NADPH has the ability to increase GSH levels through reduction of GSSG, and therefore protect cells from H_2O_2. Collectively, these studies demonstrate that SIRT3 protects cells during conditions of oxidative stress, by preventing mPTP from opening under stress conditions, and by regulating expression of antioxidative enzymes at the mitochondrial level.

1.6.3 SIRT3 and aging

Several studies suggest that members of SIR2 gene family can extend life span in diverse organisms when upregulated (Guarente, 2007; Longo & Kennedy, 2006). Over-expression of SIR2 in *Saccaromyces cerevisiae* (yeast) extends lifespan by as much as 30% (Kaeberlein et al., 1999). In addition, over-expression of the SIR2 gene in *Caenorhabditis elegans* (roundworm) increases lifespan by approximately 50% (Tissenbaum and Guarente, 2001). Genome association studies demonstrated that in humans there is variable number of tandem repeat (VNTR) polymorphism in the SIRT3 gene (Bellizzi et al., 2005). The VNTR region has an enhancer that is present in alleles containing specific sequences; this region was observed more frequently in men over 90 years of age. Therefore, the expression of SIRT3 was hypothesized to be essential for longevity.

Converging evidence has demonstrated that aging increases the susceptibility to carcinogenesis (Anisimov, 2003). An association between mitochondrial abnormalities and defects in oxidative metabolism was observed in tumour-like cells (Isshi, 2007). Tumour suppressor genes (TS) play an important role in the regulation of anti-carcinogenic mechanisms; therefore, the loss of fidelity of these genes has been implicated in the increase of the cancer-like phenotype (Anisimov, 2003). SIRT3 may hold such anti-carcinogenic capabilities, as it is linked to longevity in humans and it is a negative regulator of cellular stress pathways in mitochondria.

Surprisingly, a report by Lombard et al. (2007) has demonstrated that under basal conditions $SIRT3^{-/-}$ mice did not display any evident health deficits, and in fact they exhibited normal oxygen consumption and normal body weight. This study goes against the idea that SIRT3 plays a role in development and/or carcinogenesis, as loss of SIRT3 did not appear to be detrimental. However, Kim et al. (2010) reported that following ectopic over-expression of proto-oncogenes, $SIRT3^{-/-}$ mouse embryonic fibroblasts (MEF) displayed a decrease in ATP levels, and increased $\cdot O_2$ levels. Furthermore, $SIRT3^{-/-}$ mice developed mammary gland tumours after 24 months. These results contradicted Lombard et al. (2007), and demonstrated that mice with diminished SIRT3 levels exhibit negative phenotypic consequences. This disparity could arise because Lombard et al (2007) investigated $SIRT3^{-/-}$ mice only during short-term exposure to mild stress and under basal conditions. Whereas Kim et al (2010) demonstrated that loss of SIRT3 augments *in vitro* oncogenic transformation, and under normal conditions SIRT3 knockout would lead to a tumourigenic phenotype over a longer period of time. Taken together, SIRT3 is increasingly becoming recognized as an important modulator of mitochondrial metabolism regulating aging and carcinogenesis.

1.6.4 SIRT3 and caloric restriction

Caloric restriction (CR) is a dietary regimen low in calories without a lack of nutrition, and is speculated to slow the aging process (Koubova & Guarente, 2003). Although the mechanistic properties remain elusive, SIRT3 levels have been demonstrated to be elevated during conditions of CR (Civitarese et al., 2007; Shi et al., 2005). Because both CR and SIRT3 are proposed to regulate longevity, this encouraged further investigations of the relationship between SIRT3 and CR.

During conditions of CR, there is an enhanced catabolism of stored fat and amino acids in order to derive energy for cell functioning. To sustain metabolic processes during CR, there is a shift towards β-oxidation of fatty acids (Bruss et al., 2010). Indeed, SIRT3 is able to modulate fatty acid oxidation by deacetylating long-chain acetyl coenzyme A dehydrogenase (LCAD), a mitochondrial enzyme responsible for fatty acid oxidation (Hirschey et al., 2010). This study suggested that during fasting, SIRT3 regulates mitochondrial metabolism through fatty-acid utilization.

CR increases synthesis of acetyl-CoA, a metabolite used in the TCA cycle to produce energy (Hagopian et al., 2003). In the liver, when the levels of acetyl-CoA production exceeds the energy requirements of a cell, the excess acetyl-CoA is synthesized into ketone bodies (mainly there are two different ketone bodies produced: acetoacetate (AcAc) and 3-β-hydroxybutyrate (3HB)) (McGarry & Foster, 1980). These ketone bodies are exported from the liver and circulated throughout the body. Unlike fatty acids, ketone bodies are water soluble and are able to penetrate the blood brain barrier; thus, they are capable of being utilized by the brain as well as the heart and muscles. Therefore, ketogenesis is an important mechanism for supplying the brain with metabolites for energy during low levels of carbohydrate intake.

SIRT3 regulates the synthesis of ketone bodies within the liver. The production of 3HB is regulated by 3-hydroxy-3-methylglutaryl-CoA synthase (HMGCS2) in the matrix of liver mitochondria. SIRT3 deacetylates HMGCS2, which therefore activates the synthesis of ketone bodies (Shimazu et al., 2010). SIRT3 also regulates ketogenic metabolism, which is the action of breaking down ketone bodies in order to derive energy for the body. AceCS2 levels are elevated during ketogenic conditions, and its enzymatic function plays a role in the metabolism of ketone bodies (Fujino, 2001). Because SIRT3 activates AceCS2, it may therefore play an important role in the breakdown of ketone bodies to be used as metabolites for the TCA cycle during conditions of glucose deprivation. Therefore, the beneficial effects observed in conditions mimicking caloric restriction may be partly attributed to the mechanistic actions of SIRT3.

1.6.5 SIRT3 and the brain

Of all the mammalian sirtuins, SIRT1 has been the most extensively investigated as a potential neuroprotective factor. Over-expression of SIRT1 has been demonstrated to be protective in models of neurodegenerative diseases (Kim et al., 2007). However, the actions of SIRT1 as a neuroprotective factor are predominantly nuclear and/or cytoplasmic and it can only regulate mitochondrial functions through indirect mechanisms. As previously discussed, mitochondrial dysfunction is associated with age-related diseases, specifically neurodegenerative conditions. Altered mitochondrial function and ROS accumulation, with time, lead to neurodegenerative diseases and neuronal apoptosis.

Given that SIRT3 is a global mitochondrial acetylation levels regulator and that it targets mitochondrial proteins that regulate anti-oxidative processes, makes SIRT3 an attractive mitochondrial neuroprotective factor. To date, there have been only two studies, which have investigated the role of SIRT3 in the brain. Pfister et al (2008) demonstrated that SIRT3 over-

expression in cerebellar granule neurons results in cell death following low potassium exposure. On the other hand, Kim et al (2011) reported that over-expressing SIRT3 in cerebral cortical cultures decreases ROS genesis, and therefore is neuroprotective against N-methyl-D-asparate (NMDA)-induced cell death. These data demonstrate that the role of SIRT3 in the central nervous system (CNS) is ambiguous, and emphasizes the need for further investigations. In addition, there have only been three studies investigating SIRT3 expression within the CNS. However, these reports did not address SIRT3 expression profile in specific brain regions (Shi et al, 2005; Lombard 2007; Palacios et al, 2009). Collectively, these studies demonstrate that SIRT3 is expressed in the brain, however its functions have yet to be elucidated.

1.7 Rationale

Sirtuins are increasingly recognized to play a role in stress responses, metabolism, and aging (Huang et al., 2010; Shoba et al., 2009). To date, a large number of studies have investigated the role of SIRT1 as a cytoprotective factor in various oxidative stress models (Giannakou & Partridge 2008; Hasewaga et al., 2008; Nemoto et al., 2005) and neurodegenerative diseases (Kim et al., 2007). However, only a limited number of studies have focused on the role of the remaining six sirtuins in models of cellular stress. Is SIRT1 the only sirtuin that holds these cytoprotective functions? When focusing on the other members of the sirtuin family, SIRT3 may possess similar beneficial functions as SIRT1. While all the potential mechanisms induced by SIRT3 are not clear, SIRT3 may target some of the same substrates as SIRT1 (Law et al., 2009). As previously discussed, unlike the cytoplasmic and nuclear localization of SIRT1, SIRT3 carries out its enzymatic function directly within mitochondria by regulating global mitochondrial acetylation/deacetylation levels, increasing the entry of metabolites into the TCA cycle and targeting mitochondrial substrates involved in anti-oxidative and metabolic processes. Given that mitochondria are susceptible to oxidative stress which contributes to pathogenesis of

numerous clinical conditions, can SIRT3 be therapeutically targeted as a potential cytoprotective factor?

SIRT3 targets a number of mitochondrial proteins through deacetylation, however the consequences of these interactions have not been fully elucidated as of yet. Interestingly, cells which had their SIRT3 levels diminished have been demonstrated to be sensitive to various models of oxidative stress (Bell et al., 2011; Finley et al., 2011). While studies investigating the consequences of over-expressing SIRT3 have just began to emerge, it is still not fully understood how increasing SIRT3 levels affects mitochondrial function under basal conditions, and following conditions of oxidative stress. Furthermore, studies have demonstrated that mitochondrial dysfunction is associated with neurodegenerative diseases (Chaturvedi & Beal, 2008). Because SIRT3 is able to regulate mitochondrial function, this sirtuin may also hold neuroprotective capacity. Although SIRT3 is expressed in the brain (Lombard 2007; Palacious et al, 2009; Shi et al, 2005), these reports did not investigate regional specific expression or assess whether SIRT3 is expressed in a specific cell type. Thus before examining the role of SIRT3 within the brain, its expression profile needs to be investigated.

1.8 Hypothesis and specific aims

Hypothesis:

SIRT3 over-expression protects cells from oxidative stress

Specific Aims:

PART I – Cytoprotective role of SIRT3

1. To determine whether $\Delta\Psi_m$ is altered in cells over-expressing SIRT3
2. To determine whether ROS levels are decreased in cells over-expressing SIRT3
3. To determine whether cells over-expressing SIRT3 are less sensitive to oxidative damage, such as glucose deprivation and H_2O_2

PART II – Expression levels and localization of SIRT3 in the brain

1. To determine mRNA and protein expression levels of SIRT3
2. To determine cell specific localization of SIRT3 in cortical primary cultures

MATERIALS AND METHODS

2.1 Cell culture

Human embryonic kidney cells (HEK-293) were cultured in 10 cm dishes and grown to 80% confluency in Dulbecco's Modified Eagle Medium (DMEM, Gibco) with 1,000 mg/L of D-glucose, L-glutamine, pyridoxine hydrochloride, and 110 mg/L of sodium pyruvate supplemented with 10% fetal bovine serum (FBS) (Gibco). All transfections were performed using lipofectamine 2000 (52887, Invitrogen) as per manufacturers recommendation; 4 hours following the transfection, the medium was replaced with fresh culturing medium.

2.1.1 Establishment of stable transfectants

HEK-293 cells were transfected with 4 µg of either empty p-LKO vector or p-LKO vector containing human SIRT3 cDNA (accession code: NP 036371.1). The SIRT3 transgene contained a myc-tag on the amino-terminus, which was inserted into the EcoRI site of the p-LKO expression cassette. Expression of SIRT3-myc in HEK-293 cells was enforced by selection in Blasticidin S (20 µg/ml) (380-089-M100, Alexis Biochemicals). Stable transfectants were maintained in DMEM medium supplemented with 10% FBS, ampicilin x1, and blasticidin S at a concentration of 5 µg/ ml. Clones were preliminarily screened for the mature SIRT3 expression by Western blotting described in section 2.4.

2.2 Primary cultures

2.2.1 Coating dishes with poly-L-ornithine

Poly-L-ornithine **(**PLO) (P-4638, Sigma) stock was prepared by diluting it in ddH20 to a concentration of 10 mg/ml. The stock aliquots of 75 µl were then kept frozen at -20°C. In preparation of the fresh working solution one aliquot of PLO stock was diluted in 50 mL ddH20 resulting in a final concentration of 15 µg/ml. Borax Acid (BOR 001, Bioshop) was added (0.19 g). The pH was then corrected to 8.4. The working solution was then filtered and used to coat 24

well polystyrene plates containing sterilized glass coverslips, and then incubated at room temperature (RT) overnight. On the day of culturing, the PLO solution was washed out with sterile ddH20, and the culture plates were left to dry for 2 hours at RT.

2.2.2 Harvesting and plating primary cultures

On day 18 of gestation, fetuses were dissected out of pregnant Wistar rats in compliance with the guidelines established by the University Health Network and the Canadian Council on Animal Care. The rats were sacrificed by CO_2 asphyxiation, and the fetuses were dissected out of the abdominal cavity, and were placed in sterile phosphate buffered saline (PBS) x1 on ice. The fetuses were individually cut out of the fetal membranes, and transferred to dissecting medium on ice. Both cortical hemispheres were dissected out, and for every 3 fetuses the brains were collected by centrifugation at 1000 rpm for 2 minutes in 15 ml of dissecting medium. The dissecting medium was aspirated, and the brains were digested for 30 minutes on a shaker at 37°C in 4 ml of papain solution. Following incubation the brains were centrifuged for 5 minutes at 1000 rpm, the papain solution was then aspirated, and 5 ml of neurobasal plating solution (21103- 049, Gibco) was added. The cortices were then dissociated by tituration with a glass pipette. The volume of the plating solution was brought up to 50 ml, allowing 10-15 minutes for the debris to settle down. Cells were stained with Trypan Blue and counted using a hemocytometer. Once counted, the cells were plated on dishes containing plating medium at a density of 250,000 cells/ml to grow in 5% CO_2 at 37°C.

2.3 Immunocytochemistry

2.3.1 Validation of SIRT3 translocation to mitochondria

One set of HEK-293 cells were co-transfected with a mitochondrial-targeted green fluorescent protein (Mt-GFP) and SIRT3-myc transgene, whereas the second set of HEK-293 cells were transfected with the SIRT3-myc transgene only. After 24 hours, the second set of cells were incubated with mitochondria marker mitotracker-red (0.5 μM) for 30 minutes. Following 30 minutes of incubation, the mitotracker-red dye was washed out with PBS x 1 (3x). Both sets of cells were fixed in 4% formaldehyde in PBS for 30 minutes, and permeabilized with 0.1% Triton X-100 in PBS for 10 minutes. Following permeabilization the cells were washed two times in PBS and once with 0.5% NP40 in PBS. The coverslips were blocked for 1 hour in blocking solution (PBS plus 4% BSA, 4% Goat Serum, 0.5% Dry Milk) at RT. The coverslips were then incubated with a rabbit monoclonal antibody against the SIRT3 myc-epitope (2276, Cell Signalling) (1:500) overnight at 4°C.

After the overnight incubation, the coverslips were washed twice in PBS and once with 0.5% NP40 for 3 minutes each. Following the washes, the coverslips were blocked for 30 minutes (PBS plus 4% BSA, 4% Goat Serum, 0.5% Dry Milk). Coverslips which were labeled with mitotracker-red and transfected with SIRT3-myc were incubated for 1 hour at RT with goat-anti rabbit secondary antibody conjugated to fluorescein isothiocyanate (FITC) (1:500) to label SIRT3-myc. Whereas, coverslips transfected only with Mt-GFP, were incubated with goat-anti rabbit secondary antibody conjugated to texas red (1:500) to label SIRT3-myc. The coverslips were then washed and stained with hoechst dye 33258 (8 μg/ml) for 5 minutes, washed twice with PBS x 1, and mounted with mounting glue (S3023, Dako).

The slides were viewed using Zeiss Deconvolution Axiovert 200M microscope. This microscope is equipped with broadband mercury bulb source, as well as a set of filters to excite fluorescent dyes. Images were captured with a digital camera (Axiocam, Zeiss) using the 63x oil objective lens, and analyzed using the LSM 510 software. The photographic and microscopic settings were kept constant for comparisons between pictures.

2.3.2 Cell-specific expression of SIRT3 and SIRT1 proteins

Primary rat cells (E-18) were obtained following procedure in section 2.2 and were grown on coverslips for 10 days prior to the experiment. Cells were fixed in 4% formaldehyde, and washed by the same method outlined in the section above. The coverslips were incubated overnight at 4°C with primary antibodies: SIRT3 (C73E3, Cell Signalling) and SIRT1 (09-845, Millipore). Simultaneously, coverslips were also incubated with either astrocyte specific primary antibody, glial fibrillary acidic protein (GFAP) (63893, Sigma) or neuron specific marker primary antibody microtubule associated protein 2 (MAP2) (M1406, Sigma). The coverslips were washed as per section 2.3.1, and blocked in blocking solution (PBS plus 4% BSA, 4% Goat Serum, 0.5% Dry Milk) for 30 minutes.

Due to a very weak signal of the SIRT3 antibody, signal amplification was achieved using a streptavidin biotin technique. After blocking, coverslips were incubated with biotinylated goat anti-rabbit antibody (1:1000) for 1 hour at RT. Following 3 washes with PBS x 1, these coverslips were then incubated with secondary antibody streptavidin conjugated to dylight 549 (1:500) to detect SIRT3 (D16-500-084, Jackson Immunoresearch). No biotin amplification to detect SIRT1 was needed. Therefore, SIRT1 coverslips were incubated with goat-anti rabbit secondary antibody conjugated to dylight 549. To detect GFAP or MAP2, secondary antibody

conjugates known as quantum dots 525 (1:100) (Q11041MP, Invitrogen) were used. Coverslips were then washed, mounted and imaged as described above.

2.4 Western blot analysis

2.4.1 Sample preparation

Male Wistar rats were sacrificed at different age stages by the decapitation method in compliance with the guidelines established by the Medical Research Council of Canada and the Canadian Council on Animal Care. Animals aged 1 week, 3 week, 3 month, and 24 months were sacrificed. Tissues of interest were collected in cryovials, and snap-frozen by liquid nitrogen. Protein lysis was performed by taking 30 g of tissue and submerging it in 300 µl of ice cold tissue lysis buffer (50 mM Tris - pH 8.0, 1% NP40, 150 mM NaCl, 1mM EDTA, 1mM PMSF, 1 µg/ml Aprotinin, 1 µg/ml Leupeptin, 2 mM Na3VO4 and 1 tablet of protease inhibitor from Boehringer). The tissues were then homogenized manually with a 25 gauge syringe needle approximately 30 times, and centrifuged at 11000 rpm for 10 minutes at 4°C. The supernatant (consisting of total cell protein) was collected and total protein concentrations of individual samples were quantified using the Bio-Rad protein assay (162-0115, Biorad) at 595 nm wavelength using a spectrophotometer (Beckman model DU640).

2.4.2 Sodium dodecyl sulphate -polyacrylamide gel electrophoresis (SDS-PAGE)

The samples prepared as discussed in the section above were separated using SDS-PAGE (5% acrylamide stacking gel and 12.5% resolving acrylamide gel) in Tris-Glycine Laemelli running buffer (25 mM Tris, 192 mM glycine and 0.1% SDS) at a constant voltage of 100 V for 2 hours. The proteins resolved in the gel were then transferred to nitrocellulose membrane (BIORAD) overnight in transfer buffer (25 mM Tris, 192 mM glycine, and 0.1% SDS) at 4°C at a constant voltage of 25 V. The membranes were then blocked for 2 hours in non-fat powdered milk (5%)

in TBST washing buffer (10 mM Tris, 150 mM NaCl, 0.05% Tween 20), and probed overnight with a specific primary antibody (see section 2.4.3 below) at 4°C. The membranes were then washed 3 times for 15 minutes each in TBST. Following the washes, membranes were then incubated for 2 hours at RT with HRP-conjugated secondary antibodies (see section 2.4.3 below), which were diluted in TBST containing 5% non-fat powdered milk. After the 2 hour incubation, blots were then washed 3 times for 15 minutes each in TBST. Protein levels were detected using chemiluminescence (GE Healthcare, Amersham ECL Western Blotting Detection Reagents) onto X-Ray film (Biotex). To control for equal loading, the membranes were incubated with stripping solution (2% SDS, 0.7% BME, 6.2 mM Tris pH 6.7) for 30 minutes at 55°C and reprobed with a housekeeping protein glyceraldehyde-3-phosphate dehydrogenase (GAPDH) to check for equal protein loading.

2.4.3 Antibodies used for detection of SIRT3, GAPDH and Myc

primary antibodies:

- Anti-SIRT3 rabbit polyclonal antibody, 1:500 dilution (C73E3, Cell Signalling)
- Anti-GAPDH mouse monoclonal antibody, 1:15,000 dilution (MAB374, Chemicon)
- Anti-myc mouse monoclonal antibody, 1:1000 dilution (2276, Cell Signalling)

secondary antibodies:

- HRP-linked goat anti-rabbit antibody, 1:5000 dilution (111-036-006, Jackson)
- HRP-linked goat anti-mouse antibody, 1:5000 dilution (115-036-006, Jackson)

2.4.4 Densitometry and quantification of results

In order to quantify optical density per equal area of analysis (OD/mm2) of all protein bands, X-ray films were scanned and analyzed using Quantity One Software (BIORAD). To quantitatively analyze each sample, a rectangle was drawn around the biggest protein band and re-used via

copying and pasting for all the other bands on the same film. To control for background signal intensity, the same box was pasted above all the protein bands on the film, and the OD/mm2 was averaged to obtain an average background signal. To calculate the net band density, the average background density was subtracted from each of the band density values. All the densitometry values obtained were then normalized versus the OD/mm2 values obtained for the housekeeping protein GAPDH in the same samples.

2.5 Quantitative real time polymerase chain reaction

Quantitative real time polymerase chain reaction (qRT-PCR) is based on the general principle of polymerase chain reaction (Wong & Medrano, 2005). qRT-PCR is used to amplify and quantify mRNA expression levels of a specific gene of interest relative to a housekeeping gene. In this thesis, two distinct molecular qRT-PCR assays were used: TaqMan and SYBR Green. Both of these qRT-PCR methods allow for detection of PCR products by the generation of a fluorescent signal. Taqman probe contains a fluorophore covalently attached to it, and this probe is able to anneal to a distinct region on the mRNA template. During qRT-PCR, forward and reverse primers anneal to a specific region within the target of interest, as the polymerase replicates the template it cleaves the Taqman probe which results in fluorescence emission. On the other hand, SYBR Green assay is simply a dye and does not contain a fluorescent probe attached to it. Once the SYBR Green dye binds a gene of interest, it forms a DNA-dye complex which emits fluorescence once it is excited. Although, TaqMan and SYBR Green are of different chemistry technologies, both rely on the same principle: as the PCR products accumulate, fluorescence increases (for full review of TaqMan and SYBR Green see Wong & Medrano, 2005).

2.5.1 Sample preparation

To quantify SIRT3 mRNA and SIRT1 mRNA expression levels in the rodents, male Wistar rats and B57 mice of different age groups were sacrificed at different age stages by decapitation. This was done in compliance with the guidelines established by the University Health Network and the Canadian Council on Animal Care. Immediately after harvesting tissue of interest, samples were collected in cryovials and snap-frozen by liquid nitrogen to be stored at -80°C for RNA extraction. To quantify PGC-1α mRNA levels, HEK-293 cells stably over-expressing SIRT3-myc and HEK-293 control cells were used.

RNeasy Mini Kit (74104, Qiagen) was used to extract total RNA from the frozen tissues or cells as per manufacturer's guidelines for mammalian tissues or cells, respectively. Purified total RNA (1 ug) was then reverse transcribed into cDNA via Superscript II First Strand Synthesis System (18064-014, Invitrogen). Oligo(dT) was used to ensure that cDNA synthesis contained pure mRNA product from the initial total RNA extracted from the samples. Oligo(dT) is a primer that anneals to the poly(A) sequence at the 3' end of all mRNA templates, therefore allowing the reverse transcriptase to transcribe cDNA directly along the mRNA template.

2.5.2 Primers utilized

Pre-designed Taqman probe and primer mixtures (Applied Biosystems) were used for qRT-PCR reaction for SIRT3 (mouse - Mm00452129m1; rat - Rn01501410m1), SIRT1 (mouse – Mm01168521m1; rat - Rn01428094m1), and a reference housekeeping gene, hypoxanthine-guanine phosphoribosyltransferase (HPRT1) (mouse – Mm03024075m1; rat - Rn01527840m1).

SYBR Green Forward and reverse primers were designed for PGC-1α (F-5'tcagctgtgtcgacatggcttgggacatgtgcag'3; R-5'-agctgactgatatcttacctgcgcaagcttctctg'3), and a reference housekeeping gene, glyceraldehyde-3-phosphate dehydrogenase (GAPDH) (F-5'

cctgacctgccgtctagaaaa’3; R– 5’tgtcgctgttgaagtcagagga’3), these sequences were obtained from Chang et al. (2009) and Fukushina et al. (2005), respectively.

2.5.3 Amplification conditions used

Each of the samples were loaded on a 96-well plate, and ran in quadruplicates. Taqman master mix reagent kit (4304437, Applied Biosystems) or SYBR Green master mix reagent kit (4385612, Applied Biosystems) were used to amplify 20 ng of transcripts of interest in 10 µl reactions. The amplification reactions were carried out in 96-well plates with 7900HT Fast Real-Time PCR System (Applied Biosystems).

The thermal profile for Taqman is as follows: the initial step of enzyme activation at 50°C for 2 minutes, followed by denaturation at 95°C for 10 minutes, then 40 cycles of 95°C for 15 sec, primer annealing at 60°C for 1 minute, and template extension at 72°C for 30 sec. The thermal profile for SYBR Green is as follows: initial step of enzyme activation at 50°C for 2 minutes, followed by denaturation at 95°C for 10 minutes, then 40 cycles of 95°C for 15 sec, primer annealing at 56°C for 1 minute, and template extension at 72°C for 30 sec; with the dissociation step of 95°C for 15 sec, 60°C for 15 sec and 95°C for 15 sec. The amplification of all the primers was analyzed with sequence detection system software 2.2. Values obtained, known as the threshold cycle (CT), were averaged and normalized to HRPT1 (for SIRT1 and SIRT3) and GAPDH (for PGC-1α) for each cycle to obtain relative gene expression values.

2.6 Flow cytometry

Flow cytometry is a methodology which is able to detect and analyze cell counts, cell granularity and whether the cell contains any fluorescence (dyes or antibodies). Cells are suspended in a stream of high-speed fluid, the stream passes the cells individually through a laser beam. The laser beam is able to detect light scattering from each of the cells, which measures size (forward

scatter) and granularity (side scatter). Forward scatter measures cell size, as more light is scattered if the cell is bigger in size. Side scatter measures cell complexity, as a higher number of organelles inside a cell produce more light scattering at larger angles. In addition, the laser beam is able to excite fluorescent molecules present in the cells. The combination of all the information collected from the laser excitation, is then converted to an electronic signal by optical detectors, which then sends this information to the computer. A photodiode collects the forward scatter signal, whereas an optical detector known as photomultiplier tube (PMT) collects the information from side scatter and fluorescence signals. The output is expressed as mean fluorescence intensity of all the cells that passed through the laser. Unless stated otherwise, all of the flow cytometry experiments were performed on HEK-293 cells stably over-expressing SIRT3-myc vs. control HEK-293 cells.

Flow cytometry experiments were carried out with the BD FACScan flow cytometer (BD Biosciences, San Jose, CA) equipped with a 488 nm argon laser, and BD FACS Calibur equipped with 488 nm argon laser and 633 nm halogen laser. Forward and side scatter were used to gate the viable population of cells. In addition, unlabelled cells were used to gate out auto-fluorescence. For each experiment, at least 10,000 events were collected and analyzed for mean fluorescence intensity for positive stained cells. Cell Quest program was used to analyze results using dotplot or histograph function.

2.6.1 Analysis of basal mitochondrial membrane potential using rhodamine-123

Basal mitochondrial membrane potential ($\Delta\Psi m$) was measured using rhodamine-123 (R-302, Invitrogen), which is a cationic probe that accumulates in the mitochondrion and fluoresces proportionally with $\Delta\Psi m$ (Chen, 1988). Control and experimental cells were plated at 300,000 cells/well. After 24 hours in culture, cells were washed once with DMEM media, and incubated

for 30 minutes with 0.5 μM of rhodamine-123 at 37°C in 5% CO_2. Two specific positive controls were used in this experiment. One of the controls was carbonyl cyanide m-chloro phenyl hydrazone (CCCP) (10 μM) (Sigma, #C-2759), an uncoupler which decreases ΔΨm through facilitating proton movement across the mitochondrial membrane. CCCP was added 12 hours prior to cell harvest. The second control was a high concentration of rhodamine-123 (20 μM), to make sure the probe was not quenched.

Following incubation, cells were then centrifuged 10,000 rpm to pellet, washed once in cold DMEM media and then re-suspended in 0.5 ml of cold PBS x 1. The cells were then kept on ice until the mean fluorescence for each sample was analyzed by BD FACsort flow cytometer.

Rhodamine-123 (excitation 490 nm, emission 530 nm) was excited by a 488 nm argon laser. Once the fluorescence was emitted, it was collected by a PMT filter FL-1 (which is able to collect green emitted light between 510 nm – 545 nm). The mean rhodamine-123 fluorescence intensity in experimental and control cells depicted basal ΔΨm.

2.6.2 Analysis of basal mitochondrial membrane potential using mitotracker deep red

Prior to the experiment naive HEK-293 cells were plated at 300,000 cells/well. After 24 hours in culture, as per the transfection protocol in section 2.1, the experimental plates were co-transfected with 4 μg of SIRT3-myc and 1.5 μg of plck-GFP. The control cells were co-transfected with β-galactosidase and plck-GFP, to balance for the metabolic load. Twenty four hours post transfection, the cells were loaded with 0.5 μM of mitotracker deep red, which is a cationic probe that accumulates in the mitochondrion and fluoresces proportionally with ΔΨm . The cells were incubated with mitotracker deep red for 30 minutes at 37°C in 5% CO_2. Cells were collected as described in 2.6.1, and re-suspended in cold PBS. The cells were then kept on

ice until the average fluorescence for each sample was analyzed by FACsCalibur flow cytometry system.

Mitotracker deep red (excitation 640 nm, emission 662 nm) was excited by 633 nm halogen laser; whereas, GFP (excitation 488 nm, emission 520 nm) was excited by a 488 argon laser. Mitotracker deep red fluorescence emission was collected by a PMT filter FL-4 (which is able to collect emitted light between 653 nm – 669 nm), and GFP emission was collected by a PMT filter Fl-1 (which is able to collect emitted light between 510 nm – 545 nm).

Transfected cells were identified by GFP fluorescence. A dual fluorescence dot plot was plotted FL1 (GFP, green fluorescence) vs. (FL4) (mitochondria deep red probe, red fluorescence). A gate was made to include cells that exhibited both green and red fluorescence. Therefore, cells transfected with either SIRT3-myc or β-galactosidase (GFP positive) were analyzed for mean fluorescence intensity of mitotracker deep red.

2.6.3 Analysis of basal ROS levels using DCF

In order to measure basal intracellular ROS levels, 5-(and-6)chloromethyl-2',7' dichlorohydrofluoresceindiacetate (DCF) (D-399, Invitrogen) was utilized. DCF is a fluorescent probe, which gets converted to fluorescent oxidized form, and fluoresces proportionally with the level of free radical oxidation. Control and experimental cells were plated at 300,000 cells/well. After 24 hours in culture, cells were washed once with DMEM media, and incubated for 30 minutes with 10 μM of DCF at 37°C in 5% CO_2. 100 μM of hydrogen peroxide (H_2O_2) was used as a positive control for DCF, and was added 2 hours prior to cell harvest. Cell cultures were collected as described in 2.6.1, and re-suspended in cold PBS. The cells were then kept on ice until the average fluorescence for each sample was analyzed by FACScan flow cytometry system. DCF (excitation 490 nm, emission 517 nm); was excited by a 488 nm argon laser. Once

the fluorescence was emitted, it was collected by a PMT filter FL-1 (which is able to collect emitted light between 510 nm – 545 nm). The mean DCF fluorescence intensity in experimental and control cells depicted basal ROS levels.

2.7 Oxidative stress assays

HEK-293 naive cells were plated at a density of 250,000 cells/well on PLO coated 33 mm glass dishes. After 24 hours in culture, experimental cells were co-transfected with 4 μg SIRT3-myc and lck-GFP. The control plates were co-transfected with β-galactosidase and lck-GFP, in order to control for metabolic load. Twenty four hours after transfection, the experimental cells were exposed to either glucose deprivation (GD) or H_2O_2 challenge.

For the GD challenge, cells were incubated for up to 3 hours with GD media, which was glucose and glutamine-free DMEM medium supplemented with 10 mM of 2-deoxy-D-glucose (2DG) (Sigma, #D-8375) to impair mitochondrial glycolysis. Following GD, cells were subjected to the glucose reperfusion (GR) challenge by changing the GD medium to normal culturing medium (DMEM containing glucose and glutamine and supplemented with 10% FBS), and were incubated for 24 hours. For the H_2O_2 challenge, cells were treated with 500 μM H_2O_2 in DMEM medium (with glucose and glutamine supplemented with 10% FBS), and incubated for up to 24 hours.

2.7.1 Quantification of cell death

After subjecting cells to GD/GR or H_2O_2 insults, propidium iodide (PI) (1 μg/ml) was used to identify dead cells at specific time-points during GD (0 hours, 1 hour, 3 hours), after GR (24 hours), and at specific time-points during the H_2O_2 treatment (0 hours, 6 hours, 12 hours, 24 hours). At the specified time-points cells were visualized via the Nikon TE2000E Timelapse microscope, using 20x fluor objective. Five randomized fluorescent images were taken for each

of the experimental and control dishes. Cells that were PI-positive and GFP-expressing (containing SIRT3-myc or β-galactosidase) were identified by dual-channel confocal microscopy (Texas Red/FITC filters). For each image collected, the percentage of cell death was quantified by counting the number of double positive cells (GFP positive and PI positive), and then dividing the count by the number of total GFP positive cells in the same picture. This was performed for all the time-points and conditions stated above.

2.8 Cell proliferation assay

CyQuant cell proliferation assay kit (C7027, Invitrogen) was used to quantitfy relative cell proliferation rates between HEK-293 cells stably over-expressing SIRT3-myc and control HEK-293 cells. This assay is able to determine the relative cell number in a culture dish. CyQuant cell proliferation assay kit contains a fluorescent dye which is able to bind cellular DNA. Once the dye has binded to the nucleic acid, it fluoresces when it is excited (excitation 480 nm, emission 520 nm). Both of the cell types were seeded in 96-well PLO-coated microplates at an initial concentration of 12,500 cells/well. To obtain an initial cell count at time-point of 0 hours, cells were allowed to settle at the bottom of the wells for 30 minutes. Media was then gently removed, and the wells were washed once with 1 x PBS. After the PBS wash, the plates were immediately frozen on dry ice to be stored at -80°C until use. The same procedure was followed for cells that were cultured for 48 hours.

On the day of the assay, the 96-well plates from the time-points of 0 hours and 48 hours were taken out of the -80°C freezer and thawed at RT. CyQuant solution was prepared as per manufacturer's guidelines, and 200 µl of the solution was added to each of the wells. In order to control for auto-fluorescence, a row of blank wells was included on each plate. The blank control consisted of poly-L-ornithine-coated wells and CyQuant dye without cells. The plates were then

read fluorimetrically on a microplate reader (Molecular Devices Flexstation II). To exclude auto-fluorescence from the data, the mean fluorescence intensity of the blank values was subtracted from the mean fluorescence intensity values of the cells for each of the 96-well plates.

2.9 Statistical analysis

Statistical analysis was performed using non-paired, two-tailed Student's t-test, one-way analysis of variance (ANOVA) or two-way ANOVA in GraphPad Prism. When data was significant using one-way or two-way ANOVA, Bonferroni's post-hoc test was utilized. All results are expressed as mean ± Standard Error of Means (SEM) and a probability value (P) of less than 0.05 was accepted as a significant result.

RESULTS

3.1 Assessment of the SIRT3 construct

To assess whether ectopical over-expression of SIRT3 has any effect on cultured HEK-293 cells, a construct was engineered expressing human SIRT3 cDNA containing a myc-tag. The myc-tag was used to identify the SIRT3-myc transgene from endogenous SIRT3 within transfected HEK-293 cells. For all over-expression experiments, SIRT3-myc construct was used to transiently transfect cells or to generate stable cell lines.

Full length SIRT3 contains 3 important conserved functional motifs: mitochondrial localization sequence (MLS) (Cooper et al, 2008), mitochondrial processing peptidase (MPP) cleavage site, and the catalytic deacetylation motif (Schwer et al, 2002). SIRT3 has a predicted molecular mass of 45 kilodaltons (kDa), and is targeted to mitochondria by the MLS (Cooper et al, 2008). Upon reaching mitochondria it is imported into the inner mitochondrial matrix through a translocase of the outer membrane (TOM) and translocase of the inner membrane (TIM) complexes (Neupert, 1997). Within the matrix, MPP cleaves ~ 100 amino acids at the amino-terminus, to produce an enzymatically active 28 kDa SIRT3 protein. Because the MLS sequence is on the amino-terminus, the myc-tag was added on the carboxyl-terminus. Once SIRT3 is enzymatically active, it functions as a protein deacetylase. The human SIRT3 protein is illustrated in Figure 2A.

3.1.1 SIRT3 construct is targeted to mitochondria in HEK-293 cells

Immunocytochemistry was used to identify the subcellular localization of the SIRT3 transgene product. In order to detect whether this product is targeted to mitochondria, two independent mitochondrial markers were used: mitotracker-red and mitochondrial-targeted GFP protein (Mt-GFP). HEK-293 cells were transiently transfected with SIRT3 and counter stained with mitotracker-red. Mitotracker-red is a fluorescent probe that accumulates in active mitochondria. Mitotracker-red is sequestered to active mitochondria, and its fluorescence is proportional to the

mitochondrial membrane potential (ΔΨm). Indeed the results showed that SIRT3 immunofluorescence co-labels with the mitotracker-red signal (Figure 3A).

As an independent assessment using a different mitochondrial marker, HEK-293 cells were co-transfected with the SIRT3 construct and Mt-GFP (Figure 3B). Mt-GFP is a nuclear encoded protein containing a MLS domain. The GFP protein fluoresces only when it is folded properly following mitochondrial import (Sirk et al., 2003). Indeed, the results demonstrated that SIRT3 immunofluorescence co-labels with the Mt-GFP signal. Unlike mitotracker-red, Mt-GFP localization to mitochondria is independent of the ΔΨm. Thus, Mt-GFP provides an independent assessment. Taken together, the co-labeling of SIRT3 with both mitotracker-red and Mt-GFP confirmed that SIRT3 is targeted to mitochondria. In addition, there was no SIRT3 staining in the nucleus and/or the cytoplasm.

3.1.2 SIRT3 is processed correctly into its mature form in HEK-293 cells

To assess if the SIRT3 transgene-derived protein is correctly processed after translation, it was transfected in HEK-293 cells and SDS PAGE was performed followed by Western blot. The Western blot was probed with a myc antibody, and two distinct immunoreactive products were detected at 45 kDa and 28 kDa. The 45 kDa protein depicts the predicted size of the full length SIRT3 protein. The 28 kDa protein is of the appropriate size following post-translational modification by MPP in the mitochondrial matrix (Figure 4). Therefore, our SIRT3 product is of the predicted pro- and processed forms. Collectively, these results indicate that the product generated from the SIRT3 transgene is targeted to mitochondria, is of the predicted mass, and is correctly posttranslationally processed.

Fig. 2

A)

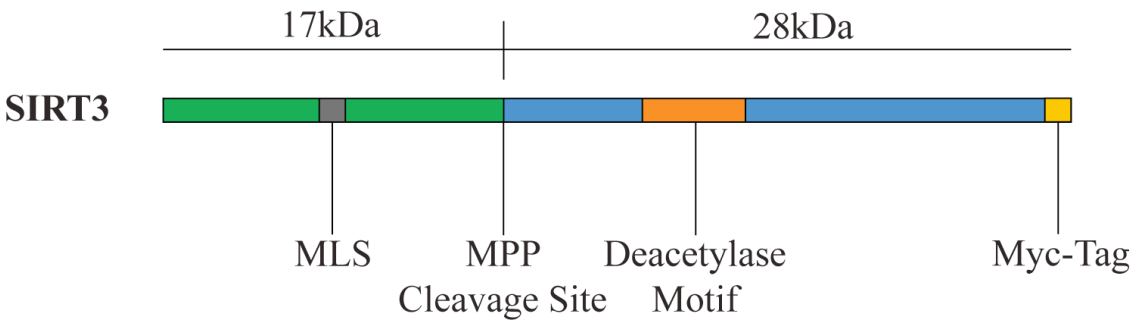
17kDa
28kDa
SIRT3
MLS
MPP
Cleavage Site
Deacetylase
Motif
Myc-Tag

B)

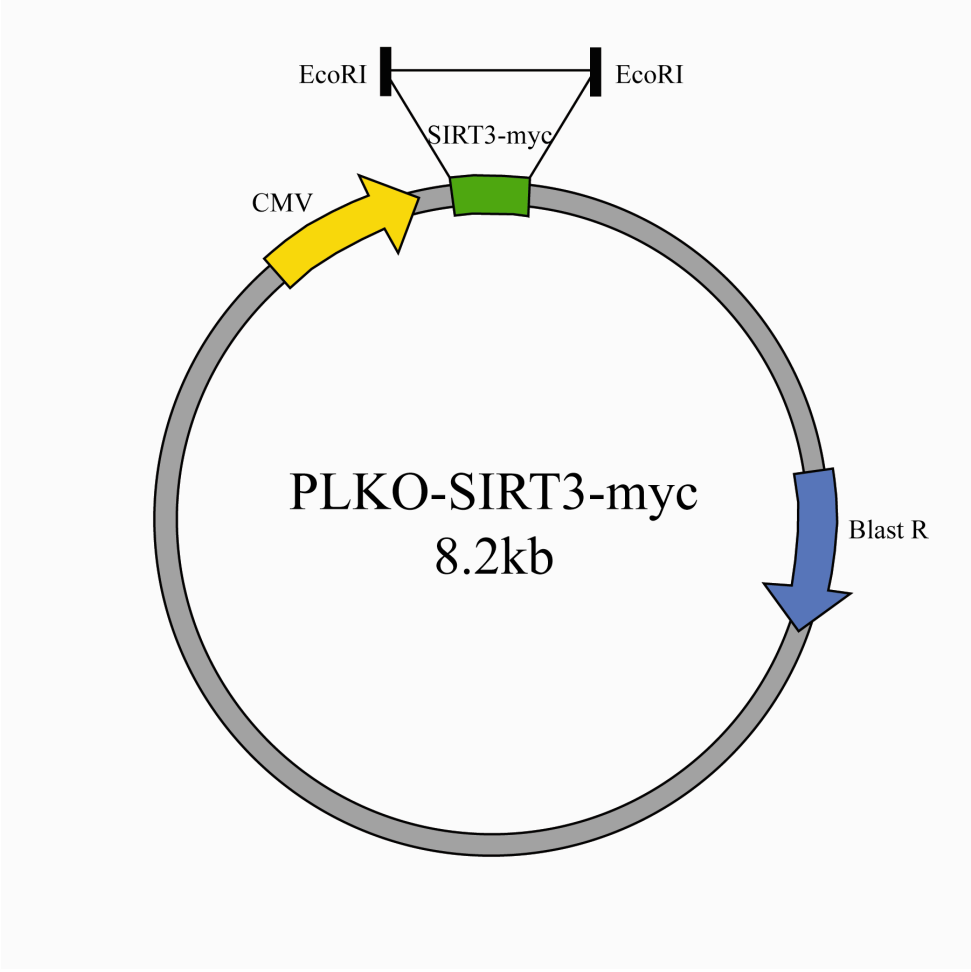
EcoRI
EcoRI
SIRT3-myc
CMV
PLKO-SIRT3-myc
8.2kb
Blast R

Figure 2: Schematic diagram of human SIRT3 protein and a map of p-LKO-SIRT3 construct

A) Schematic diagram of human SIRT3 protein. This diagram shows the 45 kDa pro-form of the SIRT3 protein (green and blue together). It is targeted to mitochondria by the MLS. Once it reaches the mitochondrial matrix, the pro-form is cleaved by MPP. This yields the enzymatically active 28 kDa processed form (green), and the deacetylation motif becomes active (orange). Depicted in the yellow is the myc-tag. Three motifs are presented: mitochondrial localization sequence (MLS), mitochondrial processing peptidase (MPP) cleavage site and the catalytic deacetylase motif.

B) Map of p-LKO-SIRT3 Construct (8.2 kb). The vector contains human SIRT3 cDNA (Accession code: NP 036371.1), encoding 399 amino acids. The expression of SIRT3 is driven by the CMV promoter. The presence of a Blasticidin antibiotic resistance gene allows for the generation of a stable cell line.

Fig. 3

A)

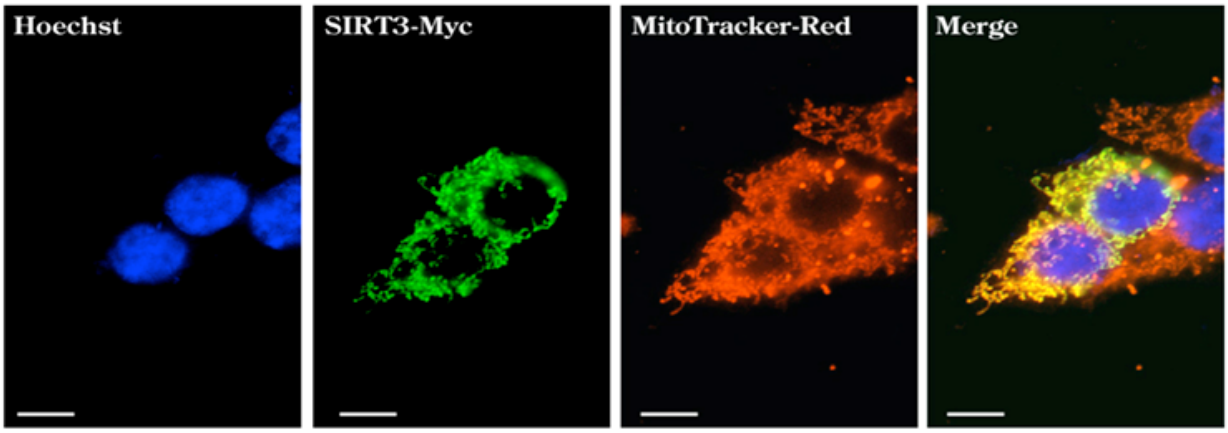
Hoechst
SIRT3-Myc
MitoTracker-Red
Merge

B)

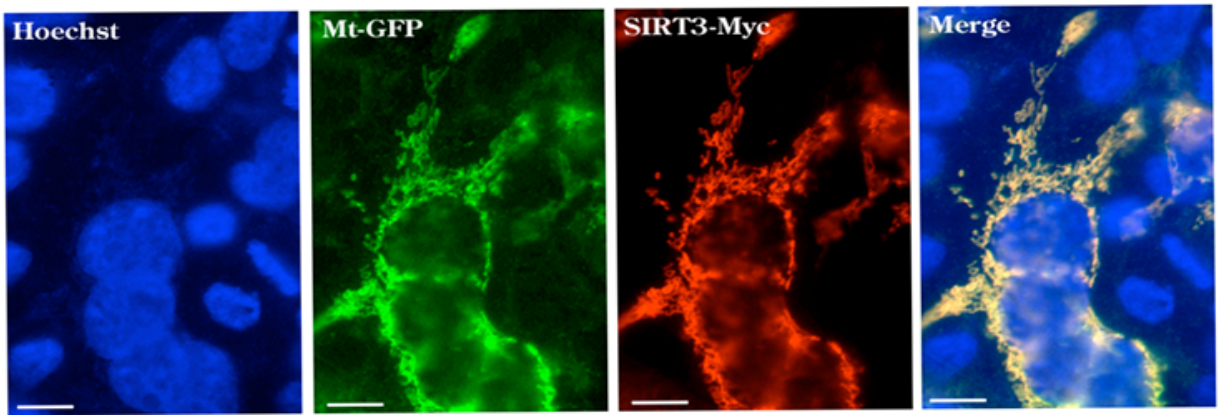
Hoechst
Mt-GFP
SIRT3-Myc
Merge

Figure 3: SIRT3 construct is targeted to mitochondria in transfected HEK-293 cells

A) SIRT3 immunofluorescence co-labels with the mitochondrial dye mitotracker-red. Triple-label immunofluorescence of HEK-293 cells transfected with SIRT3 (Green), counter-stained with mitochondrial dye mitotracker-red (Red), and the nuclei is stained with hoechst (Blue). The merged image shows co-localization between SIRT3 and mitotracker-red. There is no co-localization of SIRT3 with the nuclei staining. Images were taken with 63x objective. Bar = 10 μM.

B) SIRT3 immunofluorescence co-labels with the mitochondrial targeted GFP (Mt-GFP). Triple-label immunofluorescence of HEK-293 cells co-transfected with SIRT3 (Red) and Mt-GFP (Green), and the nuclei is stained with hoechst (Blue). The merged image shows co-localization between SIRT3 and Mt-GFP. There is no co-localization of SIRT3 with the nuclei staining. Images were taken with 63x objective. Bar = 10 μM.

Fig. 4


Positive Control
HEK-293 Naive
SIRT3-myc Transfected HEK-293
45 kDa
28 kDa
25 kDa

Figure 4: Full length 45 kDa SIRT3 construct is correctly processed into 28 kDa mature form

Representative Western blot of HEK-293 cells transiently expressing SIRT3 construct. Two immunoreactive products were detected (probed with myc antibody). The 45 kDa band represents the predicted size for the SIRT3 pro-form, whereas the 28 kDa band is the appropriate mass for the enzymatically activated SIRT3 product following post-translational cleavage. The positive control consists of a myc-tagged Grb2 plasmid.

3.2 Basal mitochondrial membrane potential is decreased in HEK-293 cells over-expressing SIRT3

Mitochondrial membrane potential ($\Delta\Psi_m$) is reduced in cells over-expressing SIRT3, however this has only been demonstrated in adipocytes (Shi et al, 2005). Thus, we assessed whether ectopical over-expression of SIRT3 would have an effect on basal $\Delta\Psi_m$ in cells other than adipocytes. Flow cytometry and a fluorescent dye rhodamine-123 were utilized to measure basal $\Delta\Psi$m in HEK-293 cells stably over-expressing SIRT3 relative to control HEK-293 cells. Rhodamine-123 is a fluorescent probe that accumulates in active mitochondria and causes cells to fluoresce proportionally to their $\Delta\Psi_m$ (Solaini et al., 2007). At high concentrations, rhodamine-123 forms aggregates resulting in quenching of the signal (Perry et al., 2011). Therefore the fluorescent signal does not fluoresce proportionally with the $\Delta\Psi_m$. To show that the concentration of rhodamine-123 used (5 μM) is not quenched, a 4x concentration of rhodamine-123 was used (depicted as the light green line in Figure 5B). Rhodamine-123 fluorescence significantly decreased in experimental cells as compared to the control cells (*$P < 0.05$) (Figure 5A; Figure 5B). This suggests that stable over-expression of SIRT3 decreases $\Delta\Psi_m$ in HEK-293 cells.

As an independent assessment, we investigated whether transient over-expression of SIRT3 decreases basal $\Delta\Psi_m$. Experimental HEK-293 cells were transiently co-transfected with SIRT3 and GFP, while the control HEK-293 cells were transiently co-transfected with β-galactosidase (to control for metabolic load) and GFP. Co-transfected cells were identified by GFP fluorescence. Flow cytometry and a fluorescent dye mitotracker deep red were utilized to measure basal $\Delta\Psi$m. Mitotracker deep red is a fluorescent dye that is able to stain active mitochondria, and its accumulation is dependent upon $\Delta\Psi_m$. The mitotracker deep red fluorescent signal was decreased significantly in experimental cells compared to that in control cells (*$P < 0.05$). These results suggest that cells transiently over-expressing SIRT3 have a lower basal $\Delta\Psi_m$

compared to the control cells transiently over-expressing β-galactosidase (Figure 6). Taken together, two independent fluorescent probes have demonstrated that over-expression of SIRT3 may regulate $\Delta\Psi_m$ under basal conditions.

Fig. 5

A)

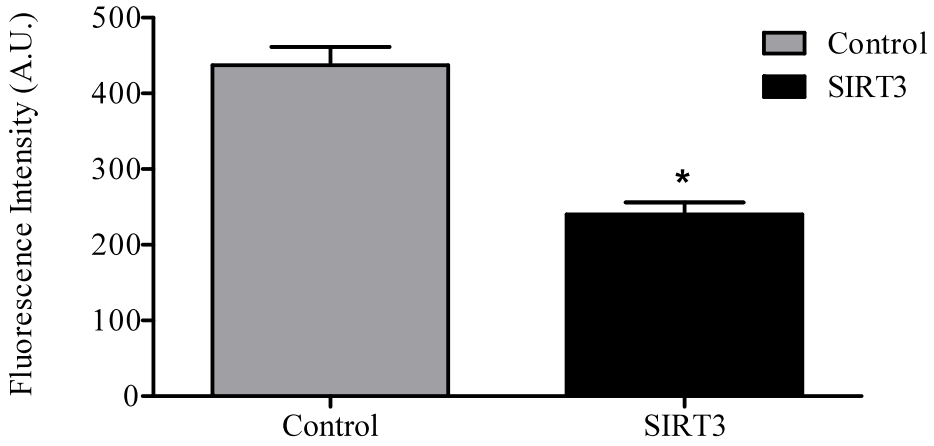
Fluorescence Intensity (A.U.)
500
400
300
200
100
0
Control
SIRT3
*
Control
SIRT3

B)

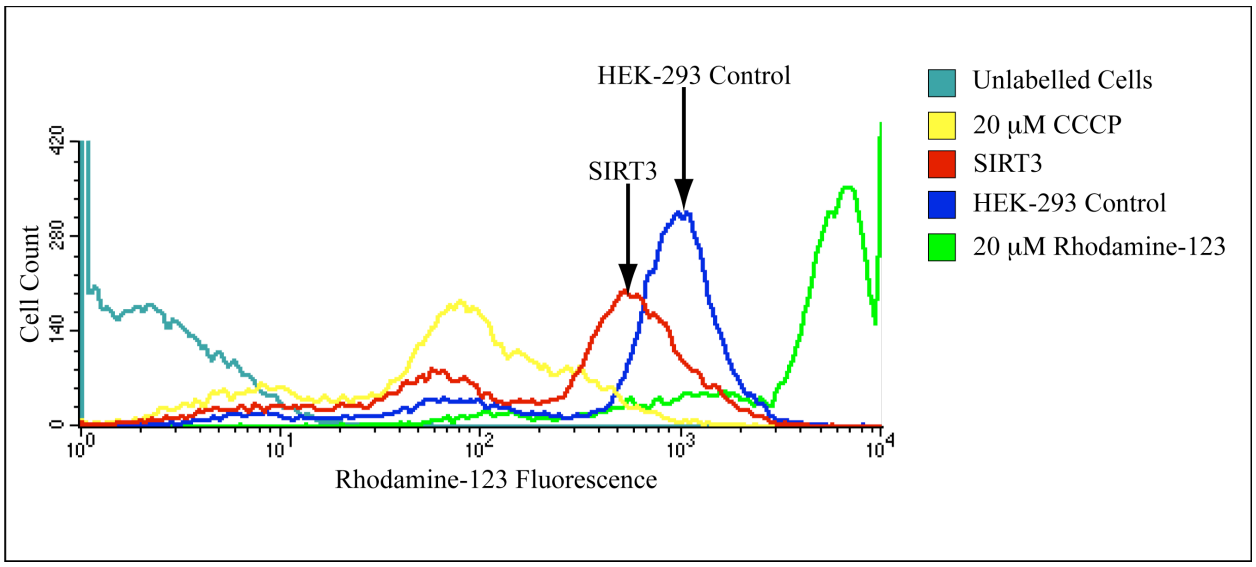
HEK-293 Control
SIRT3
Unlabelled Cells
20 µM CCCP
SIRT3
HEK-293 Control
20 µM Rhodamine-123
Cell Count
420
280
140
0
10^0
10^1
10^2
10^3
10^4
Rhodamine-123 Fluorescence

Figure 5: Basal mitochondrial membrane potential is decreased in HEK-293 cells stably over-expressing SIRT3

A) Cumulative results of arbitrary fluorescence units (A.U) represented by rhodamine-123 fluorescence intensity in HEK-293 cells stably over-expressing SIRT3 and in control HEK-293 cells. Cells over-expressing SIRT3 have significantly lower basal $\Delta\Psi_m$ (decreased rhodamine-123 fluorescence) compared to control cells (n=3, * denotes statistical significance at $P < 0.05$, non-paired, two-tailed Student's *t*-test, error bars shown are ± SEM).

B) Representative flow cytometry histogram of rhodamine-123 fluorescence intensity in HEK-293 cells stably over-expressing SIRT3 (Red line) and in control HEK-293 cells (Blue line). There is a left-shift in rhodamine-123 fluorescent intensity profile in cells over-expressing SIRT3, indicative of a lower $\Delta\Psi_m$ compared to control cells. The light green line represents a high dose of rhodamine-123 (20 μM) and the dark green line represents unlabelled cells that depict auto-fluorescence.

Fig. 6

A)

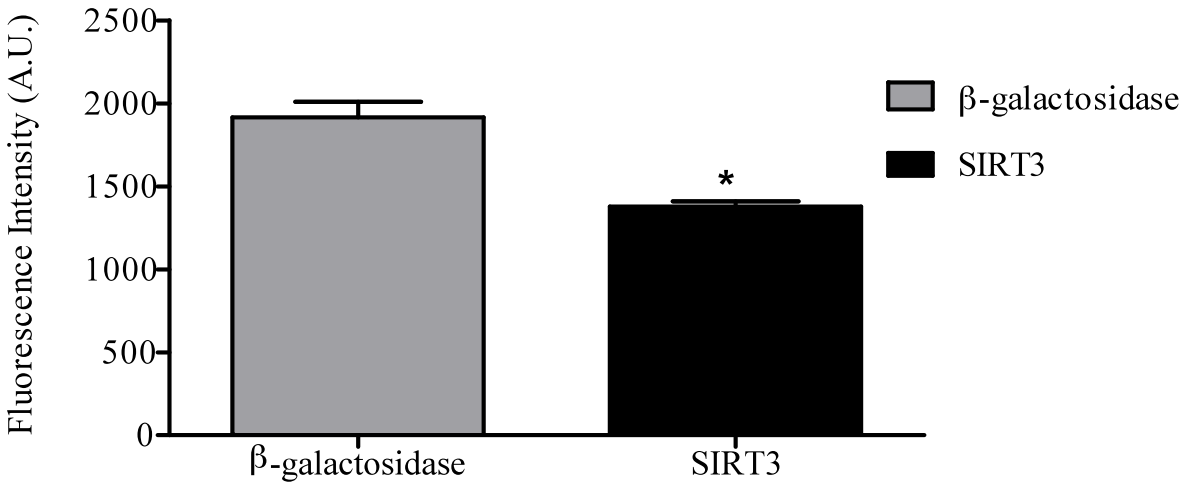
Fluorescence Intensity (A.U.)
2500
2000
1500
1000
500
0
β-galactosidase
SIRT3
*
β-galactosidase
SIRT3

B)

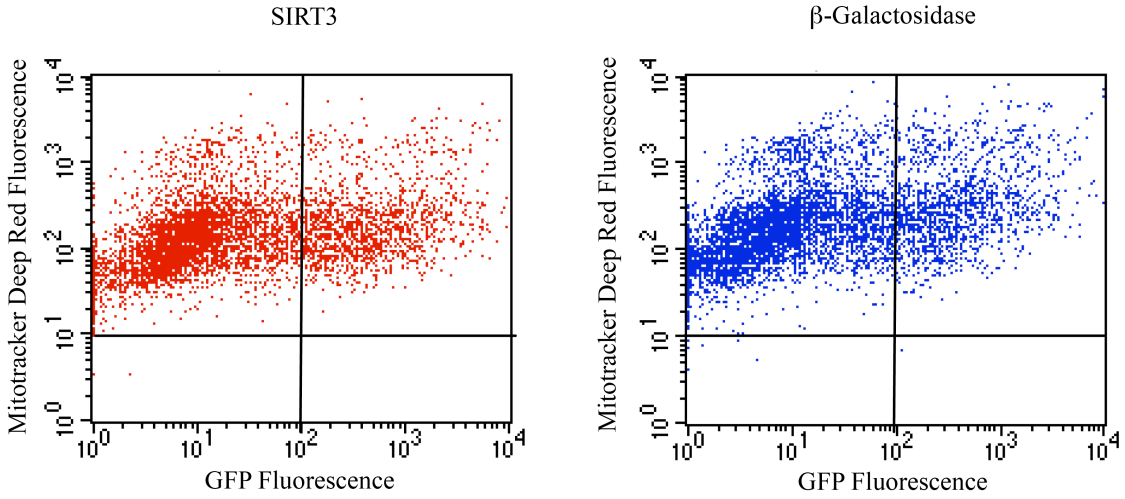
SIRT3
β-Galactosidase
Mitotracker Deep Red Fluorescence
GFP Fluorescence
Mitotracker Deep Red Fluorescence
GFP Fluorescence

Figure 6: **Basal mitochondrial membrane potential is decreased in HEK-293 cells transiently over-expressing SIRT3**

A) Cumulative results of arbitrary fluorescence units (A.U) represented by mitotracker deep red fluorescence intensity in HEK-293 cells over-expressing SIRT3 and control HEK-293 cells over-expressing β-galactosidase. Cells over-expressing SIRT3 have significantly lower basal $\Delta\Psi_m$ (decreased mitotracker deep red fluorescence) compared to control cells (n=3, *P < 0.05, non-paired, two-tailed Student's *t*-test, error bars shown are ± SEM).

B) Representative two parameter histogram dot plot displays GFP intensity on the x axis vs. mitotracker deep red intensity on the y axis. Upper Right (UR) quadrant depicts GFP positive HEK-293 cells, which represent cells expressing SIRT3 (Red Dot Plot) or β-galactosidase (Blue Dot Plot). There is a down-shift in the mitotracker deep red intensity profile in cells over-expressing SIRT3, indicative of a lower $\Delta\Psi_m$ compared to control cells.

3.3 Basal reactive oxygen species levels are decreased in HEK-293 cells stably over-expressing SIRT3

Although SIRT3 targets substrates that are involved in regulating anti-oxidative systems, only a few reports have assessed whether SIRT3 over-expression affects the production of ROS under basal conditions (Bell et al., 2011; Kong et al 2010; Shi et al, 2005). These studies have demonstrated that SIRT3 over-expression reduces basal ROS levels in adipocytes, myocardium cells and mouse embryonic fibroblasts (MEFs). Previous studies show that ROS genesis is closely linked to $\Delta\Psi_m$, and that its partial reduction correlates with lower ROS levels. The results described above indicate that $\Delta\Psi_m$ is reduced in cells over-expressing SIRT3 (Figure 5; Figure 6). Therefore, we investigated whether the observed decrease in basal ROS levels, would extend to HEK-293 cells. Flow cytometry and a fluorescent dye 5-(and-6)chloromethyl-2',7'dichlorohydrofluoresceindiacetate (DCF) were utilized to measure basal ROS levels in experimental cells vs. control cells. DCF is sequestered inside the cell where it gets cleaved by esterases, converting it to a fluorescent form (Armstrong & Whiteman, 2007). Thus, DCF fluorescence is proportional to ROS levels within the cell. Indeed the results demonstrated that HEK-293 cells stably over-expressing SIRT3 have lower basal ROS levels compared to that in the control cells ($^*P < 0.05$) (Figure 7).

Fig. 7

A)

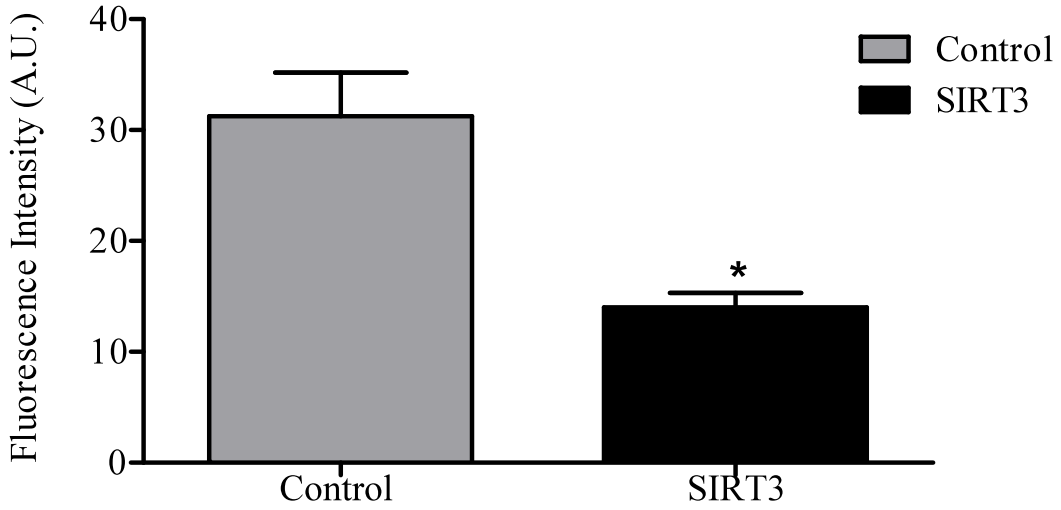
Fluorescence Intensity (A.U.)
40
30
20
10
0
Control
SIRT3
*
Control
SIRT3

B)

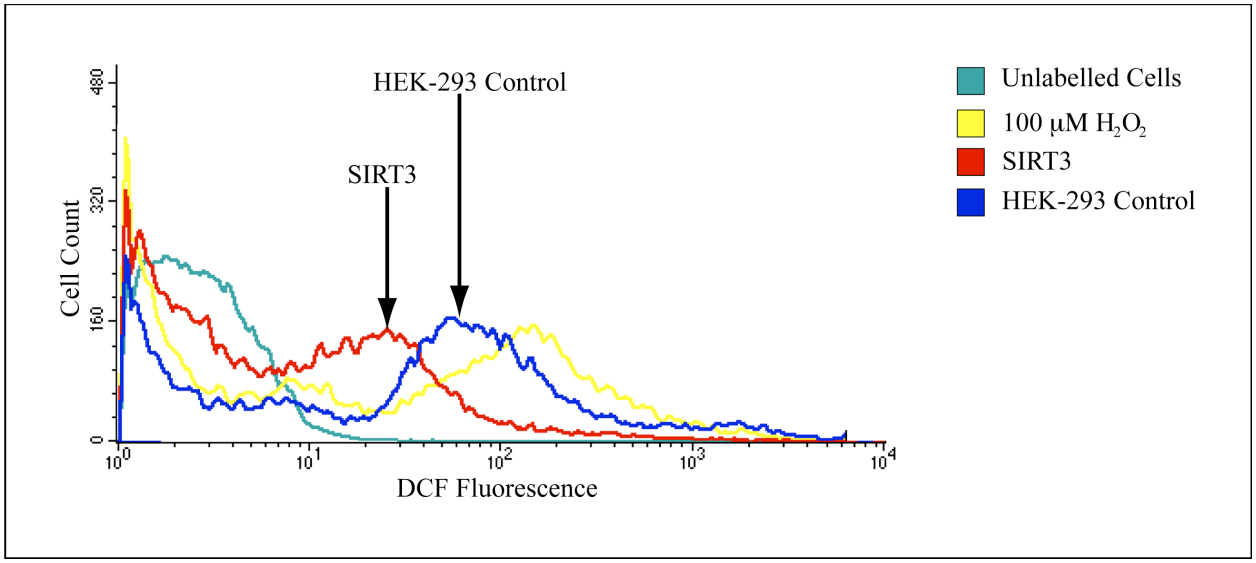
HEK-293 Control
SIRT3
Cell Count
480
320
160
0
10^0
10^1
10^2
10^3
10^4
DCF Fluorescence
Unlabelled Cells
100 μM H_2O_2
SIRT3
HEK-293 Control

Figure 7: Basal ROS levels are decreased in HEK-293 cells stably over-expressing SIRT3

A) Cumulative results of arbitrary fluorescence units (A.U) represented by DCF fluorescence intensity in HEK-293 cells stably over-expressing SIRT3 and in control HEK-293 cells. Cells over-expressing SIRT3 have significantly lower basal ROS levels (decreased DCF fluorescence) compared to control cells (n=3, * denotes statistical significance at $P < 0.05$, non-paired, two-tailed Student's *t*-test, error bars shown are ± SEM).

B) Representative flow cytometry histogram of DCF fluorescence intensity in HEK-293 cells stably over-expressing SIRT3 (Red line) and in control cells (Blue line). There is a left-shift in the DCF fluorescence intensity profile in cells over-expressing SIRT3, indicative of lower intracellular ROS concentration compared to control cells. The yellow line represents positive control (100 μM H_2O_2) and the dark green line represents unlabelled cells that depict auto-fluorescence.

3.4 HEK-293 cells over-expressing SIRT3 do not have elevated basal PGC-1α mRNA levels

Over-expression of SIRT3 increases phosphorylation of cAMP-response element binding protein (CREB) in adipocytes (Shi et al, 2006) and AMP-activated protein kinase (AMPK) in murine skeletal muscle (Palacious, 2009). Phosphorylation of CREB and AMPK are associated with induction of peroxisome proliferator-activated receptor-gamma co-activator 1 alpha (PGC-1α). PGC1-α is a transcription factor, which regulates a host of metabolic and antioxidant genes in mitochondria. Furthermore, PGC-1α increases expression of uncoupling proteins (UCPs), which play a role in dissipating the proton gradient and ultimately resulting in a decrease of the $\Delta\Psi_m$, and ROS levels. Indeed, Shi et al (2006) has demonstrated that adipocytes over-expressing SIRT3 have elevated UCP1 levels.

Our results show that HEK-293 cells over-expressing SIRT3 have lower basal $\Delta\Psi_m$ (Figure 5; Figure 6) as well as lower basal ROS levels (Figure 7). Therefore, we further investigated whether ectopic over-expression of SIRT3 has an effect on PGC-1α at the transcriptional level. Quantitative real time PCR (qRT-PCR) was used to assess whether at basal conditions PGC-1α mRNA levels are higher in HEK-293 cells over-expressing SIRT3 compared to that in HEK-293 control cells. The relative PGC-1α expression levels were then calculated by comparison with the level of the housekeeping gene, GAPDH. However, no significant difference was apparent in PGC-1α mRNA levels between the two cell lines (Figure 8). The results suggest that at least at the mRNA level, SIRT3 may not regulate PGC-1α expression.

Fig. 8

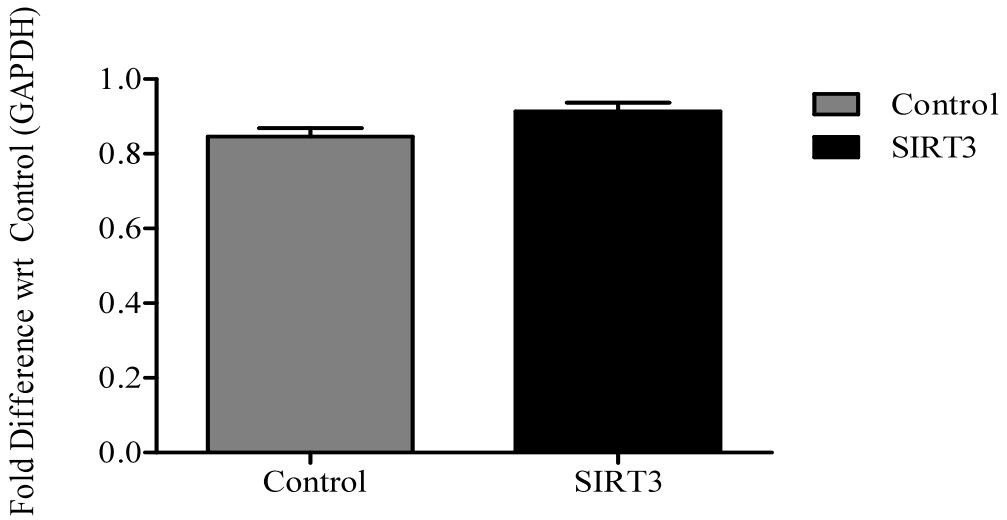
Fold Difference wrt Control (GAPDH)
1.0
0.8
0.6
0.4
0.2
0.0
Control
SIRT3
Control
SIRT3

Figure 8: HEK-293 cells over-expressing SIRT3 do not have elevated basal PGC-1α mRNA levels

Quantitative real time PCR results show that during basal conditions there was no significant difference in PGC-1α mRNA expression between SIRT3 stable over-expressing cells compared to that of control HEK-293 cells (relative to GAPDH) (n= 3, ns , non-paired, two-tailed Student's *t*-test, error bars shown are ± SEM).

3.5 SIRT3 over-expression renders HEK-293 cells less sensitive to glucose deprivation insult

Because cells over-expressing SIRT3 displayed reduced ROS levels under basal conditions (Figure 7), we investigated whether over-expressing SIRT3 renders cells less sensitive to glucose deprivation (GD)-induced cell death. GD is an oxidative insult that causes an elevation in mitochondrial ROS (Blackburn et al, 1999).

Experimental HEK-293 cells were co-transfected with SIRT3 and a GFP plasmid, and control HEK-293 cells were co-transfected with GFP and β-galactosidase (to control for metabolic load). Co-transfected cells were identified by GFP fluorescence. Random pictures were taken at 0, 1, and 3 hours post GD. Propidium iodide (PI) was used to identify dead cells. Compromised membranes in dead cells become permeabilized, and allow PI inside to stain dead nuclei. Following 3 hours of GD there was significantly lower percentage of PI positive cells over-expressing SIRT3 compared to that of the control cells (*$P < 0.05$) (Figure 9B). After 3 hours of GD, normal culturing medium was reintroduced back into the cells for 24 hours. Reintroducing media to glucose-deprived cells is a paradigm known as glucose reperfusion (GR). GR has been demonstrated to rapidly increase ROS levels through mechanisms that are not fully understood (Suh et al, 2007). Following 24 hours of GR, cells transiently over-expressing SIRT3 had significantly lower percentage of PI positive cells compared to that of the control cells (*$P < 0.05$). These data indicate that SIRT3 over-expression renders cells less sensitive to oxidative insults such as GD and GR.

Fig. 9

A)

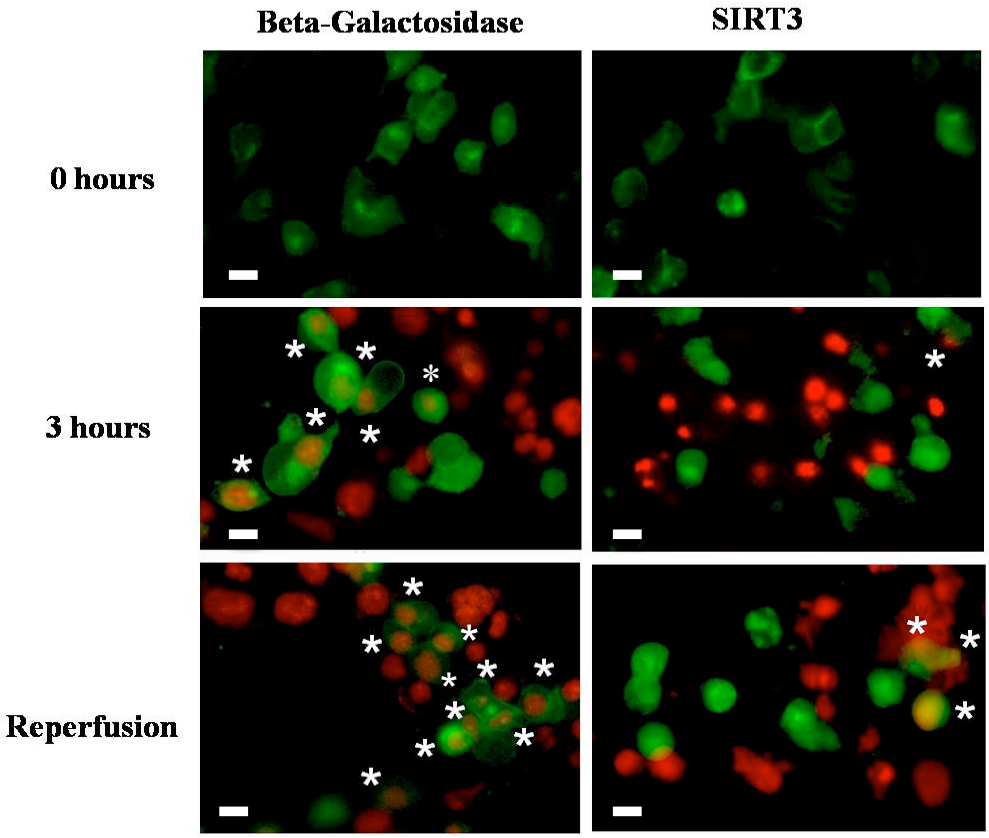
Beta-Galactosidase
SIRT3
0 hours
3 hours
Reperfusion

B)

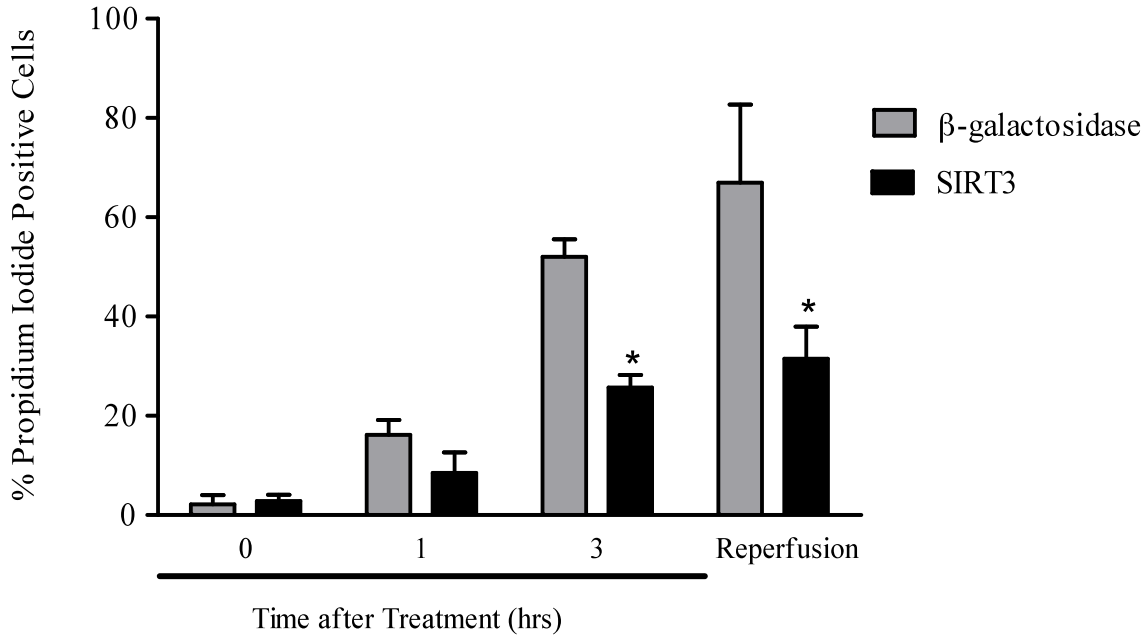
% Propidium Iodide Positive Cells
100
80
60
40
20
0
0
1
3
Reperfusion
Time after Treatment (hrs)
β-galactosidase
SIRT3

Figure 9: HEK-293 cells over-expressing SIRT3 are less sensitive to glucose deprivation

A) Dual-label confocal images of HEK-293 co-expressing GFP plasmid (Green) and either SIRT3 (experimental cells) or β-galactosidase (control cells). Dead/dying cells are identified by PI staining (Red). Displayed images were taken at the onset of GD (0 hours) and 3 hours post GD, or after 24 hours of reperfusion. Cells that are transfected and viable are GFP positive, and transfected dying/dead cells are both GFP and PI positive (represented by asterisks). There are fewer double-stained cells in the SIRT3 panel compared to that in the control panel. Images were taken at 20X magnification. Bar = 10 μM.

B) Bar graph shows the mean percentage of PI positive HEK-293 cells over-expressing SIRT3 or β-galactosidase at 0 hours, 1 hour and 3 hours post GD or following 24 hours of reperfusion. At 3 hours and following reperfusion there is a lower percentage of cells transfected with SIRT3 that are PI positive than that of cells expressing β-galactosidase (n=3, * denotes statistical significance at $P < 0.05$, two-way ANOVA analysis using % of PI positive cells and time as factors, Bonferonni post-hoc test, error bars shown are ± SEM).

3.6 HEK-293 cells transiently over-expressing SIRT3 are less sensitive to acute hydrogen peroxide insult

A potent oxidant H_2O_2 (500 μm) was used to assess whether ectopic over-expression of SIRT3 would render HEK-293 cells less sensitive to direct oxidative-stress. Experimental HEK-293 cells were co-transfected with SIRT3 and GFP, and control HEK-293 cells were co-transfected with GFP and β-galactosidase (to control for metabolic load). Co-transfected cells were identified by GFP fluorescence. PI was used to identify dead cells, at 0, 6, 12 and 24 hours following treatment with 500 μM of H_2O_2. Indeed, experimental cells had significantly lower percentage of PI positive cells than that of the control cells at 12 and 24 hours post treatment with 500 μM of H_2O_2 (*$P < 0.05$) (Figure 10B). These data indicate that SIRT3 over-expression renders cells less sensitive to H_2O_2-induced cell death.

Fig. 10

A)

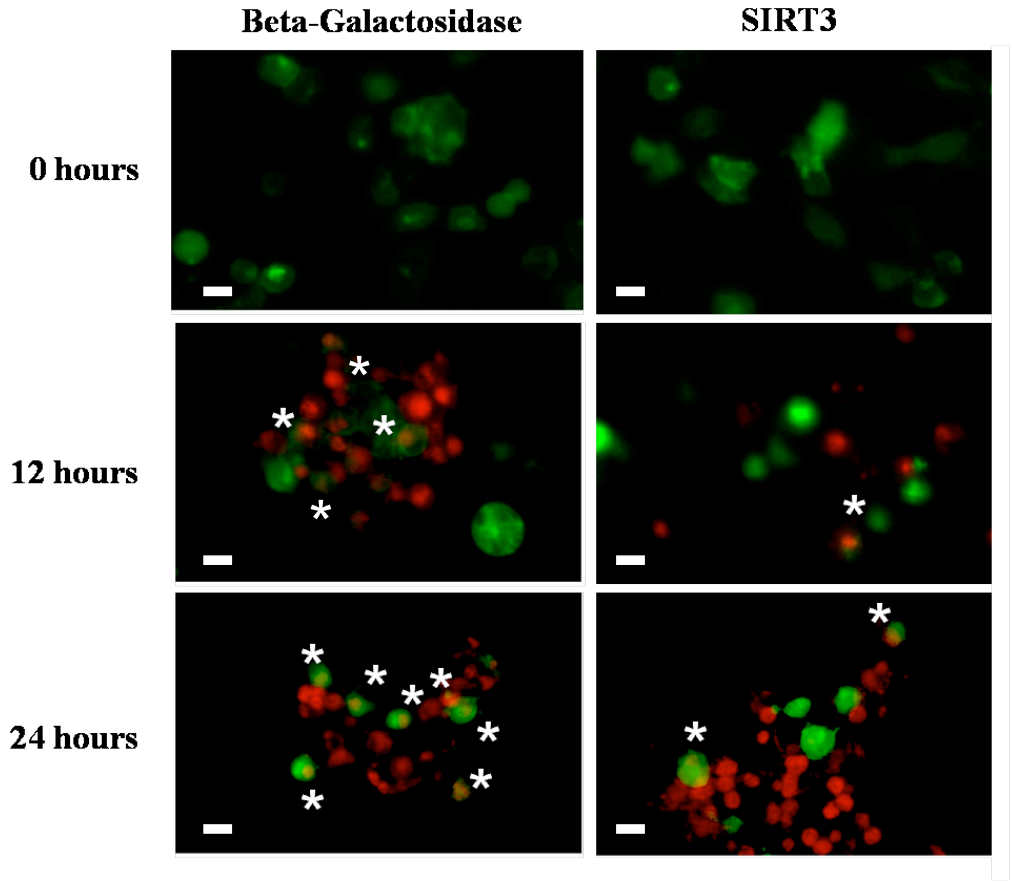
Beta-Galactosidase
SIRT3
0 hours
12 hours
24 hours

B)

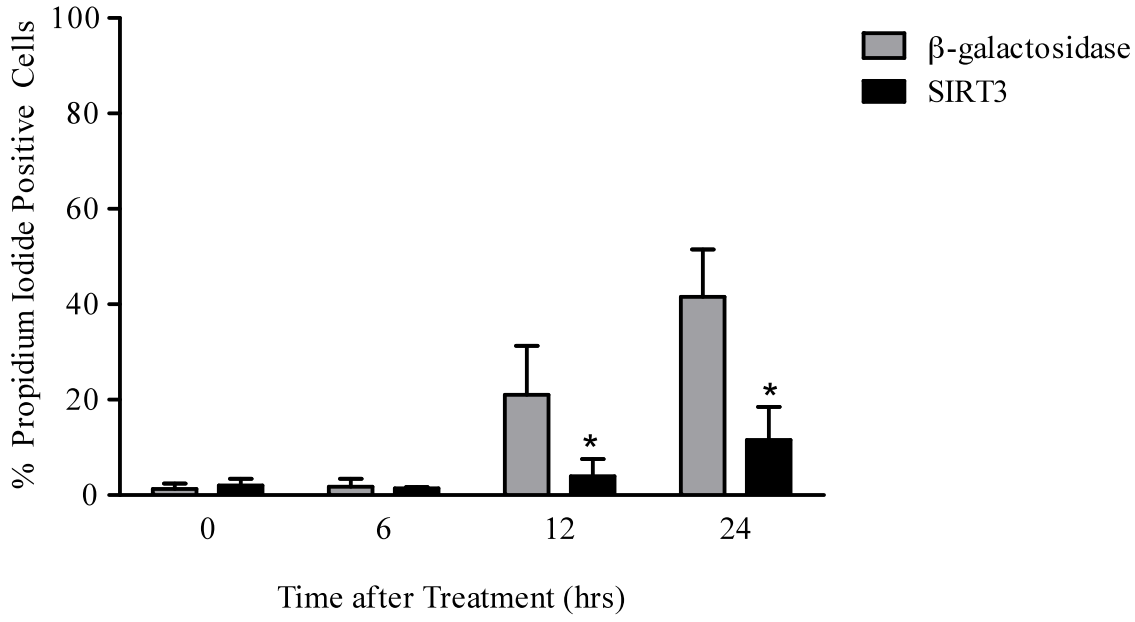
% Propidium Iodide Positive Cells
100
80
60
40
20
0
0
6
12
24
Time after Treatment (hrs)
β-galactosidase
SIRT3
*
*

Figure 10: HEK-293 cells over-expressing SIRT3 are less sensitive to hydrogen peroxide (500 μM)

A) Dual-label confocal images of HEK-293 co-expressing GFP plasmid (Green) and either SIRT3 (experimental cells) or β-galactosidase (control cells). Dead/dying cells are identified by PI staining (Red). Displayed images were taken at the onset (0 hours) and at 12 and 24 hours post a single challenge with H_2O_2. Cells that are transfected and viable are GFP positive, and transfected dying/dead cells are GFP and PI positive (represented by asterisks). There are fewer double-stained cells in the SIRT3 panel compared to the control panel. Images were taken at 20X magnification. Bar = 10 μM.

B) Bar graph shows the mean percentage of PI positive HEK-293 cells over-expressing SIRT3 or β-galactosidase at 0 hours, 6 hours, 12 hours and 24 hours post a single challenge with H_2O_2. At 12 hours and 24 hours there is a lower percentage of cells expressing SIRT3 that are PI positive than that of control cells (n=3, * denotes statistical significance at $P < 0.05$, two-way ANOVA analysis using % of PI positive cells and time as factors, Bonferonni post-hoc test, error bars shown are ± SEM).

3.7 SIRT3 over-expression decreases proliferation rates of HEK-293 cells

Caloric restriction (CR) is a dietary regimen that has been demonstrated to increase lifespan in mammals. In addition, CR can slow cell proliferation rates and attenuate ROS production **(**Hagopian, 2005; Martín-Montalvo et al., 2011). Indeed, SIRT3 levels are upregulated by CR (Shi et al., 2005). Our data demonstrates that ectopic over-expression of SIRT3 reduced ROS under basal conditions (Figure 7). Given the potential link between CR, cell proliferation and ROS levels, it was assessed whether over-expression of SIRT3 would have an effect on cell proliferation rates. The results revealed that at 48 hours in culture, HEK-293 cells stably over-expressing SIRT3 were proliferating slower than control HEK-293 cells ($*P < 0.05$) (Figure 11). This suggests that SIRT3 over-expression plays a regulatory role in cell proliferation rates.

Fig. 11

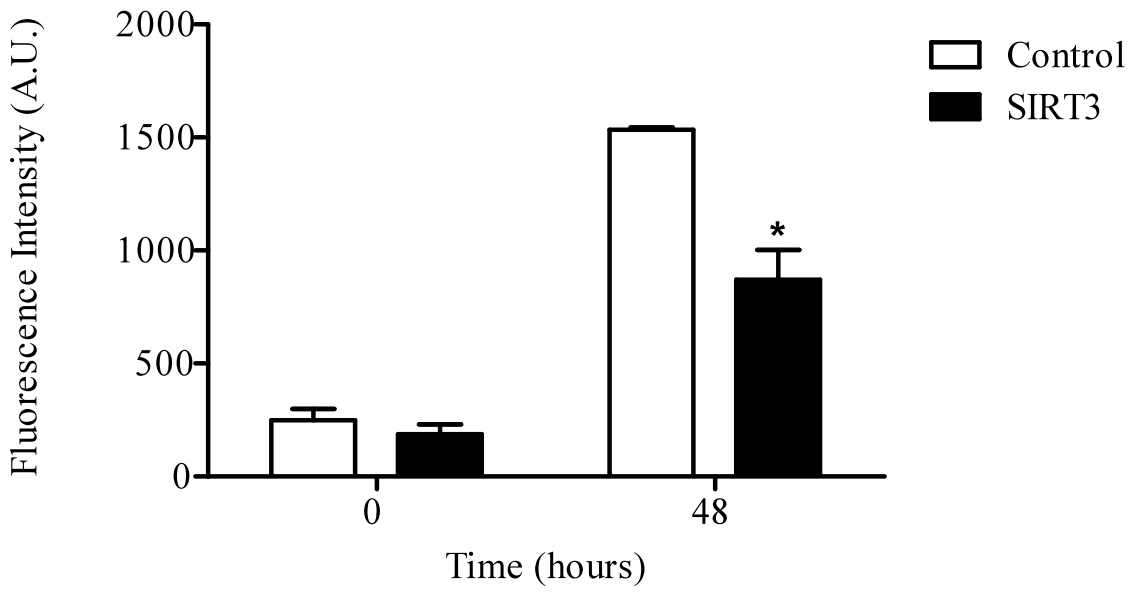
Fluorescence Intensity (A.U.)
2000
1500
1000
500
0
0
48
Time (hours)
*
Control
SIRT3

Figure 11: SIRT3 stable over-expression decreases proliferation rates of HEK-293 cells

Cumulative cell count of HEK-293 cells stably over-expressing SIRT3 and control HEK-293 cells represented by arbitrary fluorescence units (A.U) of CyQuant dye fluorescence intensity at 0 hours and after 48 hours in culture. Cells stably over-expressing SIRT3 had a significantly lower cell count (lower CyQuant dye fluorescence intensity) compared to control cells at the 48 hour time-point (n=3, * denotes statistical significance at $P < 0.05$, non-paired, two-tailed Student's *t*-test, error bars shown are ± SEM).

3.8 Assessment of SIRT1 and SIRT3 mRNA expression levels in mouse and rat tissue

3.8.1 SIRT3 mRNA is expressed at higher levels than SIRT1 mRNA levels in the peripheral and central nervous system

Collectively, the results presented above suggest that SIRT3 resides in mitochondria (Figure 3) and its ectopic over-expression results in a reduction of basal $\Delta\Psi_m$ (Figure 5; Figure 6) and ROS levels (Figure 7). SIRT3 over-expression also renders HEK-293 cells less sensitive to oxidative-type insults (Figure 10; Figure 11). Taken together, these results suggest that over-expression of SIRT3 plays a cytoprotective role, which raises the possibility that these effects may extend to the cells in the central nervous system (CNS). However, to date no studies have quantified SIRT3 expression levels in brain tissue.

In order to fully understand the functional role of SIRT3 in the brain, we need to investigate its expression profile. Of the seven mammalian sirtuins, SIRT1 has been the most extensively studied in the brain. Numerous reports have demonstrated that SIRT1 over-expression is neuroprotective in models of amyotropic lateral sclerosis and Alzheimer's disease (Kim et al, 2007). Thus, we sought to compare SIRT3 expression pattern to the extensively studied SIRT1. However, no studies have quantified the expression of endogenous SIRT1 within the brain.

To address this issue, quantitative real-time polymerase chain reaction (qRT-PCR) was used to investigate relative mRNA expression profiles of SIRT1 and SIRT3 in the brain as well as in peripheral tissues. Two age-groups of the wild-type mice were used (3 and 24 month-old), as it is conceivable that expression profiles of these sirtuins may change as a function of age. Developing rats and mice reach the adult stage at about 3 months of age, and the 24 month-old animals are classified as aged. The relative gene expression levels were then calculated by comparison with the level of the housekeeping gene, HPRT1.

First, the mRNA levels of SIRT3 and SIRT1 in peripheral tissues such as lung, liver, heart, kidney, and intestine were assessed. qRT-PCR data showed that in both age groups, SIRT3 mRNA is expressed at higher levels than SIRT1 mRNA levels in the heart, kidney and in the liver samples (*P < 0.05) (Figure 12). Additionally, there was no significant age-dependent difference in either SIRT1 and SIRT3 mRNA levels in any of the peripheral tissues examined.

To investigate SIRT3 and SIRT1 mRNA expression levels in the CNS, whole brain samples were derived from 3 and 24 month-old mice. In both of the age groups, SIRT3 mRNA levels were significantly higher than that of SIRT1 mRNA levels (Figure 13). There was no significant difference in SIRT1 mRNA expression levels in 3 month-old whole brain samples compared to that of the 24 month-old whole brain samples. On the other hand, SIRT3 mRNA expression levels were significantly higher in the 24 month than that of the 3 month-old whole brain samples (*P < 0.05). These results suggest that SIRT3 mRNA levels increase as the brain ages.

Furthermore, SIRT3 and SIRT1 mRNA endogenous levels were assessed in hippocampal, striatal and cerebellar brain regions in 3 and 24 month-old mice (Figure 14). In all of the regions investigated SIRT3 mRNA was consistently expressed at significantly higher levels than that of SIRT1 mRNA levels (*P < 0.05). However, there were no age-dependent differences in either SIRT1 or SIRT3 mRNA levels in any of the brain regions examined.

3.8.2 SIRT3 protein levels are expressed at higher levels in peripheral tissues than in the brain of 3 month-old rats

To assess SIRT3 protein levels in wild-type rat brain regions (cortex, cerebellum, striatum, hippocampus) and other tissues (heart and kidney), Western blot was performed (Figure 15). SIRT3 protein levels were significantly higher in the heart compared to the levels in the cortex, cerebellum and striatum (*P < 0.05). SIRT3 levels in the kidney were significantly higher than

that in the cortex and cerebellum (# $P < 0.05$). However, no significant differences were found between SIRT3 protein levels in the hippocampus compared to the rest of the tissues examined.

Fig. 12

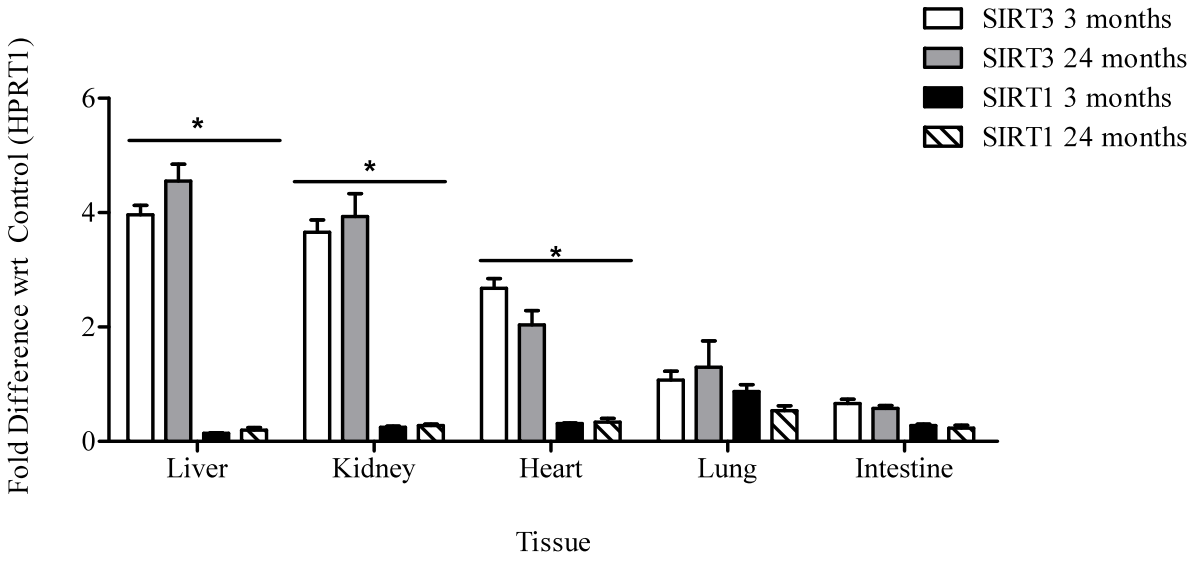
SIRT3 3 months
SIRT3 24 months
SIRT1 3 months
SIRT1 24 months
Fold Difference wrt Control (HPRT1)
6
4
2
0
*
*
*
Liver
Kidney
Heart
Lung
Intestine
Tissue

Figure 12: SIRT3 mRNA is expressed at higher levels than SIRT1 mRNA levels in peripheral tissues of 3 and 24 month-old wild-type mice

Bar graph shows qRT-PCR data for endogenous SIRT3 mRNA levels compared to SIRT1 mRNA levels in the heart, liver, kidney, lung and intestine of 3 and 24 month-old mouse tissues (relative to HPRT1). SIRT3 mRNA was expressed at significantly higher levels than that of SIRT1 mRNA in the heart, kidney as well as liver in both age groups (n= 4, * denotes statistical significance at $P < 0.05$ compared between all peripheral tissues, one way ANOVA with Bonferonni *post-hoc* test, error bars shown are ± SEM).

Fig. 13

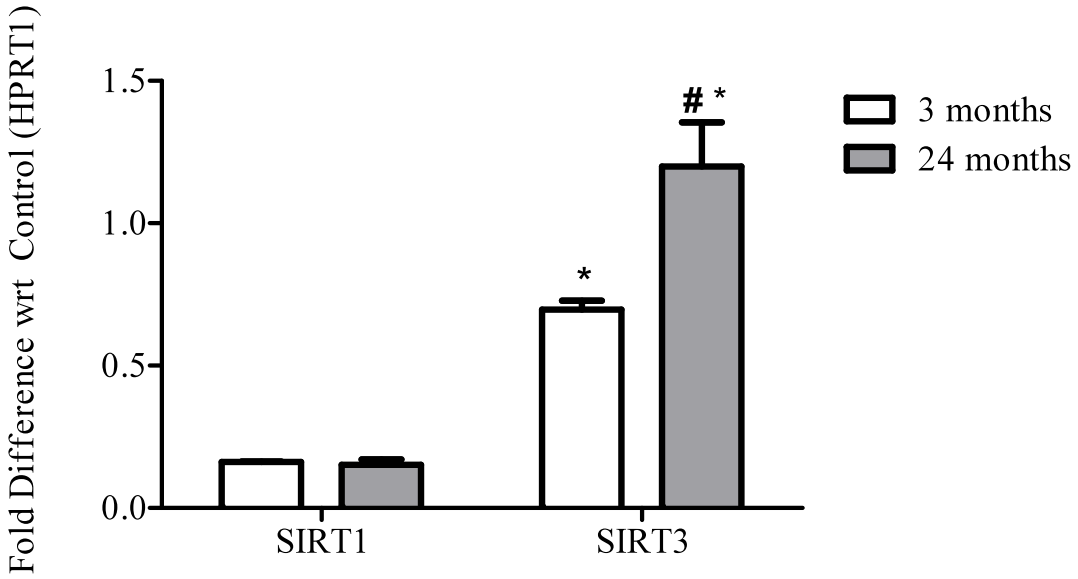
Fold Difference wrt Control (HPRT1)
1.5
1.0
0.5
0.0
*
*
SIRT1
SIRT3
3 months
24 months

Figure 13: SIRT3 mRNA expression levels are higher in the whole brain of 24 months old wild-type mice compared to that of 3 months old mice

Bar graph shows qRT-PCR data for SIRT3 mRNA expression levels compared to SIRT1 mRNA expression levels in the whole brain tissue of 3 month and 24 month-old mice (relative to HPRT1). SIRT3 mRNA was expressed at significantly higher levels in the 24 month-old mice than that in the whole brain tissues of 3 month-old mice (#$P < 0.05$). In both age groups SIRT3 mRNA levels were higher than that of SIRT1 mRNA levels (*$P < 0.05$) (n= 4, * and # denote statistical significance at $P < 0.05$, non-paired, two-tailed Student's *t*-test, error bars shown are ± SEM).

Fig. 14

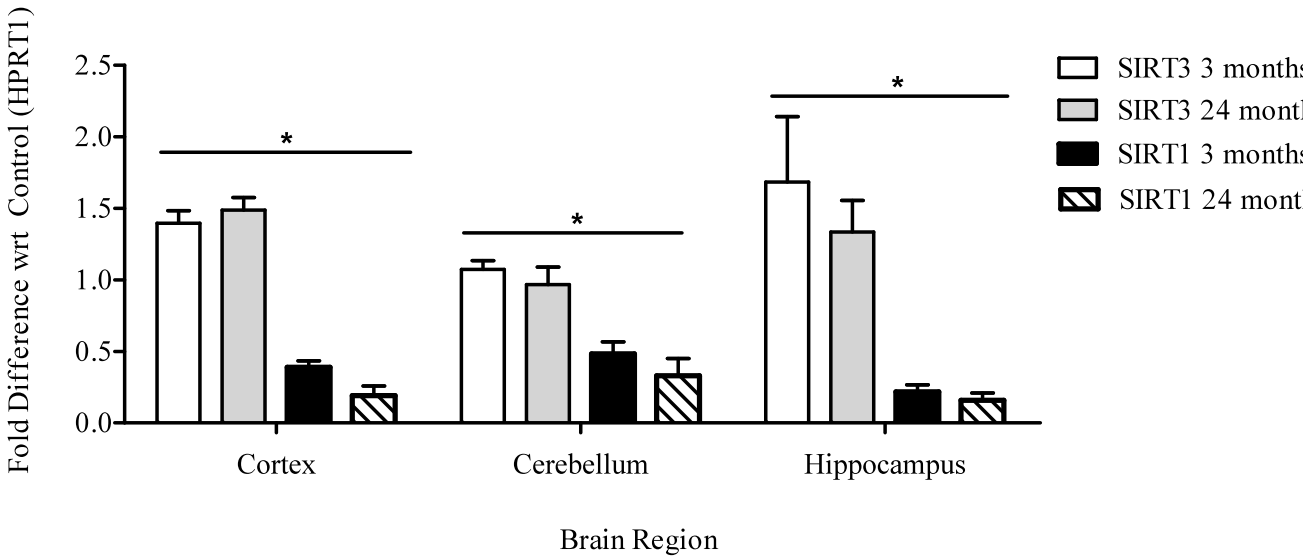
Fold Difference wrt Control (HPRT1)
2.5
2.0
1.5
1.0
0.5
0.0
*
*
*
Cortex
Cerebellum
Hippocampus
Brain Region
SIRT3 3 months
SIRT3 24 month
SIRT1 3 months
SIRT1 24 month

Figure 14: SIRT3 mRNA expression levels are higher than SIRT1 mRNA levels in the cortex, cerebellum and hippocampus of 3 and 24 month-old wild-type mice

Bar graph shows qRT-PCR data for SIRT3 mRNA expression levels compared to SIRT1 mRNA expression levels in the cortex, cerebellum and hippocampus of 3 and 24 month-old wild-type mouse tissues (relative to HPRT1). In both age groups SIRT3 mRNA was expressed at higher levels than that of SIRT1 mRNA levels in all regions examined. There were no significant differences in either SIRT3 or SIRT1 mRNA levels between the two age groups (n= 4, * denotes statistical significance at $P < 0.05$, one way ANOVA with Bonferonni *post-hoc* test, error bars shown are ± SEM).

Fig 15

A)

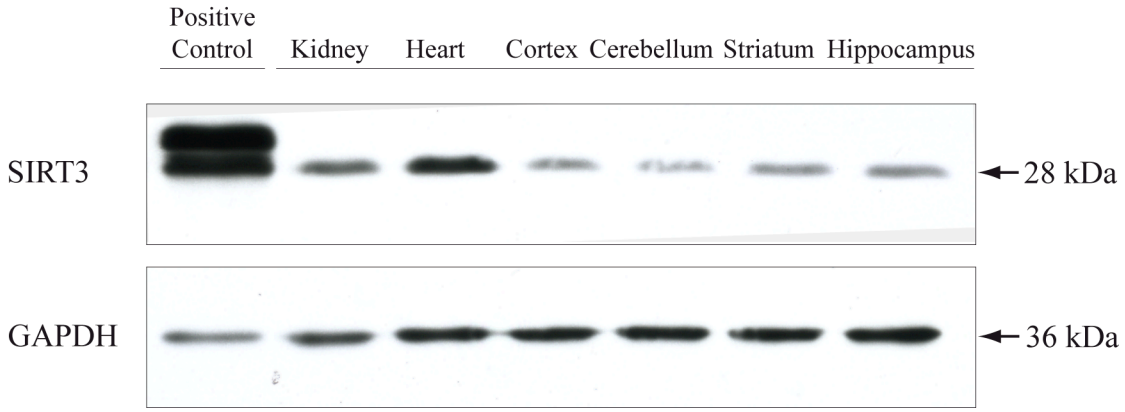
Positive Control
Kidney
Heart
Cortex
Cerebellum
Striatum
Hippocampus
SIRT3
28 kDa
GAPDH
36 kDa

B)

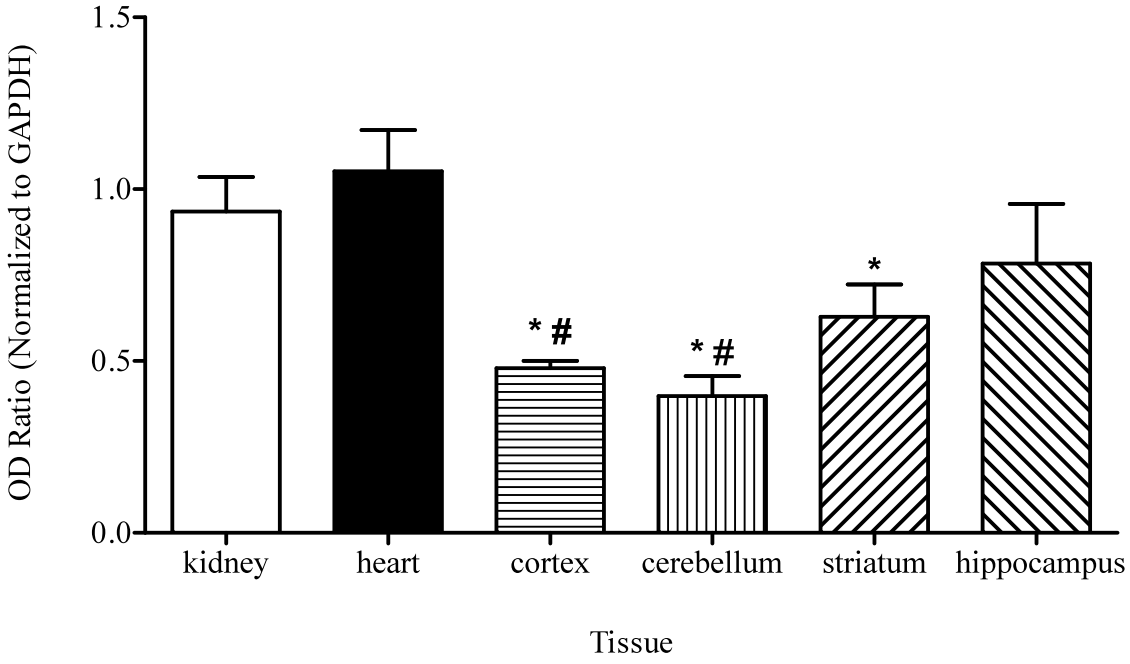
OD Ratio (Normalized to GAPDH)
1.5
1.0
0.5
0.0
* #
* #
*
kidney
heart
cortex
cerebellum
striatum
hippocampus
Tissue

Figure 15: SIRT3 protein expression levels are higher in peripheral tissues than in the brain of 3 month-old wild-type rats

A) Representative Western blot of endogenous SIRT3 expression levels in the kidney, heart, cortical, cerebellar, striatal and hippocampal regions of adult rats (3 month-old). GAPDH was used as a loading control.

B) Bar graph shows densitometric data for SIRT3 protein expression levels in 3 month-old rat regions. Values represented are means of OD ratio between all samples normalized against GAPDH. SIRT3 protein was significantly expressed at a higher level in the heart compared to the SIRT3 levels in the cortex, cerebellum and striatum (*$P < 0.05$). SIRT3 protein was significantly expressed at a higher level in the kidney compared to that of levels in the cortex and cerebellum (#$P < 0.05$). There were no significant differences in SIRT3 protein levels in the hippocampus compared to that of the other tissues examined. The positive control consists of HEK-293 cells over-expressing SIRT3 (n= 3, * and # denote statistical significance at $P < 0.05$, one way ANOVA with Bonferonni *post-hoc* test, error bars shown are ± SEM).

3.9 Assessment of SIRT3 mRNA and protein expression levels throughout developing and aging brain regions

3.9.1 SIRT3 mRNA expression levels increase in the hippocampus and in the striatum of the developing rat brain

To date, no studies have examined expression profile of SIRT3 or SIRT1 at different stages of brain development. SIRT3 and SIRT1 mRNA expression profiles were quantified throughout the developmental course of 1 week, 3 weeks, and 3 months in wild-type rat brain regions, and in the aged 24 month-old rats. qRT-PCR was used to measure SIRT3 and SIRT1 mRNA levels in cortical, hippocampal, striatal and cerebellar regions. In the hippocampus, 3 week-old rats had significantly higher SIRT3 mRNA levels compared to that in 1 week-old rats, and these levels remained constant throughout the development after the 3 week time-point (*$P < 0.05$). SIRT3 mRNA levels in the striatum increased significantly in the 24 month-old rats (*$P < 0.05$). There was no significant change in SIRT3 mRNA levels in the cortical or the cerebellar regions between any of the age groups examined (Figure 16A). On the other hand, SIRT1 mRNA levels in the cortex, hippocampus and striatum decreased significantly in the 3 week-old rats from their levels of 1 week and remained constant (*$P < 0.05$) (Figure 16B). In the cerebellum, SIRT1 mRNA decreased significantly in the 3 month-old rats (*$P < 0.05$). Taken together, these data show that the mRNA expression profiles of SIRT3 and SIRT1 are age and brain region dependent.

3.9.2 SIRT3 protein expression levels increase in the cortex, hippocampus and cerebellum of the developing rat brain

To assess whether the observed age-dependent changes in the SIRT3 mRNA levels correspond to the protein levels**,** Western blotting was used to measure SIRT3 protein levels in the cortex, hippocampus and cerebellum. SIRT3 protein levels were quantified throughout the developmental course of 1 week, 3 weeks, and 3 month-old rats and in the aged (24 month-old)

rats. Because mRNA analysis cannot distinguish between the pro- and processed forms of SIRT3, the SIRT3 protein levels were analyzed two-fold. Firstly, the total SIRT3 protein levels (45 kDa and 28 kDa) were quantified in order to compare protein data to the mRNA data. Secondly, the protein levels of the processed form (28 kDa) were assessed, as this is the form that resides within mitochondria and is responsible for regulating mitochondrial protein acetylation levels (Lombard et al., 2007). These independent assessments were done because the SIRT3 processed levels may change independently to the total levels of SIRT3 at different stages of development.

Our results demonstrate that SIRT3 protein levels increased in cortical (Figure 17), hippocampal (Figure 18) and cerebellar (Figure 19) rat regions from their relative levels at the 1 week developmental time-point. In the cortex and hippocampus, both the total and the processed SIRT3 protein levels were significantly higher in the 3 week-old rats compared to that of 1 week-old rats ($*P < 0.05$), and the levels further increased at the 3 months time-point ($*P < 0.05$). SIRT3 processed levels in the cerebellum were elevated in the 3 month-old rats compared to that of 1 week-old rats, and then stayed at consistent levels in the 24 month-old rats ($*P < 0.05$). The total SIRT3 protein levels in the cerebellum also increased in the 3 month old rats ($*P < 0.05$), however decreased again in the 24 month-old rats. SIRT3 protein expression levels were different from the mRNA expression profile depicted in Figure 16. Unlike the protein data, there were no significant differences in SIRT3 mRNA expression levels throughout development in the cerebellar or cortical brain regions. Taken together, these data indicate that SIRT3 protein expression levels increase as the brain develops, and that SIRT3 mRNA and SIRT3 protein levels do not correlate.

Fig. 16

A)

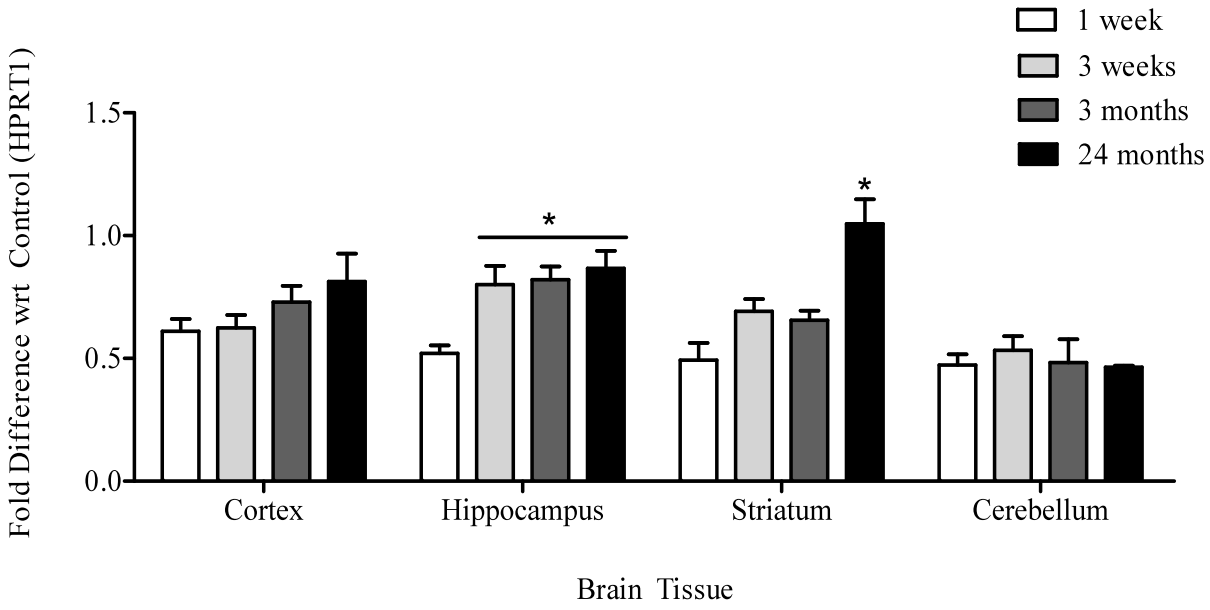
1 week
3 weeks
3 months
24 months
Fold Difference wrt Control (HPRT1)
1.5
1.0
0.5
0.0
*
*
Cortex
Hippocampus
Striatum
Cerebellum
Brain Tissue

B)

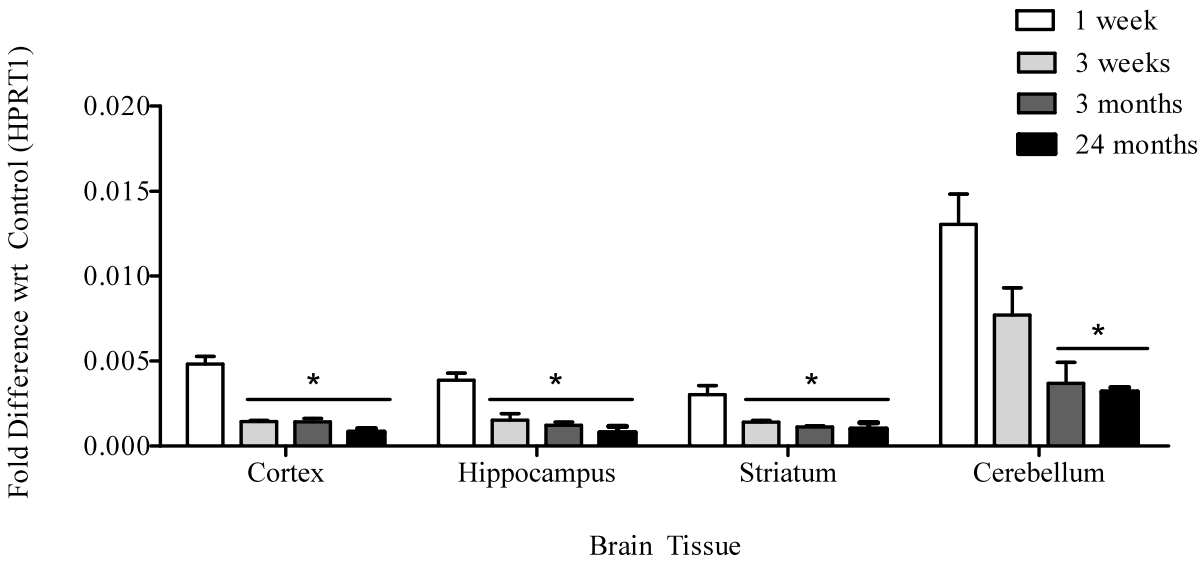
1 week
3 weeks
3 months
24 months
Fold Difference wrt Control (HPRT1)
0.020
0.015
0.010
0.005
0.000
*
*
*
*
Cortex
Hippocampus
Striatum
Cerebellum
Brain Tissue

Figure 16: mRNA expression levels of SIRT1 and SIRT3 in the cortex, hippocampus, striatum, and cerebellum of 1 week, 3 week, 3 month and 24 month-old wild-type rats

A) Bar graph shows qRT-PCR data for SIRT3 mRNA expression levels in the cortex, hippocampus, striatum and cerebellum of wild-type rats (relative to HPRT1). In the hippocampus SIRT3 mRNA levels were significantly higher in the 3 week-old rats and stayed elevated up to and including the 24 months of age. In the striatum, SIRT3 mRNA levels increased significantly in the 24 month-old rats. There were no significant differences in SIRT3 mRNA levels in the cortex or the cerebellum between the different age stages (n= 6, * denotes statistical significance at $P < 0.05$ compared between age groups within brain regions, one way ANOVA with Bonferonni *post-hoc* test, error bars shown are ± SEM).

B) Bar graph shows qRT-PCR data for SIRT1 mRNA expression levels in the cortex, hippocampus, striatum and cerebellum of wild-type rats (relative to HPRT1). SIRT1 mRNA levels in the cortex, hippocampus and striatum were significantly lower at the 3 week, 3 months and 24 months time-points compared to the levels in 1 week old rats. In the cerebellum, SIRT1 mRNA levels were significantly lower in 3 and 24 month-old rats compared to that of 1 week old rats (n= 6, * denotes statistical significance at $P < 0.05$ compared between age groups within brain regions, one way ANOVA with Bonferonni *post-hoc* test, error bars shown are ± SEM).

Fig. 17

A)

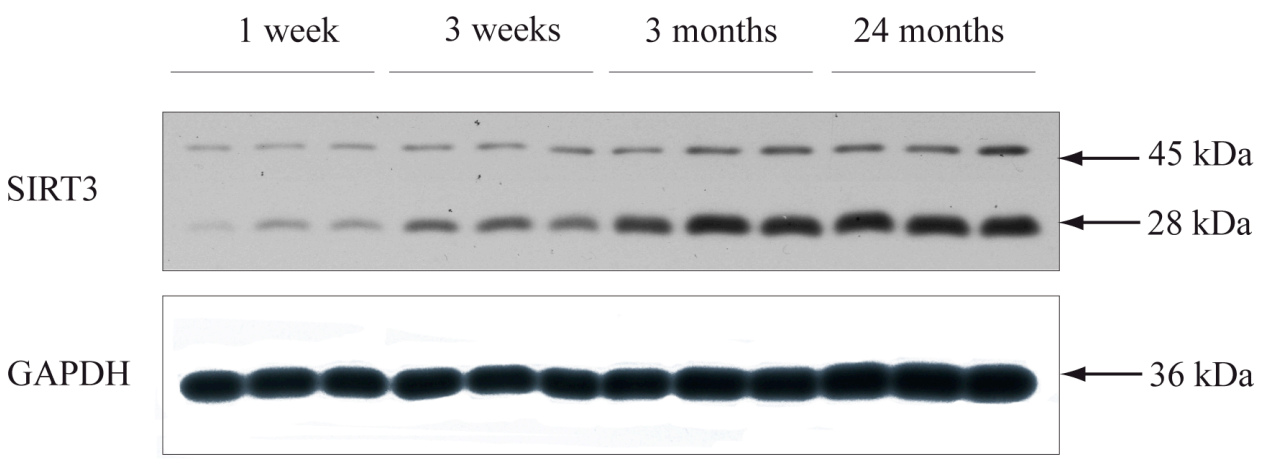
1 week
3 weeks
3 months
24 months
SIRT3
45 kDa
28 kDa
GAPDH
36 kDa

B)

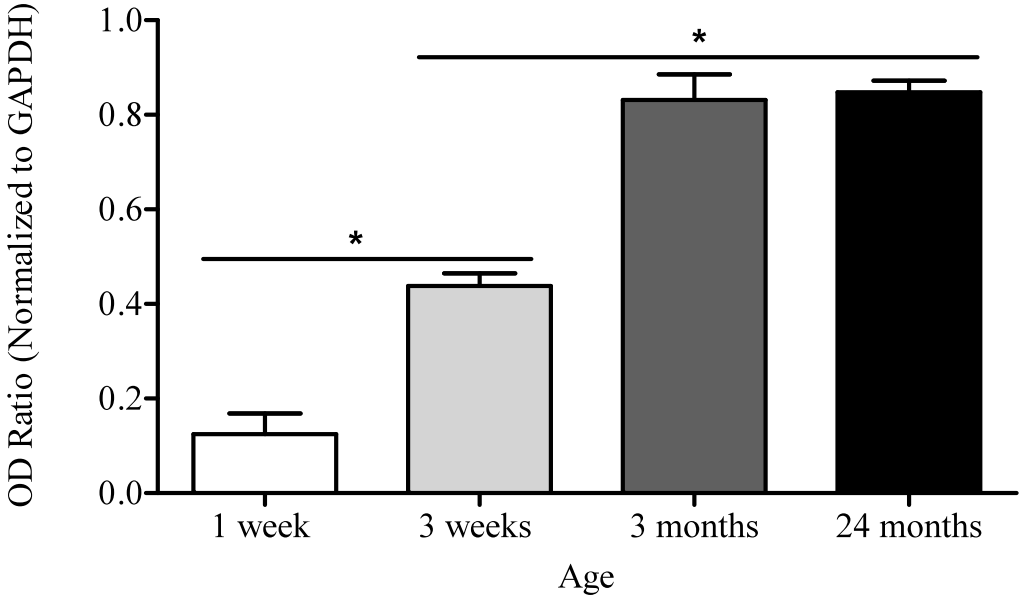
OD Ratio (Normalized to GAPDH)
1.0
0.8
0.6
0.4
0.2
0.0
*
*
1 week
3 weeks
3 months
24 months
Age

C)

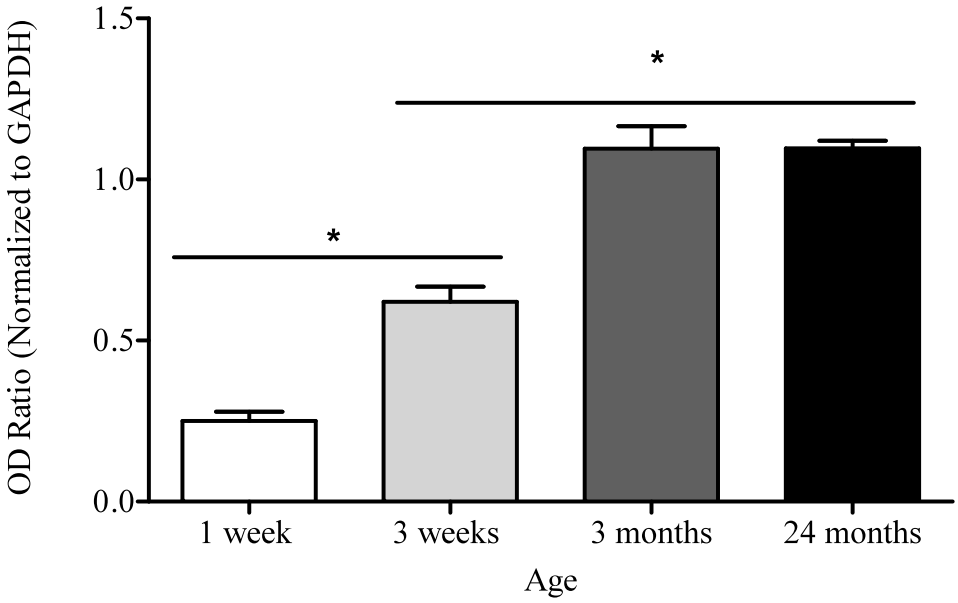
1.5
1.0
0.5
0.0
OD Ratio (Normalized to GAPDH)
*
*
1 week
3 weeks
3 months
24 months
Age

Figure 17: SIRT3 protein expression levels increase in the cortex of wild-type rats throughout development

A) Representative Western blot of endogenous SIRT3 protein expression in the cortex of 1 week, 3 week, 3 month and 24 month-old rats. GAPDH was used as a loading control.

B) Bar graph shows the densitometric data of processed SIRT3 protein expression levels in the cortex of 1 week, 3 week, 3 month and 24 month-old rats. Values represented are means of optical density (OD) ratio normalized against GAPDH. SIRT3 protein levels in 3 week-old rats were significantly higher compared to the levels in 1 week-old rats. SIRT3 protein levels in 3 and 24 month-old rats were significantly higher compared to the levels in 3 week-old rats (n= 3, * denotes statistical significance at $P < 0.05$ compared between age groups within t, one way ANOVA with Bonferonni *post-hoc* test, error bars shown are ± SEM).

C) Bar graph shows the densitometric data of total SIRT3 protein expression levels in the cortex of 1 week, 3 week, 3 month and 24 month-old rats. Values represented are means of OD ratio normalized against GAPDH. SIRT3 protein levels at 3 weeks were significantly higher compared to the levels in 1 week-old samples. SIRT3 protein levels in 3 and 24 month-old rats were significantly higher compared to the levels in of 3 week-old rats (n= 3, * denotes statistical significance at $P < 0.05$ compared between age groups within brain region, one way ANOVA with Bonferonni *post-hoc* test, error bars shown are ± SEM).

Fig. 18

A)

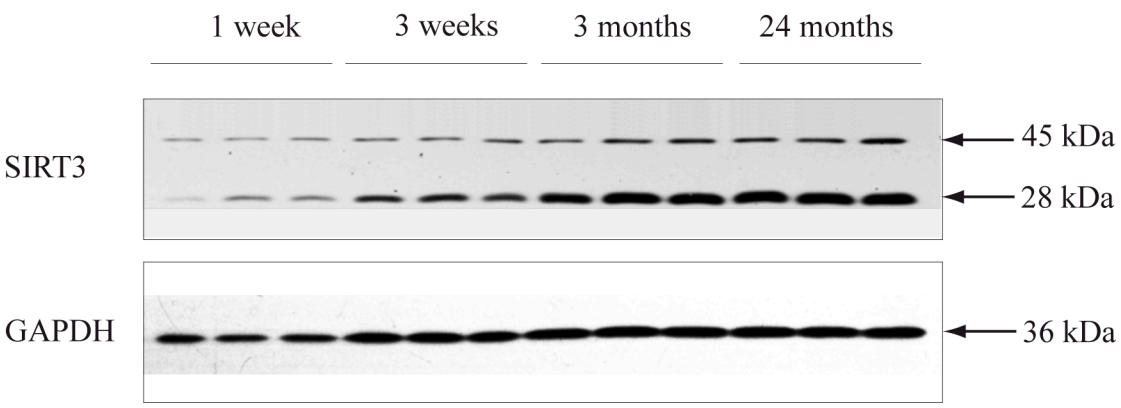
1 week
3 weeks
3 months
24 months
SIRT3
45 kDa
28 kDa
GAPDH
36 kDa

B)

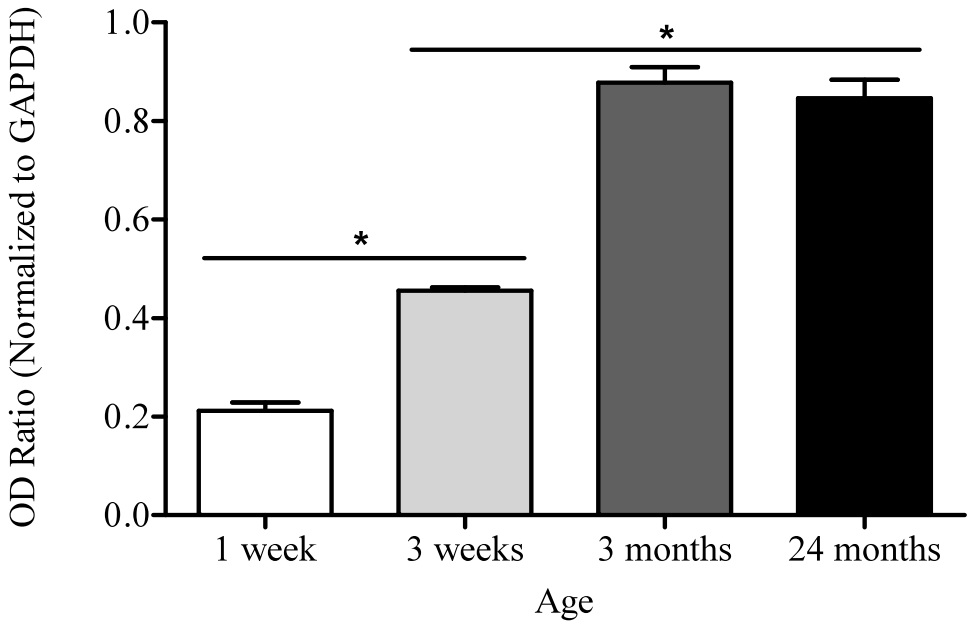
OD Ratio (Normalized to GAPDH)
1.0
0.8
0.6
0.4
0.2
0.0
*
*
1 week
3 weeks
3 months
24 months
Age

C)

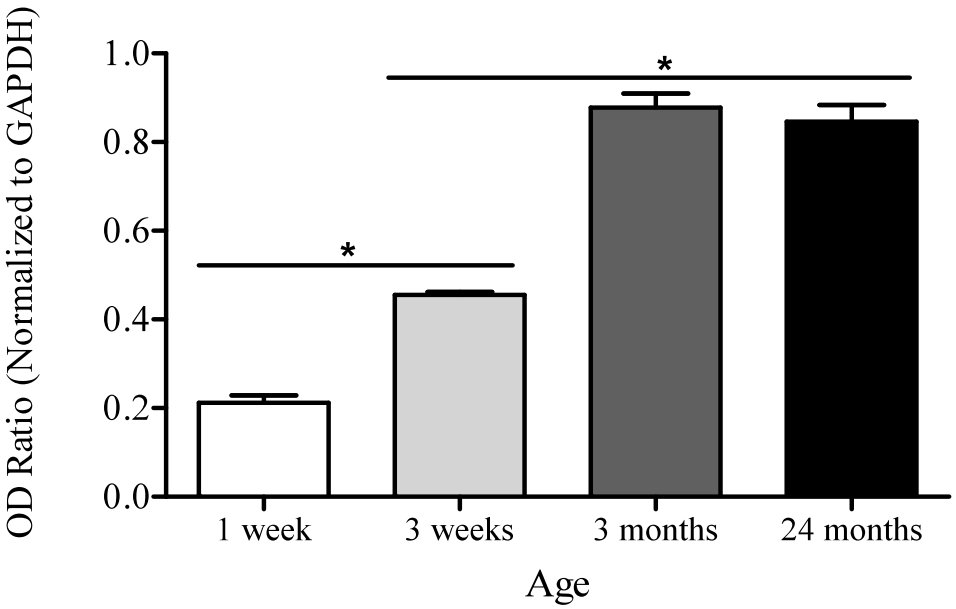
OD Ratio (Normalized to GAPDH)
1.0
0.8
0.6
0.4
0.2
0.0
*
*
1 week
3 weeks
3 months
24 months
Age

Figure 18: SIRT3 protein expression levels increase in the hippocampus of wild-type rats throughout development

A) Representative Western blot of endogenous SIRT3 protein expression in the hippocampus of 1 week, 3 week, 3 month and 24 month-old rats. GAPDH was used as a loading control.

B) Bar graph shows the densitometric data of processed SIRT3 protein expression levels in the hippocampus of 1 week, 3 week, 3 month and 24 month-old rats. Values represented are means of OD ratio normalized against GAPDH. SIRT3 protein levels in 3 week-old rats were significantly higher compared to the levels in 1 week-old rats. SIRT3 protein levels in 3 and 24 month-old rats were significantly higher compared to the levels in 3 week-old rats (n= 3, * denotes statistical significance at $P < 0.05$ compared between age groups within brain region, one way ANOVA with Bonferonni *post-hoc* test, error bars shown are ± SEM).

C) Bar graph shows the densitometric data total SIRT3 protein expression levels in the hippocampus of 1 week, 3 week, 3 month and 24 month-old rats. Values represented are means of OD ratio normalized against GAPDH. SIRT3 protein levels in 3 week-old rats were significantly higher compared to the SIRT3 protein levels in 1 week-old rats. SIRT3 protein levels of 3 and 24 month-old rats were significantly higher compared to the levels in 3 week-old rats (n= 3, * denotes statistical significance at $P < 0.05$ compared between age groups within brain region, one way ANOVA with Bonferonni *post-hoc* test, error bars shown are ± SEM).

Fig. 19

A)

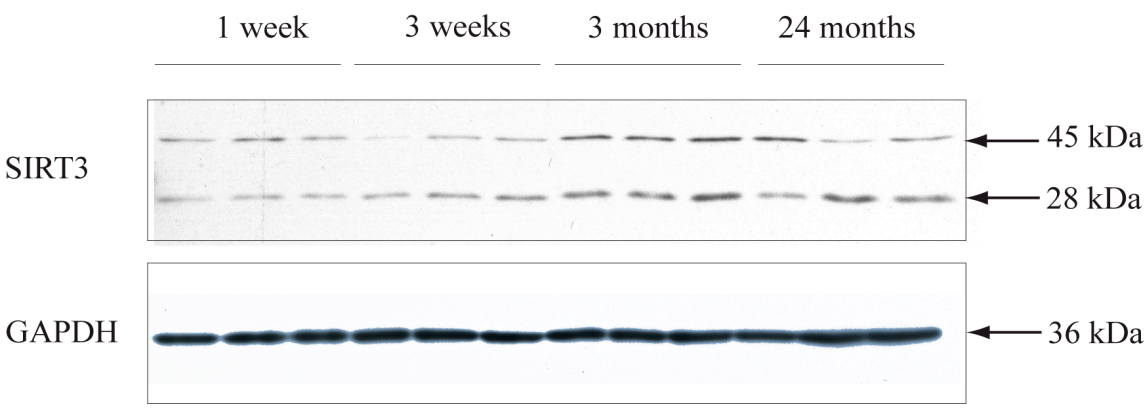
1 week
3 weeks
3 months
24 months
SIRT3
45 kDa
28 kDa
GAPDH
36 kDa

B)

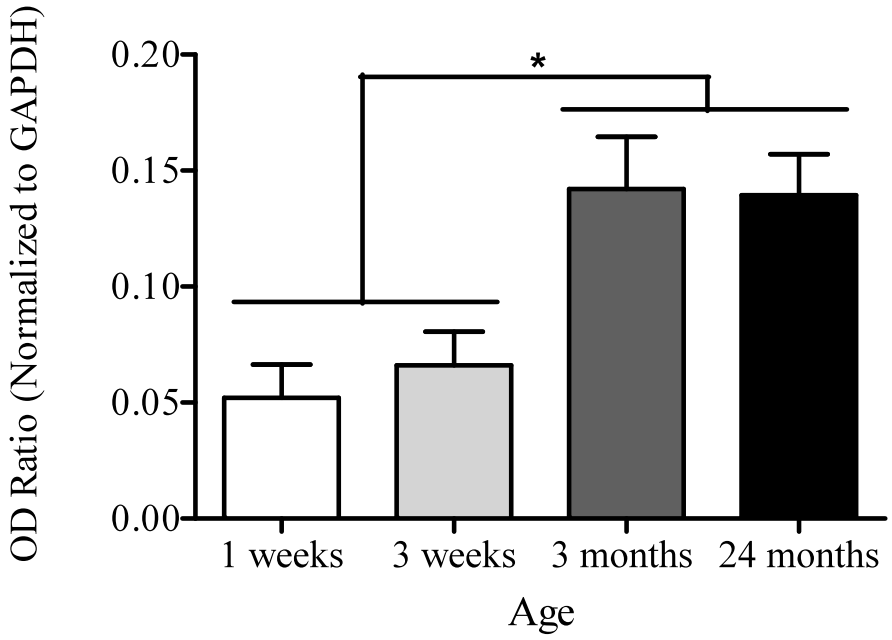
OD Ratio (Normalized to GAPDH)
0.20
0.15
0.10
0.05
0.00
*
1 weeks
3 weeks
3 months
24 months
Age

C)

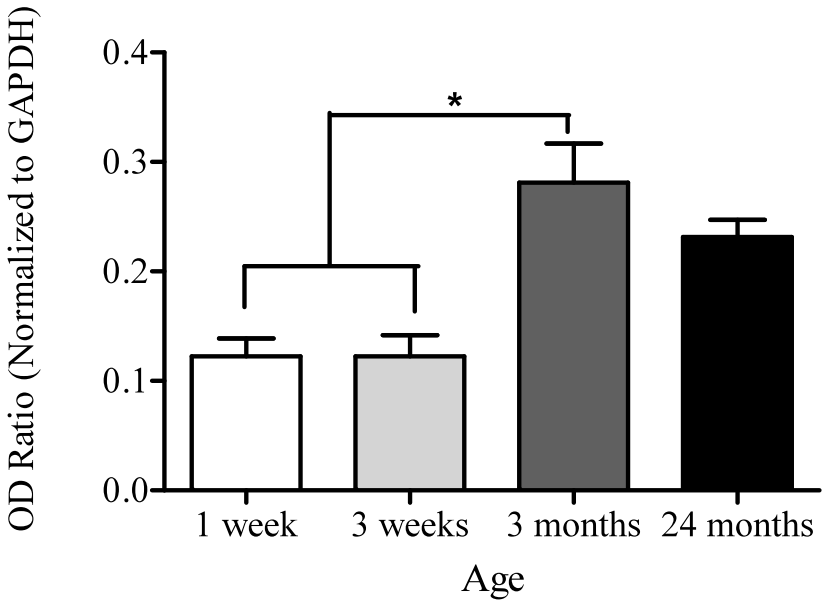
OD Ratio (Normalized to GAPDH)
0.4
0.3
0.2
0.1
0.0
*
1 week
3 weeks
3 months
24 months
Age

Figure 19: SIRT3 protein expression levels increase in the cerebellum in adult wild-type rats

A) Representative Western blot of endogenous SIRT3 protein expression in the cerebellum of 1 week, 3 week, 3 month and 24 month-old rats. GAPDH was used as a loading control.

B) Bar graph shows the densitometric data of processed SIRT3 protein expression levels in the cerebellum of 1 week, 3 week, 3 month and 24 month-old rats. Values represented are means of OD ratio normalized against GAPDH. SIRT3 protein levels in 3 and 24 month-old rats were significantly higher compared to the levels in 1 week-old rats (n= 3, * denotes statistical significance at $P < 0.05$ compared between age groups within brain region, one way ANOVA with Bonferonni *post-hoc* test, error bars shown are ± SEM).

C) Bar graph shows the densitometric data of total SIRT3 protein expression levels in the cerebellum of 1 week, 3 week, 3 months and 24 month-old rats. Values represented are means of OD ratio normalized against GAPDH. SIRT3 protein levels in 3 month-old rats were significantly higher than 1 week, 3 week and 24 month-old samples (n= 3, * denotes statistical significance at $P < 0.05$ compared between age groups within brain region, one way ANOVA with Bonferonni *post-hoc* test, error bars shown are ± SEM).

3.9.3 SIRT3 is predominately expressed in astrocytes in rat primary cortical culture

Our results suggest that SIRT3 is robustly expressed in the brain, however the data obtained cannot distinguish if SIRT3 resides in a specific cell type. Immunocytochemistry was performed in order to assess whether the SIRT3 protein is predominately expressed in astrocytes or in neurons of E18 rat primary cortical cultures. To identify a specific cell type, glial fibrillary acidic protein (GFAP) and microtubule associated protein-2 (MAP2) were used. GFAP and MAP2 are markers of astrocytes and neurons, respectively. In culture mostly GFAP positive cells co-label with SIRT3 (Figure 20A), and no co-labeling was observed between SIRT3 and MAP2 positive cells (Figure 20B). On the other hand, MAP2 positive cells were co-labeled with SIRT1 (Figure 21A), whereas no co-labeling was observed between SIRT1 and GFAP positive cells (Figure 21B). These results suggest that within the rat primary cortical cells SIRT3 and SIRT1 are expressed in distinct cell populations. SIRT3 is predominately expressed in astrocytes and SIRT1 is predominately expressed in neurons. This suggests that SIRT3 plays an important role in astrocyte physiology, whereas SIRT1 plays a role in the physiology of neurons.

Fig. 20

A)

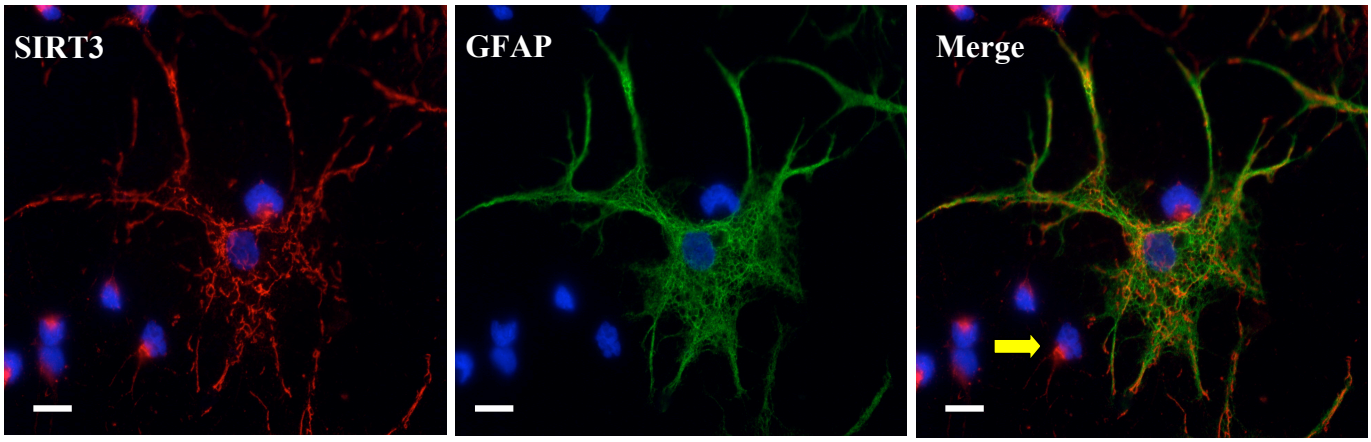

B)

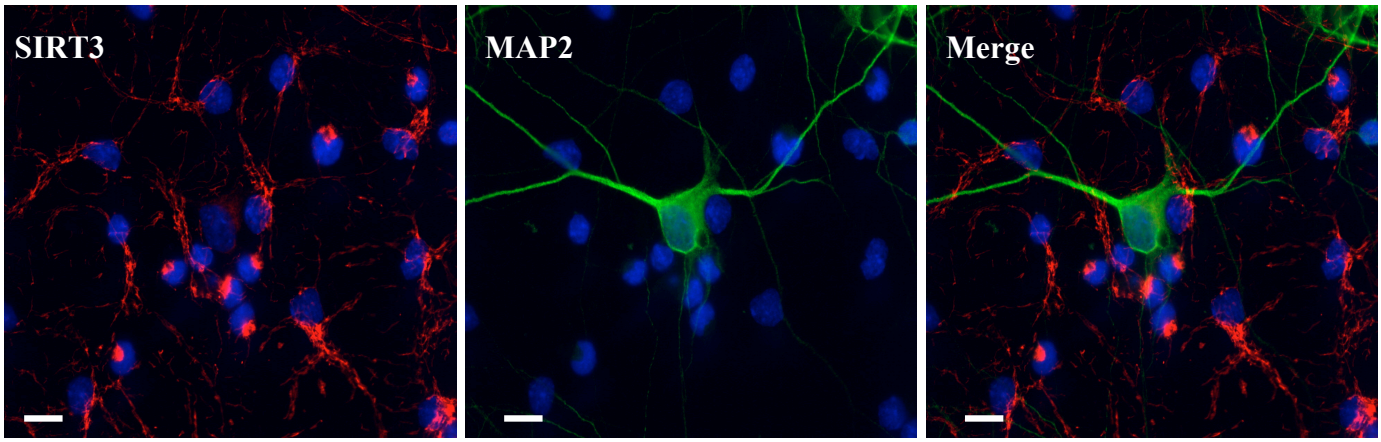

Figure 20: SIRT3 is robustly expressed in astrocytes in rat primary cortical culture

A) SIRT3 co-labels with GFAP. Triple-label immunofluorescence staining of endogenous SIRT3 (Red), GFAP (Green) and nuclei staining (Blue) in rat primary cortical culture. Merged image indicates that the cell that is labelled with GFAP is also SIRT3 positive. A cell type that is not GFAP positive is also positively stained with SIRT3 (arrowhead in merged image). Images were taken with 63x fluor objective. Bar = 10 μM.

B) SIRT3 does not co-label with MAP2. Triple-label immunofluorescence staining of endogenous SIRT3 (Red), MAP2 (Green) and nuclei staining (Blue) in rat primary cortical culture. Merged image indicates that MAP2 positive cell does not co-localize with SIRT3. Images were taken with 63x fluor objective. Bar = 10 μM.

Fig. 21

A)

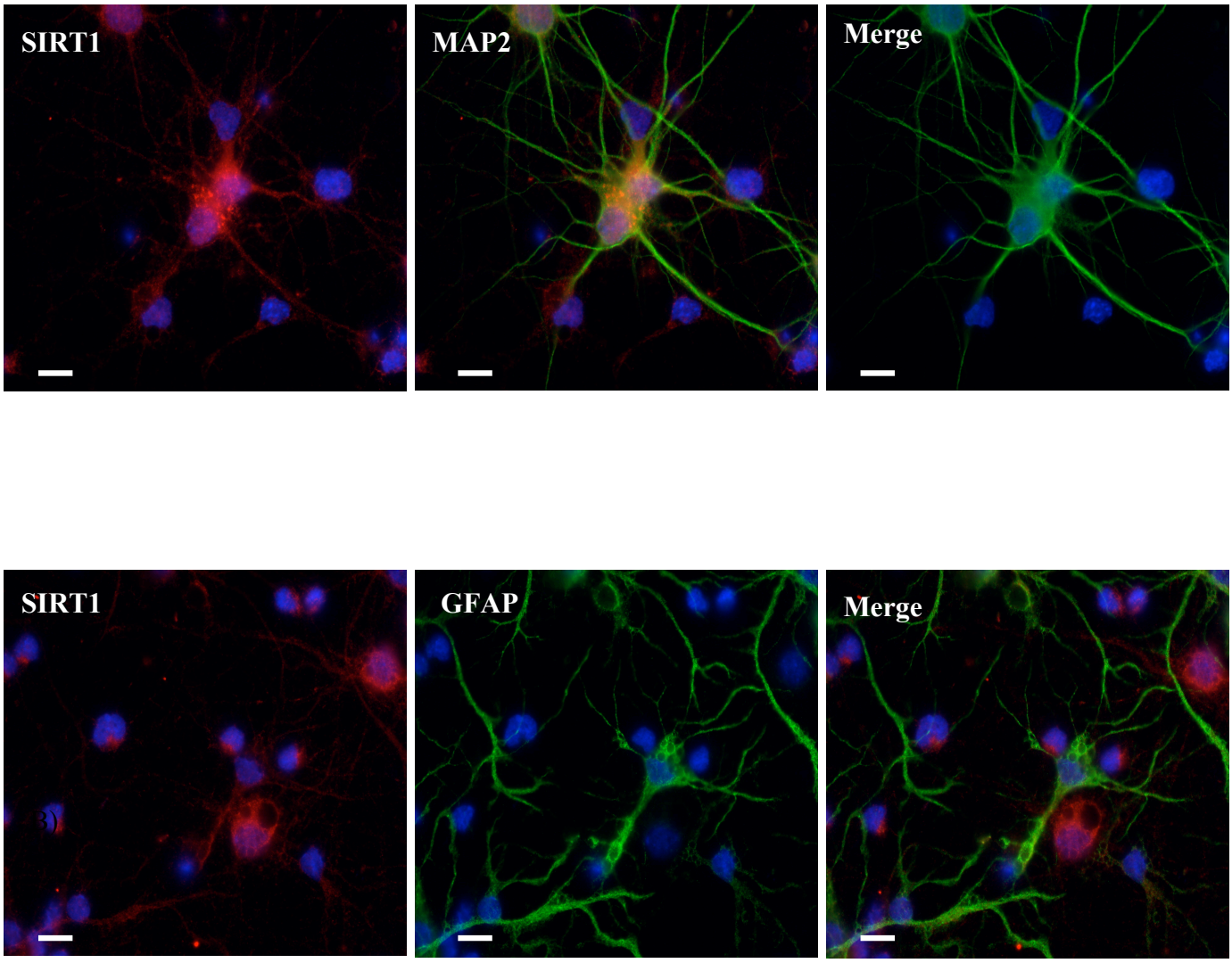

Figure 21: SIRT1 is robustly expressed in neurons in rat primary cortical culture

A) SIRT1 co-labels with MAP2. Triple-label immunofluorescence staining of endogenous SIRT1 (Red), MAP2 (Green) and nuclei staining (Blue) in rat primary cortical culture. Merged image depicts that SIRT1 positive cell co-localizes with MAP2 and the nucleus. Images were taken with 63x fluor objective. Bar = 10 μM.

B) SIRT1 does not co-label with GFAP. Triple-label immunofluorescence staining of endogenous SIRT1 (Red), GFAP (Green) and nuclei staining (Blue) in rat primary cortical culture. Merged image depicts that the GFAP positive cell does not co-localize with SIRT1. Images were taken with 63x fluor objective. Bar = 10 μM.

DISCUSSION

4.1 PART I: Effect of SIRT3 over-expression in HEK-293 cells

4.1.1 Summary

The significance of abnormal mitochondrial function is becoming increasingly recognized in many degenerative diseases. Thus, much focus has been placed in identifying targets that improve mitochondrion's functioning, in anticipation that such agents would render the cell less sensitive to cytotoxic insults. Members of the sirtuin family have been speculated to possess such potential. Of the seven mammalian sirtuins, the majority of research has focused on SIRT1. Recently a mitochondrial sirtuin, namely SIRT3, has been implicated as a potential mediator of mitochondrial metabolic processes (Huang et al., 2010; Pillai, 2010; Yu & Auwerx, 2009). These observations suggest that SIRT3 may also be a target for cytoprotective interventions. To date, however, the precise function of SIRT3 within the mitochondrion remains to be fully elucidated. Based on the data available, however, it is hypothesized that enhancing the activity or prevalence of SIRT3 could prove to be beneficial to cells. Thus, the first aim of this thesis project was to assess how ectopic SIRT3 over-expression affects HEK-293 cells. In addition, SIRT3 expression profile in different regions or cell types of the brain remains unknown. Thus, the second aim of this thesis project was to determine the expression profile of SIRT3 in the rodent brain at different stages of brain development.

Four main conclusions can be drawn from these studies. Firstly, over-expression of SIRT3 decreases mitochondrial membrane potential ($\Delta\Psi m$) and ROS levels under basal conditions in HEK-293 cells. Secondly, over-expression of SIRT3 decreases the sensitivity of HEK-293 cells to cytotoxic insults. Thirdly, SIRT3 mRNA and protein levels are highly expressed in different regions of the rodent brain, and increase throughout development. Fourthly, SIRT3 is predominately expressed in astrocytes within the brain. Taken together, these results support the

hypothesis that SIRT3 possesses cytoprotective potential. In addition, the predominant actions of SIRT3 in the brain regulate astrocyte physiology.

4.1.2 SIRT3 is targeted to mitochondria

Currently there is conflicting data regarding the subcellular localization of SIRT3. Different studies suggest that SIRT3 resides within the mitochondrion, the cytoplasm, or within the nucleus (Hallows et al., 2008; Jin et al., 2009). Initially, SIRT3 was identified as being mitochondrial in studies that employed human SIRT3 (hSIRT3), which possesses a clear mitochondrial targeting sequence towards its amino-terminus (Cooper & Spelbrink, 2008; Onyango et al., 2002) (Figure 2A). However, early studies that used a murine SIRT3 (mSIRT3) reported a nuclear and cytosolic localization of SIRT3 in ectopic expression systems (Scher et al., 2007; Yang et al., 2000). The mSIRT3 form used in these studies, however, lacked an amino terminal region present in the hSIRT3 form, and thus lacked the amino-terminus mitochondrial targeted sequence. Initially, there was speculation that mSIRT3 may not function equivalently to hSIRT3 due to these differential intracellular localization patterns (Nakamura et al., 2008; Scher et al., 2007). This view has been recently challenged though, as mouse SIRT3 cDNA clones have been isolated that do contain an amino-terminal sequence and mitochondrial localization sequence (MLS) comparable to that of a human one (Jin et al., 2009). It is quite likely, therefore, that the originally cloned mouse SIRT3 form was truncated and lacking its correct amino terminus, and thus the subcellular localization reports are suspect. While there still remains debate on this issue, the use of a truncated SIRT3 form could explain at least some of the inconsistencies in the literature on the function of SIRT3 in the cell. For example, the truncated form would not be targeted to mitochondria, and therefore its functions would be restricted to substrates in the cytoplasm or the nucleus. Essentially, in this context SIRT3 would have similar homology and localization as SIRT1, and therefore could regulate many of the same factors

normally regulated by SIRT1. Thus, the results obtained from these studies using the apparently truncated mSIRT3 form may not reflect true mechanisms and outcomes relating to SIRT3 *in vivo*. Indeed, Lombard et al (2007) has now reported that endogenous mouse SIRT3 does exclusively reside within the mitochondria in mouse tissue. To avoid the confusion existing with mSIRT3, this study used the hSIRT3 form uniformly agreed to reside within mitochondria for the ectopic expression studies. As expected, our data show no evidence for SIRT3 residing outside the mitochondria: our immunoblot results show that the ectopically expressed 45 kilodalton (kDa) pro-form of SIRT3 is processed to a 28 kDa form in transfected HEK-293 cell lines, and immunocytochemistry shows that the expressed SIRT3 resides strictly within mitochondria (Figure 3A; Figure 3B). Thus, these results provide no evidence to support any nuclear actions of SIRT3, and suggest that some of the results attributed to SIRT3 in the literature may be artifacts of the truncated SIRT3 simply behaving like SIRT1.

4.1.3 Over-expression of SIRT3 decreases basal mitochondrial membrane potential

While the physiological role of SIRT3 in cells remains contentious, the first study to investigate SIRT3 function reported it to be a key factor involved in thermogenic regulation (Shi et al., 2005). This study found that over-expression of SIRT3 in brown adipocytes caused a decrease in $\Delta\Psi m$ due to the induction of the mitochondrial uncoupling protein 1 (UCP1). Uncoupling factors such as UCP1 allow protons (H+) to leak across the inner mitochondrial membrane, which promotes heat, but as a consequence diminishes $\Delta\Psi m$ (Andrews et al., 2005). In the previously mentioned study, SIRT3 was found to induce the expression of UCP1 indirectly by activating cAMP-response element binding protein (CREB), which in turn increased the expression of the transcription factor (peroxisomal proliferator-activated receptor-gamma coactivator-1α) PGC-1α. PGC-1α is recognized to activate a host of mitochondrial biogenesis genes, as well as to upregulate genes involved in antioxidant capacity, such as catalase and MnSOD (Lin, 2009;

Olmos et al., 2009; Wu et al., 1999). Furthermore, PGC-1α is expressed near ubiquitously throughout the body, and is able induce the expression of other members of the UCP family, such as UCP2 (Yonezawa et al., 2009). However, UCP1, which remains to date the only UCP member shown to be regulated positively by SIRT3, is not expressed in tissues other than brown adipose (Jacobsson et al., 1985). Thus, while SIRT3 activity has been linked to an uncoupling family member, it remains unclear whether the effect observed in brown adipose tissue will extend to other cell types. Our results are consistent with this hypothesis, as ΔΨm was significantly diminished in HEK-293 cells over-expressing SIRT3 under basal conditions (Figure 5; Figure 6). Thus, these results indicate that SIRT3 is able to regulate ΔΨm, and this function is not restricted to brown adipose cells.

Moreover such an effect on ΔΨm could potentially be either of benefit or detriment to the cells over-expressing SIRT3. For example, the collapse of the ΔΨm causes a progressive halt in the oxidative phosphorylation, which is necessary for ATP production (Crompton, 1999). Conditions involving loss of ATP induce overall metabolic imbalance, which trigger the opening of mitochondrial permeability transition pore (mPTP). The opening of mPTP leads to the release of cytochrome c into the cytosol and the activation of pro-apoptotic cascades (Crompton, 1999). On the other hand, a *partial* reduction in ΔΨm can be associated with cytoprotection (Andrews et al., 2005). Electrons can leak out as they pass through the electron transfer chain (ETC). This premature leak of electrons through the complexes leads to an incomplete reduction of O_2, which results in elevated superoxide ($O_2^{\bullet -}$) levels (Andreyev et al., 2005). UCPs increase permeability of the inner mitochondrial membrane, and allow protons (H+) to leak back into the matrix (Andrews et al., 2005). This partially uncouples oxidative phosphorylation from electron transport, which lowers ΔΨm and concomitantly ROS genesis. In contrast, conditions that

increase ΔΨm correlate with higher oxidative phosphorylation rates, and also generate more ROS.

Using two different flow cytometry fluorescence probes, our results collectively show that ectopic over-expression of SIRT3 decreases basal ΔΨm (Figure 5; Figure 6). However, there was no increase in PGC-1α mRNA levels in cells over-expressing SIRT3 (Figure 8). This suggests that at least at the transcriptional level, SIRT3 over-expression has no effect on PGC-1α levels. Thus, while my results clearly show that ΔΨm is regulated by SIRT3, the mechanism through which this effect occurs may not directly relate to, or involve, the PGC-1α pathway proposed by Shi et al. (2005) and Palacios et al. (2009). However, this does not discount the fact that PGC-1α may be regulated by SIRT3 through an unknown posttranslational modification. Further studies are needed to identify the nature of the SIRT3/PGC-1α axis, and assess whether UCP levels/activity are increased by SIRT3 over-expression.

4.1.4 Over-expression of SIRT3 decreases basal ROS levels

Despite its predominant localization in the mitochondrial matrix, only a few studies have investigated whether ectopic over-expression of SIRT3 affects ROS levels under basal conditions (Kong et al., 2010; Shi et al., 2005; Bell et al., 2011). One of the studies demonstrated that ROS levels are reduced following SIRT3 over-expression in brown adipocytes (Shi et al., 2005). As discussed in the section above, diminished ROS in adipocytes over-expressing SIRT3 was attributed to partial reduction of the ΔΨm through the PGC-1α/UCP1 axis. The second study also found that over-expressing SIRT3 in C_2C_{12} muscle cells decreased intracellular ROS levels (Kong et al., 2010). The authors hypothesized that SIRT3 is able to phosphorylate CREB, which upregulates PGC-1α expression and therefore subsequently stimulates the expression of anti-oxidative genes. Collectively, these two studies suggest that SIRT3 may regulate intracellular

ROS levels through pathways that increase transcriptional induction of PGC-1α. However, as illustrated in Figure 8, our results did not support an increase in PGC-1α mRNA expression levels in cells over-expressing SIRT3.

Given that ΔΨm was decreased in cells over-expressing SIRT3 (Figure 5; Figure 6), we therefore tested whether basal ROS levels would also be diminished. Indeed, in agreement with the studies described above, our results showed that basal ROS levels are lower in HEK-293 cells over-expressing SIRT3 (Figure 7). While the specific mechanism of this effect remains to be defined, potential explanations include the SIRT3-mediated attenuation of ΔΨm and/or the induction/activation of the antioxidant defense system.

As previously described in section 1.5.1, partial uncoupling of oxidative phosphorylation slows down the electron flow through the complexes of the ETC, and thereby decreases the generation of ROS by-products from these sites. In addition, reduction in ROS levels could also be due to SIRT3-induced elevation of substrates involved in antioxidant pathways. Transgenic mice over-expressing SIRT3 exhibited elevated mRNA levels of manganese superoxide dismutase (MnSOD) and catalase (Sundaresan et al., 2009). The authors suggested that SIRT3 deacetylates FOXO3a in the nucleus, which is a transcription factor driving the expression of these antioxidant genes. It is important to note that the mice used in this study were generated using the cDNA encoding mSIRT3 (28 kDa short form). This truncated mSIRT3 form lacks an amino-terminus containing the MLS, and thereby its expression is restricted to the cytoplasm or the nucleus. Because SIRT3 is localized to mitochondria (see Figure 3), the results in the previously mentioned study may be due to the truncated SIRT3 simply behaving like SIRT1 (see section 4.1.2 for discussion). Indeed, SIRT1 has been demonstrated to deacetylate and activate FOXO3a (Brunet et al., 2004). Interestingly, Jacobs et al (2008) proposed that SIRT3 and FOXO3a do

interact, however directly in mitochondria. Jacobs et al (2008) suggested that this interaction is able to promote the nuclear localization of FOXO3a, which then it is able to act as a transcription factor to upregulate these antioxidative genes.

Furthermore, Tao et al (2010) demonstrated that SIRT3 interacts directly with MnSOD in mitochondria. By deacetylating MnSOD on lysine 122, SIRT3 was able to increase MnSOD enzymatic activity. Intriguingly, it was also shown that high MnSOD expression levels do not necessarily reflect high enzyme activity. These data suggest that MnSOD requires to be deacetylated by SIRT3 directly in mitochondria in order to function as an active antioxidant.

Similar to SIRT3, SIRT1 over-expression can also induce elevation of anti-oxidative substrates involved in the regulation of mitochondrial ROS (Brunet et al., 2004; Hasewaga et al., 2008). SIRT1-mediated regulation of antioxidative defense mechanisms in mitochondria is through indirect mechanisms linked to the SIRT1/PGC-1α (Nemoto et al., 2005) and the SIRT1/FOXO3a pathways (Brunet et al., 2004). Given the mitochondrial localization of SIRT3, it is therefore possible that *both* sirtuins regulate basal ROS levels from two distinct locations within the cell. Since SIRT3 is a mitochondrial enzyme, it may act as the primary metabolic sensor and the regulator of ROS levels within mitochondria; whereas, SIRT1 may regulate antioxidant defenses in mitochondria through secondary response mechanisms. Collectively, our results demonstrate that SIRT3 over-expression decreases basal ROS formation in HEK-293 cells. The decrease in ROS levels in SIRT3 over-expressing cells can be attributed to an increase in antioxidative capacity and to partial reduction in $\Delta\Psi m$ (Figure 5; Figure 6). It would be interesting to see whether other members of the antioxidant defense system within mitochondria are directly activated by SIRT3.

4.1.5 SIRT3 over-expression renders cells less sensitive to glucose deprivation treatment

Upon observing a decrease in ROS in HEK-293 cells over-expressing SIRT3 under basal culturing conditions, we assessed whether the diminished ROS levels would protect cells during oxidative stress. It was investigated whether SIRT3 over-expression would protect cells from glucose deprivation (GD)-induced cell death with or without glucose reperfusion (GR). GD is able to elevate mitochondrial ROS levels (Blackburn et al, 1999). These authors suggested that depriving cells from glucose reduces the progression of glycolysis and shifts mitochondrial metabolism to oxidative phosphorylation in order to meet ATP demand. This in turn, would increase the rate of oxidative phosphorylation, which leads to passive electron leak through the ETC complexes, and an increase in ROS levels. Although the mechanism and the source behind the elevation of ROS following GR are still not clear, GR induces a rapid surge in ROS levels within mitochondria (Suh et al., 2007). Thus, one common mechanism of GD/GR-induced cell death is via an increase in metabolic oxidative stress.

No study to date has evaluated the role that SIRT3 plays in glucose-deprived cells. Thus, this study is the first to focus on the effects of SIRT3 over-expression during GD, which is an *in vitro* model of hypoglycemia. Indeed cells over-expressing SIRT3, demonstrated relatively lower percentage of cell death in both GD and GR conditions (Figure 9A; Figure 9B). Several potential mechanisms may explain why cells over-expressing SIRT3 are less sensitive to these oxidative insults.

Glycolysis is a source of metabolites for pathways requiring glucose. Following GD, the stalling of glycolysis results in a decrease of NADPH production; NADPH levels decline due to the inability for the pentose phosphate pathway to proceed (Spitz et al., 2000). NADPH is responsible for reduction of oxidized glutathione (GSSG) to glutathione (GSH), which has the

antioxidant capacity to metabolize H_2O_2 into H_2O (Andreyev et al, 2005; Mari et al., 2009). SIRT3 deacetylates, and therefore activates enzymes of the TCA cycle, isocitrate dehydrogenase 2 (IDH2) (Schlicker et al., 2010; Someya et al., 2010) and glutamate dehydrogenase (GDH) (Lombard et al., 2007). Both enzymes produce α-ketoglutarate to be used as a TCA cycle intermediate by using isocitrate and glutamate as their substrates, respectively. Intriguingly, these enzymes have the capacity to generate NADPH from NADP+ as a consequence of converting their substrates to α-ketoglutarate. This suggests that even if NADPH levels decrease due to stalling of the glycolytic pathway following GD, SIRT3 is able to preserve the activity of enzymes responsible for NADPH production within the TCA cycle. A recent study has demonstrated that HEK-293 cells over-expressing both SIRT3 and IDH2 have elevated NADPH levels (Someya, 2010). This suggests that SIRT3 increases NADPH levels through deacetylating and therefore activating IDH2. Such an increase in NADPH concentration arising from SIRT3 over-expression would increase the antioxidant capacity of the cell. Therefore, SIRT3 over-expression may result in increased GSH/GSSG ratio within the mitochondria, which would decrease ROS levels and protect cells from oxidative stress.

SIRT3 over-expression has been demonstrated to increase expression of antioxidant genes such as MnSOD and catalase, which would be expected to diminish acute oxidative stress in cells exposed to GD/GR. Furthermore, as GD is speculated to impede glycolysis, the rate of oxidative phosphorylation must increase in order to meet ATP demand (Blackburn et al., 1999). This would further increase the rate of electrons passing through the ETC, resulting in $\cdot O_2^-$ production caused by the electron leakage at the complexes. Because SIRT3 over-expression decreases basal $\Delta\Psi m$ (Figure 5; Figure 6), this in turn would slow the electron flux through the complexes and ultimately decrease ROS genesis and therefore protect from cell death. Future experiments

investigating whether specific antioxidant or anti-apoptotic substrates are upregulated during GD or following GR in cells over-expressing SIRT3 would be worthwhile.

4.1.6 SIRT3 over-expression renders cells less sensitive to H_2O_2 treatment

A protective effect was observed in cells over-expressing SIRT3 following the GD/GR treatment. Because GD/GR involve oxidative stress, it was further tested whether SIRT3 is protective against the direct addition of a potent oxidant, hydrogen peroxide (H_2O_2). Indeed, our results demonstrate that cells over-expressing SIRT3 are less sensitive to H_2O_2-induced cell death (Figure 10A, Figure 10B). Another group also showed that SIRT3 over-expression plays a protective role against H_2O_2-induced cell death (Someya et al., 2010). Collectively these results suggest that an increase in SIRT3 levels is sufficient to protect cells from the H_2O_2 insult.

When complex I activity is partially inhibited, mitochondria become more vulnerable to the oxidative stress that arises from acute H_2O_2 treatment (Chinopolous & Adam-Vizi, 2001). Ahn et al (2008) has reported that H_2O_2 treatment in MEFs causes SIRT3 to dissociate from complex I of the ETC. SIRT3 associates with complex I at basal levels, and one of its ascribed functions is to maintain the enzymatic stability of this complex (Ahn et al., 2008). Therefore, it may seem counter-intuitive that SIRT3 dissociates from complex I after H_2O_2 treatment, as this would decrease the overall enzymatic activity of the complex. It should be noted, that this dissociation of SIRT3 involved the normal endogenous levels of mitochondrial SIRT3. However, an increase in SIRT3 prevalence would likely diminish the degree to which the total pool of SIRT3 dissociates from complex I. Therefore, ectopic over-expression of SIRT3 would increase the association of SIRT3 with complex I, and thus maintain the functional integrity of this complex.

In conclusion, SIRT3 over-expression is protective against H_2O_2 exposure, which is remarkably consistent with recent studies. In addition to these ectopic expression scenarios, endogenous

SIRT3 mRNA levels increase following sub-lethal H_2O_2 treatment in H9c2 cells (Yu et al., 2009). Should this response extend to other cell types, it would suggest that oxidative stress can directly elevate SIRT3 endogeneous levels to provide cytoprotective effects. In support of our hypothesis, our data show that over-expression of SIRT3 protects cells from oxidative stress. This can be attributed to the ability of SIRT3 to attenuate ROS levels.

4.1.7 SIRT3 over-expression decreases cell proliferation rates

Normal cell cycle progression is a genetically complex process affected by a multitude of factors. One influencing factor is the progressive accumulation of genetic mutations within a cell, which tend to decrease the fidelity of the genome (Sinclair & Oberdoerffer, 2009). This process is accelerated by chronic oxidative stress that progressively increases damage to nucleic acids, lipids and proteins over time (Larsson, 2010; Ma et al., 2009; Sanz et al., 2006). This damage is inherited across cell generations, which collectively can lessen the efficiency of daughter cell function. Given this, cells displaying increased proliferation rates would be expected to speed up the process of deteriorative aging, because of the generation of more daughter cells with accrued genetic damage.

Caloric restriction (CR), without malnutrition, is well recognized to increase lifespan and increase longevity in numerous species. This effect is attributed at least in part to a decrease in ROS levels and slower cell proliferation rates (Hagopian et al., 2005; Martin-Montalvo et al., 2011). Given that SIRT3 levels are upregulated by CR (Shi et al., 2005), and its over-expression decreases ROS levels (Figure 7), it was therefore assessed whether over-expressing SIRT3 slows cell proliferation rates. As anticipated, the results showed that HEK-293 cells stably over-expressing SIRT3 displayed significantly reduced cell proliferation rates (Figure 11).

Tumour cells display an increased rate of cell proliferation and rely on the increase of glucose uptake as their main energy source in order to support their survival (Deberardinis et al., 2008). Therefore, high glycolysis rate is recognized as one of the main hallmarks of cells undergoing a metabolic shift towards carcinogenesis. Two distinct studies reported that SIRT3 is able to decrease the activity of the hypoxia-inducible factor-1α (HIF1α), which is a transcription factor regulating the expression of genes involved in glycolysis (Bell et al., 2011; Finley et al., 2011). These studies showed that SIRT3-depleted MEFs displayed higher proliferation rates and elevated ROS levels. In addition, Finley et al. (2011) showed that $SIRT3^{-/-}$ mice have increased glucose uptake. Therefore, it was suggested that SIRT3 is able to repress glycolysis by decreasing ROS genesis, as elevated ROS is able to increase HIF1α transcription activity. Furthermore, Kim et al (2010) reported SIRT3 to possess tumour suppressor activity, as $SIRT3^{-/-}$ MEFs exhibited higher ROS levels, increased glycolytic activity and enhanced cell proliferation rates.

As previously discussed**,** UCPs attenuate ROS levels by partially reducing the ΔΨm by uncoupling the proton gradient. UCP2 has also been demonstrated to play a role in cell proliferation and fatty acid oxidation (Pecqueur et al, 2009), and a decrease in its activity is involved in the initiation and progression of tumour development (Derdak et al., 2006). Given that there is a link between SIRT3 and UCP1, it is possible that over-expression of SIRT3 may elevate UCP2 activity/levels. A recent study showed that $UCP2^{-/-}$ CHO cells display a decrease in fatty acid oxidation, which in turn, increased glycolysis and proliferation rates (Pecqueur et al., 2008). This study suggests that UCP2 specifically plays a key role in the entry of fatty acids into mitochondria. The authors hypothesized that loss of UCP2 led to depletion of acetyl-CoA production from fatty acid sources. Acetyl-CoA is an important metabolite, and depending on cellular proliferation rate, acetyl-CoA can be derived from either pyruvate or fatty acids. Cells

that are rapidly proliferating preferentially tend to extract acetyl-CoA from pyruvate, whereas slower proliferating cells metabolize acetyl-CoA derived from both sources (Pecqueur et al., 2008). Therefore, in UCP2$^{-/-}$ cells, glycolysis is augmented in order to increase pyruvate levels to generate acetyl CoA, as fatty acid sources are not readily available. This glycolytic shift increases cellular proliferation rates, as long as glucose is available (Gogvadze et al., 2008). Thus, over-expression of SIRT3 could lead to the facilitation of fatty acid entry into the mitochondria for use in acetyl-CoA synthesis. As discussed above, this would also be expected to slow proliferation rates and lower ROS genesis.

Collectively these data suggest that SIRT3 over-expression may negatively control carcinogenesis by slowing down cell proliferation rates. SIRT3 may slow down proliferation rates by elevating of UCP2 activity/levels, increasing anti-oxidative capacity, decreasing ROS levels, and by decreasing HIF1α activation. Future studies should investigate whether SIRT3 over-expressing cells increase the levels/activity of UCP2.

4.2 PART II: EXPRESSION

Mitochondrial dysfunction brings a greater risk of neurodegenerative diseases, which can arise from an overall reduction of antioxidative defenses and the increased genesis of ROS (Sanz et al., 2006). Identifying means by which mitochondrial activity can be strengthened, and ways to reduce ROS production is the focus of current research on potential neuroprotective agents. To date, only two studies have investigated the role of SIRT3 in the CNS. Pfister et al (2008) demonstrated that SIRT3 over-expression in cerebellar granule neurons results in increased cell death following exposure conditions of low potassium. However, whether this low potassium condition holds physiological relevance is questionable. Inversely, Kim et al (2007) demonstrated that SIRT3 is a neuroprotective factor against N-methyl-D-aspartate (NMDA)-

mediated excitoxicity. Over-expression of SIRT3 in cerebral cortical cultures attenuated ROS genesis and protected neurons from cell death induced by NMDA. These data demonstrate that the role of SIRT3 in the CNS is not fully understood, and highlights the need for further investigations in this context. Our results demonstrate that SIRT3 exhibits cytoprotective properties, and its over-expression induces beneficial effects. These observations provide a strong rationale for testing whether or not these effects extend to the CNS. Work along this direction is currently underway in our lab.

4.2.1 SIRT3 mRNA levels are higher than SIRT1 mRNA levels in the peripheral and central nervous system

While there is a paucity of data relating to SIRT3, SIRT1 has been demonstrated to hold neuroprotective properties in neurodegenerative models such as Alzheimer's disease and amyotrophic lateral sclerosis (Kim et al, 2007). Surprisingly, these studies were carried out without the endogenous expression pattern of SIRT1 in the brain being clearly elucidated. To address this issue, the relative expression pattern of SIRT3 and SIRT1 was characterized within the rodent brain during the course of development. To date, there are only three reports in which SIRT3 expression within the CNS was briefly mentioned (Shi et al, 2005; Lombard 2007; Palacious et al, 2009). Shi et al. (2005) used Northern blotting to assess the abundance of SIRT3 mRNA levels in mouse tissues, with brain constituting one sample on their Northern blot panel. Similarly, Lombard et al. (2007) and Palacious et al. (2009) examined SIRT3 expression by Western blot across a range of tissues, once again the brain represented one sample in their panel. Lombard et al. (2007) and Shi et al. (2005) did not employ any quantitative measures of SIRT3 expression, nor did any of these studies address specific regions of the brain.

We first investigated SIRT3 and SIRT1 mRNA expression levels in a host of peripheral tissues and brain regions of adult mice (3 months old). These results showed that the relative expression

of SIRT3 was higher than SIRT1 in whole brain (Figure 13) as well as in all peripheral tissues tested (Figure 12). In fact, SIRT3 mRNA levels exceeded those of SIRT1 by 2 to 4 fold in all tissues except in the small intestine. Having observed that SIRT3 is expressed at higher levels than that of SIRT1 in the whole brain, it was investigated whether there are any brain regional differences. Indeed, SIRT3 mRNA is expressed at a higher level than SIRT1 mRNA in the cerebellum, cortex, and hippocampus (Figure 14). These results suggest that at least at the mRNA level, SIRT3 is expressed at higher levels than that of the extensively studied SIRT1.

Mitochondrial function as well as its protein content and/or activity has been reported to gradually decline in the aged brain due to the progressive oxidative damage (Sanz et al., 2006). Because SIRT3 is a mitochondrial resident, we investigated whether the expression levels of this enzyme decrease as a function of age. However, SIRT3 mRNA levels were significantly higher in whole brain extracts derived from aged mice compared to that of the adult mice. Observing an increase in SIRT3 mRNA levels in the aged brain suggests that a decrease in mitochondrial function does not result directly from a loss of SIRT3. In fact, the maintained SIRT3 levels in the aged brain may work to stabilize the increased progressive oxidative damage in mitochondria. Inversely, there were no age-dependent differences in SIRT1 mRNA levels. Given that SIRT3 and SIRT1 differ in their expression levels in all tissues investigated, it is highly probable that these sirtuins carry out different cellular functions.

Hypoxanthine-guanine phosphoribosyltransferase (HPRT1) is widely used as an endogenous housekeeping gene because it is expressed ubiquitously and stably in all tissues (Fischer et al., 2005; Stout, 1985). Since SIRT3 mRNA levels in the adult mouse brain showed approximately equal expression to HPRT1 levels (Figure 13), it is therefore suggestive that SIRT3 is expressed at moderate-to-high levels in the CNS. Furthermore, SIRT3 mRNA levels in some of peripheral

tissues examined were expressed were at least 2-fold higher relative to HPRT1 levels (Figure 12). Our quantified Western blot results support this pattern, as the SIRT3 protein levels are significantly higher in peripheral tissues than in specific regions of the brain that were examined (Figure 15). Taken together, these results suggest that SIRT3 is expressed at high levels in the brain, and even at higher levels in some of the peripheral tissues.

Although the high expression of SIRT3 is intriguing, Lombard et al (2007) suggested that it is not required for the functionality of these tissues. Mice deficient in SIRT3 developed normally, and displayed no impairments of either heart or kidney function under basal conditions. However, this study did not investigate the health outcomes in these mice during conditions of prolonged stress. Indeed, deficits in cardiac stress became evident in SIRT3-deficient mice when they were subjected to hypertrophy (Sundaresan et al., 2009). Therefore, one can speculate that increasing SIRT3 levels may give the cells more tolerance to various stresses.

Collectively, our expression data show that SIRT3 is robustly expressed in all regions examined, and that SIRT3 mRNA levels are higher than SIRT1 in both peripheral and brain regions. This study is the first to examine the expression profile of SIRT3 mRNA and protein levels in specific brain regions. If future studies demonstrate SIRT3 to hold neuroprotective abilities, its high expression levels may hold potential in targetable gene therapy.

4.2.2 SIRT3 mRNA levels increase in the hippocampus and striatum of the developing rat brain

Given the robust SIRT3 mRNA expression levels in the adult rodent brain, we next examined its expression at different time-points during development. These assays focused on the cortex, cerebellum, hippocampus and striatum of the rat throughout developmental stages of 1 week, 3 weeks and 3 months and in the brain regions of 24 month-old senescent rats (Figure 16).

Analysis via qRT-PCR revealed that hippocampal SIRT3 mRNA levels increased at 3 weeks of age relative to their levels at 1 week of age, and this level remained constant up to the 24 month time-point. Striatal SIRT3 mRNA, on the other hand, remained at constant levels throughout development, and its levels increased in the 24 month-old senescent animals. No significant changes in SIRT3 mRNA levels were detected within the cortical or cerebellar regions at any of the stages of development.

In contrast to SIRT3, however, SIRT1 mRNA levels displayed significant changes in all brain regions examined (Figure 17). Specifically, SIRT1 mRNA levels were at their highest in the 1 week old tissue samples. Relative to the levels of 1 week old animals, SIRT1 mRNA levels decreased significantly in the 3 week old animals in the cortex, hippocampus, and striatum, and remained at consistent levels for the rest of the examined age groups. Within the cerebellum, SIRT1 mRNA levels were significantly diminished from the 1-week levels by 3 months of age, and remained at this level in the senescent 24 months old rats.

Overall, these results show that SIRT3 and SIRT1 have distinct regional patterns of mRNA expression in the brain. SIRT3 mRNA levels increase in the hippocampal and striatal tissues, whereas SIRT1 mRNA levels decrease in all tissues examined. The observed increase of SIRT3 mRNA levels suggests that it may play an anti-oxidative role to compensate for the increase of cellular oxidative damage that occurs as an organism ages**.** However this hypothesis contrasts the observed decrease in the expression profile of SIRT1 mRNA levels, as this sirtuin also holds anti-oxidative properties. Therefore, future studies should focus on delineating the role of these sirtuins on the brain as the function of age. This is the first study to investigate endogenous gene expression of both SIRT3 and SIRT1 at different age stages.

4.2.3 SIRT3 protein levels increase in the rat brain throughout development

The observed age-dependent alterations in SIRT3 mRNA levels show that SIRT3 levels change as a function of age. However, the alterations were very minimal and did not extend to all brain tissues examined (Figure 16). It was next assessed whether the changes observed at the mRNA level would be recapitulated in specific brain regions at the protein level. SIRT3 protein expression levels were investigated in the cortical (Figure 17), hippocampal (Figure 18) and cerebellar (Figure 19) rat brain regions. For this, SIRT3 protein levels were assessed two-fold. Firstly, mRNA analysis cannot distinguish between the pro- and processed forms of SIRT3. Therefore, in order to compare protein data to the mRNA data, the total SIRT3 protein was quantified; e.g., the pro-form plus the processed form. Secondly the SIRT3 levels of the processed form were assessed, as this is the form that is present in mitochondrial matrix and is responsible for regulating mitochondrial protein acetylation levels (Cooper & Spelbrink, 2008; Hallows et al., 2008; Onyango et al., 2002). These independent assessments were done, as it is conceivable that the processed levels of SIRT3 could change independent to the total SIRT3 levels at different stages of development, as well as in the senescent brain.

Our results demonstrated that both, total and processed SIRT3 protein levels, increased with age in all brain regions examined. In both cortical and hippocampal tissues, SIRT3 protein levels were expressed at higher levels at 3 weeks relative to their levels at 1 week, and then increased again at 3 months. In both of these brain tissues, there was no difference in SIRT3 protein levels between adult brain regions (3 months) and aged brain regions (24 months). SIRT3 protein levels in the cerebellum also showed divergence from their relatively constant mRNA levels throughout development. However in the cerebellum, both the processed and total SIRT3 expression protein levels did not increase until the animals reached the adult stage.

Taken together, these results demonstrate that levels of both the pro-form and the processed form of the SIRT3 protein increase throughout development in the rat brain, and maintain their levels as the senescent animals. Given that the processed form of SIRT3 is conceivably the catalytically active form, our results suggest that SIRT3 does not lose its enzymatic potential in the aged brain. However, these results also indicate that mRNA levels cannot be used to reliably extrapolate SIRT3 protein levels.

The observed discrepancy between SIRT3 mRNA and protein levels suggests that post-transcriptional regulation of SIRT3 production likely occurs in the brain. Frequently, mRNA contain regulatory elements are present in the 3′ untranslated region (3′UTR). These can include negative control elements that regulate the repression of protein translation via shortening of poly(A) tail (deadenylation), and the subsequent cleavage of the 7-methylguanosine cap and exonucleolytic degradation of the mRNA message (Coller & Parker, 2004). Another possible type of translational repression is regulated via microRNAs (miRNAs), which through mechanisms not fully understood, bind to the complementary sequence of mRNA to repress protein synthesis (Fabian et al., 2010). Converging studies have demonstrated that miRNAs induce translation repression through deadenylation, and therefore subsequent degradation of the mRNA (Fabian et al 2010). Interestingly, after executing a scan using a program called "Regulatory RNA Motifs and Elements Finder", a number of motifs were found holding complimentary sequences to miRNAs in the 3'UTR region, which may regulate SIRT3 mRNA translation. These mechanisms could potentially explain the disconnect between mRNA and protein levels. Although, we cannot discount other binding motifs, which may be present and could regulate the translation of SIRT3 mRNA. Alternatively, the half-life of the SIRT3 protein due to various chaperones or ubiquitination processes could differ between tissues at different stages of development.

Collectively, the observed increase in SIRT3 expression throughout development suggests that it may play functional role in these brain regions at different age stages. However, the precise role of SIRT3 within the brain remains to be further investigated.

4.2.4 SIRT3 is robustly expressed in astrocytes

The robust expression of SIRT3 in the brain encouraged us to investigate whether it is ubiquitously expressed throughout the CNS or is localized to a specific cell type. Double immunofluorescence revealed that SIRT3 immunofluorescence signal predominately co-labels with glial fibrillary acidic protein fluorescence (GFAP) in rat embryonic cortical primary culture (Figure 20A). GFAP is an intermediate filament (IF) protein that is used as a specific marker for astrocytes in the CNS (Zhang, 2001). On the other hand, SIRT3 did not co-label with the microtubule-associated protein 2 (MAP2), which is a neuron-specific cytoskeleton protein marker (Matus, 1988). Taken together, these results suggest that SIRT3 may be localized predominantly in astrocytes, and it does not appear to be expressed in neurons (Figure 20B). However, there is a need for future experiments to test for SIRT3 expression in other glial cell types such as oligodendrocytes and microglia. We next assessed whether the extensively studied SIRT1 displays the same localization pattern as SIRT3. However, our results show that SIRT1 immunofluorescence signal robustly co-labels with MAP2 and not with GFAP (Figure 21A; Figure 21B). These results suggest that SIRT1 is predominantely expressed in neurons and not in astrocytes. This observed neuronal expression is in agreement with a number of previous studies (Araki et al., 2004; Michan et al., 2010). This suggests that both sirtuins are distinctly localized to two different cell types within the CNS. However, we cannot rule out that these sirtuins are not expressed in other cell types, vascular cells or stem cells should also be examined in order to fully elucidate expression of these sirtuins within the brain.

Our observed SIRT3 protein expression profile in rat brain regions throughout development closely resembles the expression pattern of astrocytes. Indeed, astrocytes display an increase in expression during the first 3 weeks of rodent postnatal life and an increase again in 3 month-old rodents (Bjorklund et al., 1985; Freeman, 2010), after which the levels then stabilize. The similarity between SIRT3 and astrocytic protein expression throughout development further supports our results that SIRT3 resides within astrocytes.

In addition to providing nutrients and regulate growth and excitability of neighbouring neurons, astrocytes have recently been emerging as key players in protecting neurons from oxidative stress (Belanger & Magistretti, 2009). For example, reports have demonstrated that astrocytes possess greater concentrations of glutathione and enzymes involved in glutathione metabolism than the neurons (Wilson, 1997; Makar et al., 1994). Because of the large glutathione antioxidant capacity, astrocytes have been reported to be more resilient to oxidative stress than the neurons. During stroke and other brain insults, astrocytes supplement neuronal antioxidant capacities by shuttling glutathione to them (Anderson et al., 2003). Our results showing that SIRT3 holds anti-oxidative capacity, and its localization in astrocytes suggest that SIRT3 may play an important role in the antioxidant defense system of the brain. Our results are the first to investigate the cellular localization of SIRT3 within the CNS.

Our results indicate that SIRT1 and SIRT3 may reside in completely different cell types within the brain. It is possible that they can induce their beneficial effects, not just from different subcellular localizations, but also from distinct cell types within the brain. Therefore, these sirtuins may target different pools of substrates, and therefore carry out different functions. In addition, it may be possible to use pharmacological interventions to target either astrocytic or neuronal function using different drugs directed either at SIRT3 or SIRT1.

4.2.5 Summary and proposed model

SIRT3 is a primary mitochondrial protein deacetylase, which target mitochondrial factors involved in regulating metabolic processes. However, the role of SIRT3 in mitochondria has not been fully investigated. In order to elucidate the role of SIRT3 in the cell, HEK-293 cells ectopically over-expressing SIRT3 were used as the model system. My results demonstrate that: 1) under basal culture conditions over-expression of SIRT3 results in a decrease in ΔΨm, ROS and cell proliferation; 2) SIRT3 over-expression renders cells less sensitive to cytotoxic insults such as GD/GR and H_2O_2.

Moreover, this study examined endogenous SIRT3 expression profile and its cell-specific localization in the rodent brain. These results show that: 1) Although SIRT1 is the sirtuin that is extensively studied throughout the brain, SIRT3 mRNA is expressed at higher levels in all brain regions examined; 2) SIRT3 and SIRT1 are distinctly localized to astrocytes and neurons respectively; 3) SIRT3 protein levels increase throughout development in the rat cortex, hippocampus and cerebellum. Taken together, these results support the hypothesis that SIRT3 holds cytoprotective potential. In addition, the robust presence of SIRT3 in the brain allows for future investigations in its potential neuroprotective abilities. Furthermore, SIRT3 may induce its cytoprotective properties in the brain through astrocytic physiology.

Reviewing data from this thesis alone, two working models are proposed on the consequences of SIRT3 over-expression. The working models describe the effects of SIRT3 over-expression under basal culture conditions (Figure 22A), and during conditions of oxidative stress (Figure 22B). The first working model illustrates of the effects of SIRT3 over-expression under basal culture conditions. Our results show that SIRT3 over-expression reduces ROS levels (Figure 7), ΔΨm (Figure 5; Figure 6) and proliferation rates (Figure 11). The second working model

consists of the effect of SIRT3 over-expression during conditions of oxidative stress. Our results have demonstrated that SIRT3 over-expression renders cells less sensitive to H_2O_2-induced oxidative stress (Figure 10), as well as GD/GR insult (Figure 9).

Collectively, we propose 2 different working models that encapsulate our findings in addition to the current research of what has been established on the role of SIRT3 in mitochondria. The first model illustrates the function of SIRT3 under basal conditions (Figure 23), the second model proposes the mechanisms that SIRT3 exudes following oxidative stress (Figure 24).

Under basal conditions, SIRT3 lowers ΔΨm and decreases ROS levels. These results agree with Shi et al (2005), that SIRT3 decreases basal ROS levels by decreasing ΔΨm. Family members of UCPs have the capacity to uncouple the proton gradient resulting in partial reduction of the ΔΨm, and subsequently a decrease in ROS levels (Andrews et al., 2005; Wu et al., 1999). Given that SIRT3 was proposed to increase expression levels of UCP1 through the PGC-1α axis (Shi et al., 2005), it may have similar effects on other family members of UCPs. However, our results demonstrated that there is no difference in PGC-1α mRNA levels between SIRT3 over-expressing cells and control cells (Figure 8), thus it is still unclear whether SIRT3 regulates PGC-1α expression/activation. However, this does not discount the fact that SIRT3 may regulate PGC-1α function at the protein level. In addition, UCPs regulate fatty acid entry into mitochondria (Pecquer et al., 2008). The metabolism of fatty acids in mitochondria results in generation of acetyl-CoA for the TCA cycle. It has been demonstrated that slow proliferating cells use acetyl-CoA derived from fatty acid oxidation and have lower ROS levels compared to fast proliferating ells which only use acetyl-CoA derived from pyruvate (Pfeiffer et al., 2001). Furthermore, reduced ROS levels lead to a decrease in activation of the transcription factor HIF1α (Bell et al., 2011). A decrease in HIF1α activation results in a reduction of glycolytic

gene expression, resulting in slower cell proliferation rates. Taken together, these data suggest that over-expressing SIRT3 may result in an increase of UCP levels, that reduce ΔΨm and concomitantly ROS levels, which further decreases cell proliferation rates (Figure 23).

The second model proposes the function of SIRT3 under oxidative stress. SIRT3 over-expression is able to attenuate oxidative stress through a number of potential mechanisms. SIRT3 prevents the opening of the mPTP by deacetylation, which protects cells from ROS and cell death (Hafner et al., 2010). In addition, SIRT3 over-expression may increase MnSOD levels through induction of PGC-1α (Kong et al., 2008), and through deacetylation of FOXO3a within mitochondria (Jacobs et al., 2008). SIRT3 also increases MnSOD enzymatic activity directly in mitochondria (Tao et al., 2011). Furthermore, SIRT3 is able to deacetylate IDH2 and GDH, which generate NADPH as a by-product. NADPH is able to reduce GSSG to produce GSH (Someya et al., 2010). Therefore, SIRT3 may reduce ROS genesis due to increased levels of these anti-oxidative enzymes. In addition, because SIRT3 over-expression reduces ΔΨm (Figure 5; Figure 6), this mechanism may also contribute to reduced ROS formation during oxidative stress. Collectively, SIRT3 over-expression is able to reduce detrimental consequences of ROS formation during oxidative stresses by convergent mechanisms of ΔΨm reduction, prevention of mPTP opening and increased antioxidant capacity through upregulation of GSH, MnSOD and catalase (Figure 24).

Fig. 22

A)

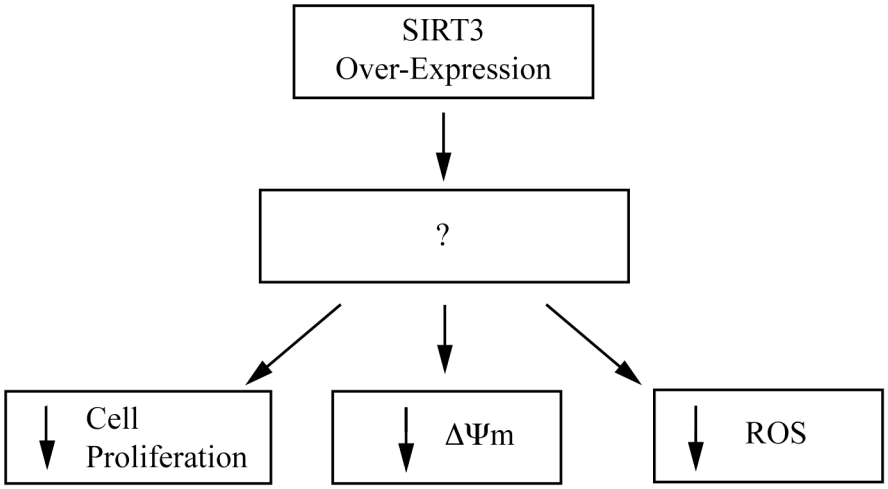
SIRT3
Over-Expression
?
Cell
Proliferation
ΔΨm
ROS

B)

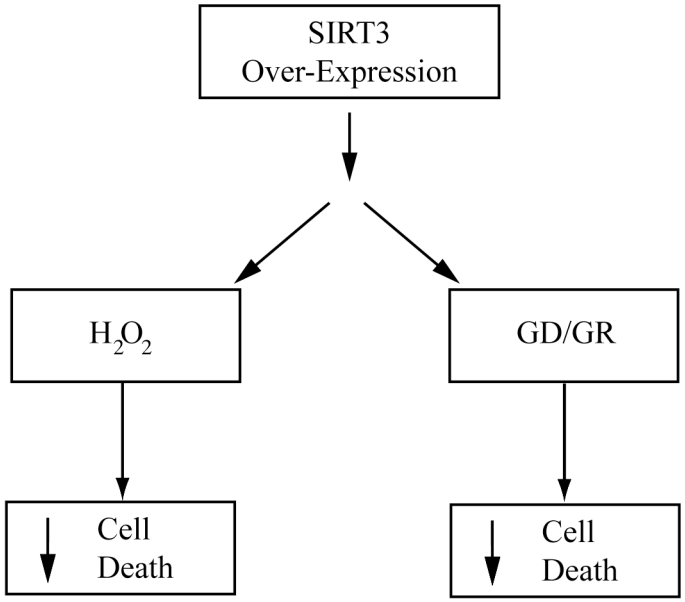
SIRT3
Over-Expression
H2O2
GD/GR
Cell
Death
Cell
Death

Figure 22: Working model of SIRT3 functions under basal and oxidative stress conditions

A) Over-expression of SIRT3 in HEK-293 cells under basal conditions. Over-expression of SIRT3 results in a reduction in cell proliferation, $\Delta\Psi m$ and ROS levels through unknown mechanisms.

B) Over-expression of SIRT3 in HEK-293 cells under conditions of oxidative stress. Over-expression of SIRT3 results in a reduction of cell death following H_2O_2 or GD/GR insults through unknown mechanisms.

Fig. 23

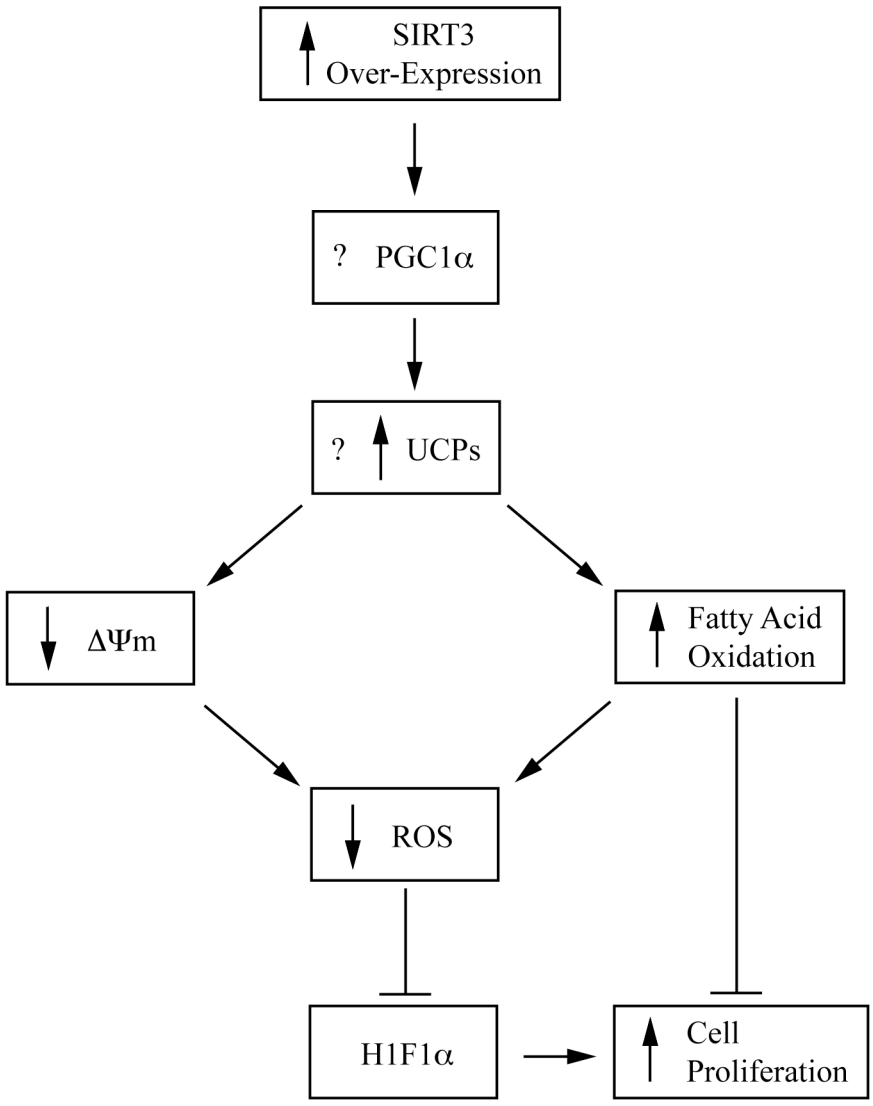
SIRT3
Over-Expression
? PGC1α
? UCPs
ΔΨm
Fatty Acid
Oxidation
ROS
H1F1α
Cell
Proliferation

Figure 23: Proposed model of SIRT3 mechanisms under basal conditions

SIRT3 over-expression under basal conditions may increase activation/expression of PGC-1α. PGC-1α elevates UCP levels/activity, resulting in a decrease in ΔΨm, as well as ROS levels. An increase in UCP levels/activity may increase fatty acid derived acetyl-CoA within mitochondria, which lowers basal ROS levels and slows cell proliferation. Reduced ROS also leads to a decrease in cell proliferation rates by not activating HIF1α transcriptional activity.

Fig. 24

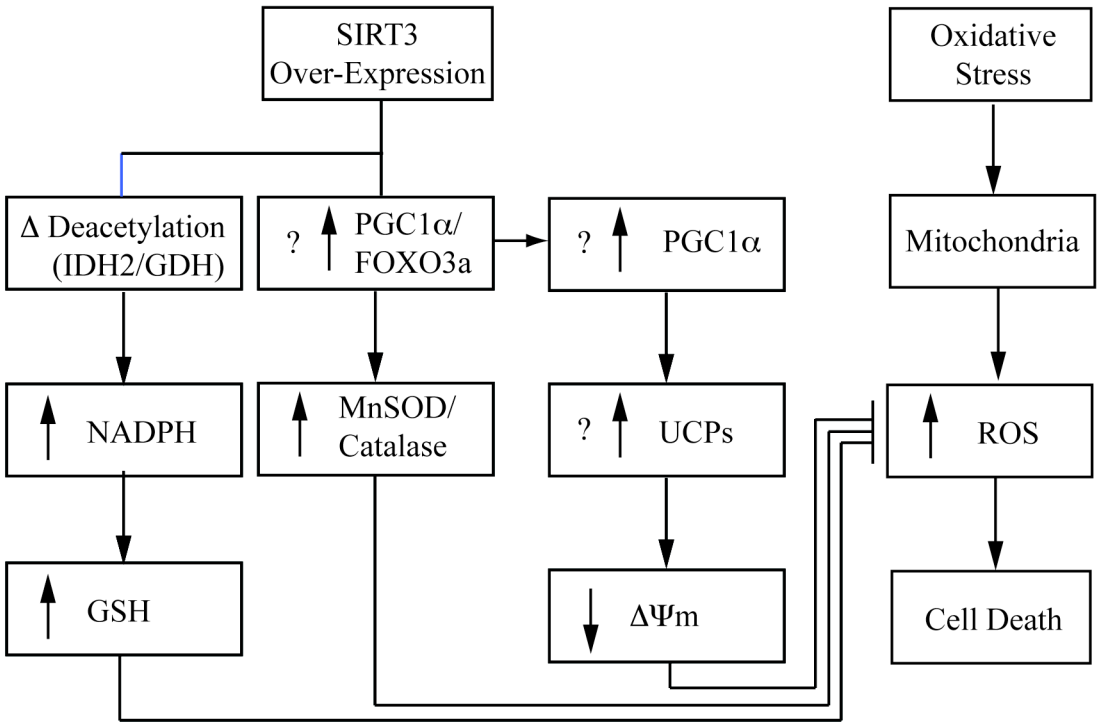
SIRT3
Over-Expression
Oxidative
Stress
Δ Deacetylation
(IDH2/GDH)
? PGC1α/
FOXO3a
? PGC1α
Mitochondria
NADPH
MnSOD/
Catalase
? UCPs
ROS
GSH
ΔΨm
Cell Death

Figure 24: Proposed model SIRT3 mechanisms under conditions of oxidative stress

SIRT3 over-expression may increase activation/expression of PGC-1α and/or FOXO3a, which increase MnSOD and catalase levels. SIRT3 activates IDH2 and GDH through deacetylation. Activated IDH2 increases levels of the antioxidant known as GSH due to the regeneration of NADPH levels. GDH activation may also be able to increase GSH levels. Lowered ΔΨm may concomitantly reduce basal ROS levels. Collectively, SIRT3 reduces ROS levels and thus protects from cell death caused by oxidative stress.

4.2.6 Future Directions

1. It has been demonstrated that SIRT3 increases expression levels of UCP1 in adipocytes (Shi et al., 2005), future studies should investigate whether SIRT3 over-expression increases the expression level/activity of other UCP family members under basal and stress conditions. UCP members have been demonstrated to decrease ROS levels, regulate fatty acid metabolism, and decrease $\Delta\Psi m$. Because the same effects are observed following over-expression of SIRT3, it is possible that SIRT3 may induce its beneficial effects through regulation of UCPs.
2. This study has showed that SIRT3 holds cytoprotective capacity and that it is expressed in astrocytes. This has opened new avenues in testing the role of SIRT3 within the brain. Future studies should selectively over-express SIRT3 in astrocytes of primary cultures to characterize whether this would lead to enhanced neuroprotection during oxidative stress-like insults. Neuroprotection can be assessed first by measuring expression levels of pro-apoptotic genes, ROS levels, DNA damage and cell death in neuronal cultures only. It should then be tested whether co-culturing with astrocytes over-expressing SIRT3 would prove to have more neuroprotective capacity than co-culturing with astrocytes expressing a control vector.
3. Someya et al (2010) demonstrated that SIRT3 deacetylates IDH2 and generates NADPH as a by-product. NADPH reduces GSSG to GSH, which holds anti-oxidative capacity. SIRT3 also targets GDH, a matrix enzyme that can produce NADPH as a by product. Therefore, future studies should investigate whether over-expressing SIRT3 increases NADPH levels not only through IDH2 mechanism, but also through GDH.

4.2.7 Clinical Implications

Mitochondrial dysfunction and oxidative stress play a crucial role in metabolic diseases, oncogenesis, as well as a host of neurodegerative conditions (Lin & Beal, 2006; McCabe, 1992). Therefore, identifying means by which mitochondrial activity can be strengthened, and/or less ROS generated may protect or slow down the progression of these disorders. Our study indicates that SIRT3 resides in the mitochondria, and induces beneficial effects by attenuating ROS levels. Collectively, these results suggest that SIRT3 regulates mitochondrial functions and may have strong positive implications in conditions involving oxidative stress.

Observing that SIRT3 is expressed in the brain suggests its role in neural regulation. Should SIRT3 over-expression prove to have neuroprotective potential, this sirtuin may be a *bona fide* target for therapeutic strategies. Because SIRT3 is expressed at high levels within the rodent brain, suggests that it can be targeted by drugs, which is a preferred method rather than using gene replacement therapy. Our results demonstrated that both SIRT3 and SIRT1 reside within astrocytes and neurons, respectively. Numerous studies have speculated that SIRT1 has neuroprotective potential against oxidative-stress like damage (Kim et al, 2007; Milner, 2009; Pallas et al., 2008). Overall, this suggests that both SIRT1 and SIRT3 may induce their neuroprotective abilities in different cell types within the brain. In addition to being principal housekeeping cells of the central nervous system, astrocytes play a fundamental role in conditions involving ischemic injury by producing antioxidants defenses (Wilson, 1997). Neurons, however, depend on metabolic support from surrounding astrocytes during normal development as well as during metabolic stress (Wilson, 1997). Because SIRT3 resides within

astrocytes, it could have potential benefits in ischemia-like injury, by supplying neurons with the needed nutrients and increasing their antioxidant capacity. In addition, the distinct localizations of the two sirtuins within the brain allow for specific pharmaceutical targeting system. Overall, delineating the potential mechanism of SIRT3 within mitochondria and astrocytes promises novel strategies in clinical intervention of neurodegenerative and metabolic diseases.

REFERENCES

Ahn, B. H., Kim, H. S., Song, S., Lee, I. H., Liu, J., Vassilopoulos, A., et al. (2008). A role for the mitochondrial deacetylase Sirt3 in regulating energy homeostasis. *Proceedings of the National Academy of Sciences of the United States of America, 105*(38), 14447-14452.

Ahuja, N., Schwer, B., Carobbio, S., Waltregny, D., North, B. J., Castronovo, V., et al. (2007). Regulation of insulin secretion by SIRT4, a mitochondrial ADP-ribosyltransferase. *The Journal of Biological Chemistry, 282*(46), 33583-33592.

Anderson, M. F., Blomstrand, F., Blomstrand, C., Eriksson, P. S., & Nilsson, M. (2003). Astrocytes and stroke: Networking for survival? *Neurochemical Research, 28*(2), 293-305.

Anderson, R. M., & Weindruch, R. (2010). Metabolic reprogramming, caloric restriction and aging. *Trends in Endocrinology and Metabolism: TEM, 21*(3), 134-141.

Andrews, Z. B., Diano, S., & Horvath, T. L. (2005). Mitochondrial uncoupling proteins in the CNS: In support of function and survival. *Nature Reviews.Neuroscience, 6*(11), 829-840.

Andreyev, A. Y., Kushnareva, Y. E., & Starkov, A. A. (2005). Mitochondrial metabolism of reactive oxygen species. *Biochemistry.Biokhimiia, 70*(2), 200-214.

Anisimov, V. N. (2003). The relationship between aging and carcinogenesis: A critical appraisal. *Critical Reviews in oncology/hematology, 45*(3), 277-304.

Araki, T., Sasaki, Y., & Milbrandt, J. (2004). Increased nuclear NAD biosynthesis and SIRT1 activation prevent axonal degeneration. *Science (New York, N.Y.), 305*(5686), 1010-1013.

Armstrong, J. S., & Whiteman, M. (2007). Measurement of reactive oxygen species in cells and mitochondria. *Methods in Cell Biology, 80*, 355-377.

Auten, R. L., & Davis, J. M. (2009). Oxygen toxicity and reactive oxygen species: The devil is in the details. *Pediatric Research, 66*(2), 121-127.

Bao, J., Scott, I., Lu, Z., Pang, L., Dimond, C. C., Gius, D., et al. (2010). SIRT3 is regulated by nutrient excess and modulates hepatic susceptibility to lipotoxicity. *Free Radical Biology & Medicine, 49*(7), 1230-1237.

Belanger, M., & Magistretti, P. J. (2009). The role of astroglia in neuroprotection. *Dialogues in Clinical Neuroscience, 11*(3), 281-295.

Bell, E. L., Emerling, B. M., Ricoult, S. J., & Guarente, L. (2011). SirT3 suppresses hypoxia inducible factor 1alpha and tumor growth by inhibiting mitochondrial ROS production. *Oncogene, 7*2, 507-527.

Bellizzi, D., Rose, G., Cavalcante, P., Covello, G., Dato, S., De Rango, F., et al. (2005). A novel VNTR enhancer within the SIRT3 gene, a human homologue of SIR2, is associated with survival at oldest ages. *Genomics, 85*(2), 258-263.

Bjorklund, H., Eriksdotter-Nilsson, M., Dahl, D., Rose, G., Hoffer, B., & Olson, L. (1985). Image analysis of GFAP-positive astrocytes from adolescence to senescence. *Experimental Brain Research.Experimentelle Hirnforschung.Experimentation Cerebrale, 58*(1), 163-170.

Blackburn, R. V., Spitz, D. R., Liu, X., Galoforo, S. S., Sim, J. E., Ridnour, L. A., et al. (1999). Metabolic oxidative stress activates signal transduction and gene expression during glucose deprivation in human tumor cells. *Free Radical Biology & Medicine, 26*(3-4), 419-430.

Bordone, L., Motta, M. C., Picard, F., Robinson, A., Jhala, U. S., Apfeld, J., et al. (2006). Sirt1 regulates insulin secretion by repressing UCP2 in pancreatic beta cells. *PLoS Biology, 4*(2), e31.

Borra, M. T., Langer, M. R., Slama, J. T., & Denu, J. M. (2004). Substrate specificity and kinetic mechanism of the Sir2 family of NAD+-dependent histone/protein deacetylases. *Biochemistry, 43*(30), 9877-9887.

Brachmann, C. B., Sherman, J. M., Devine, S. E., Cameron, E. E., Pillus, L., & Boeke, J. D. (1995). The SIR2 gene family, conserved from bacteria to humans, functions in silencing, cell cycle progression, and chromosome stability. *Genes & Development, 9*(23), 2888-2902.

Braunstein, M., Rose, A. B., Holmes, S. G., Allis, C. D., & Broach, J. R. (1993). Transcriptional silencing in yeast is associated with reduced nucleosome acetylation. *Genes & Development, 7*(4), 592-604.

Braunstein, M., Sobel, R. E., Allis, C. D., Turner, B. M., & Broach, J. R. (1996). Efficient transcriptional silencing in saccharomyces cerevisiae requires a heterochromatin histone acetylation pattern. *Molecular and Cellular Biology, 16*(8), 4349-4356.

Brunet, A., Sweeney, L. B., Sturgill, J. F., Chua, K. F., Greer, P. L., Lin, Y., et al. (2004). Stress-dependent regulation of FOXO transcription factors by the SIRT1 deacetylase. *Science (New York, N.Y.), 303*(5666), 2011-2015.

Bruss, M. D., Khambatta, C. F., Ruby, M. A., Aggarwal, I., & Hellerstein, M. K. (2010). Calorie restriction increases fatty acid synthesis and whole body fat oxidation rates. *American Journal of Physiology.Endocrinology and Metabolism, 298*(1), E108-16.

Bustin, S. A. (2002). Quantification of mRNA using real-time reverse transcription PCR (RT-PCR): Trends and problems. *Journal of Molecular Endocrinology, 29*(1), 23-39.

Cai, J., Yang, J., & Jones, D. P. (1998). Mitochondrial control of apoptosis: The role of cytochrome c. *Biochimica Et Biophysica Acta, 1366*(1-2), 139-149.

Chaturvedi, R. K., & Beal, M. F. (2008). Mitochondrial approaches for neuroprotection. *Annals of the New York Academy of Sciences, 1147*, 395-412.

Chinopoulos, C., & Adam-Vizi, V. (2001). Mitochondria deficient in complex I activity are depolarized by hydrogen peroxide in nerve terminals: Relevance to parkinson's disease. *Journal of Neurochemistry, 76*(1), 302-306.

Cimen, H., Han, M. J., Yang, Y., Tong, Q., Koc, H., & Koc, E. C. (2010). Regulation of succinate dehydrogenase activity by SIRT3 in mammalian mitochondria. *Biochemistry, 49*(2), 304-311.

Civitarese, A. E., Carling, S., Heilbronn, L. K., Hulver, M. H., Ukropcova, B., Deutsch, W. A., et al. (2007). Calorie restriction increases muscle mitochondrial biogenesis in healthy humans. *PLoS Medicine, 4*(3), e76.

Coller, J., & Parker, R. (2004). Eukaryotic mRNA decapping. *Annual Review of Biochemistry, 73*, 861-890.

Cooper, H. M., & Spelbrink, J. N. (2008). The human SIRT3 protein deacetylase is exclusively mitochondrial. *The Biochemical Journal, 411*(2), 279-285.

Crompton, M. (1999). The mitochondrial permeability transition pore and its role in cell death. *The Biochemical Journal, 341 (Pt 2)*(Pt 2), 233-249.

Davis, M., Whitely, T., Turnbull, D. M., & Mendelow, A. D. (1997). Selective impairments of mitochondrial respiratory chain activity during aging and ischemic brain damage. *Acta Neurochirurgica.Supplement, 70*, 56-58.

Deberardinis, R. J., Sayed, N., Ditsworth, D., & Thompson, C. B. (2008). Brick by brick: Metabolism and tumor cell growth. *Current Opinion in Genetics & Development, 18*(1), 54-61.

Delcuve, G. P., Rastegar, M., & Davie, J. R. (2009). Epigenetic control. *Journal of Cellular Physiology, 219*(2), 243-250.

Derdak, Z., Fulop, P., Sabo, E., Tavares, R., Berthiaume, E. P., Resnick, M. B., et al. (2006). Enhanced colon tumor induction in uncoupling protein-2 deficient mice is associated with NF-kappaB activation and oxidative stress. *Carcinogenesis, 27*(5), 956-961.

DiMauro, S., & Schon, E. A. (2008). Mitochondrial disorders in the nervous system. *Annual Review of Neuroscience, 31*, 91-123.

Dlaskova, A., Hlavata, L., Jezek, J., & Jezek, P. (2008). Mitochondrial complex I superoxide production is attenuated by uncoupling. *The International Journal of Biochemistry & Cell Biology, 40*(10), 2098-2109.

Du, J., Jiang, H., & Lin, H. (2009). Investigating the ADP-ribosyltransferase activity of sirtuins with NAD analogues and 32P-NAD. *Biochemistry, 48*(13), 2878-2890.

Elmore, S. (2007). Apoptosis: A review of programmed cell death. *Toxicologic Pathology, 35*(4), 495-516.

Fabian, M. R., Sonenberg, N., & Filipowicz, W. (2010). Regulation of mRNA translation and stability by microRNAs. *Annual Review of Biochemistry, 79*, 351-379.

Finkel, T., Deng, C. X., & Mostoslavsky, R. (2009). Recent progress in the biology and physiology of sirtuins. *Nature, 460*(7255), 587-591.

Finley, L. W., Carracedo, A., Lee, J., Souza, A., Egia, A., Zhang, J., et al. (2011). SIRT3 opposes reprogramming of cancer cell metabolism through HIF1alpha destabilization. *Cancer Cell, 19*(3), 416-428.

Fischer, M., Skowron, M., & Berthold, F. (2005). Reliable transcript quantification by real-time reverse transcriptase-polymerase chain reaction in primary neuroblastoma using normalization to averaged expression levels of the control genes HPRT1 and SDHA. *The Journal of Molecular Diagnostics : JMD, 7*(1), 89-96.

Ford, E., Voit, R., Liszt, G., Magin, C., Grummt, I., & Guarente, L. (2006). Mammalian Sir2 homolog SIRT7 is an activator of RNA polymerase I transcription. *Genes & Development, 20*(9), 1075-1080.

Fox, C. A., & McConnell, K. H. (2005). Toward biochemical understanding of a transcriptionally silenced chromosomal domain in saccharomyces cerevisiae. *The Journal of Biological Chemistry, 280*(10), 8629-8632.

Freeman, M. R. (2010). Specification and morphogenesis of astrocytes. *Science (New York, N.Y.), 330*(6005), 774-778.

Frye, R. A. (2000). Phylogenetic classification of prokaryotic and eukaryotic Sir2-like proteins. *Biochemical and Biophysical Research Communications, 273*(2), 793-798.

Fujino, T., Kondo, J., Ishikawa, M., Morikawa, K., & Yamamoto, T. T. (2001). Acetyl-CoA synthetase 2, a mitochondrial matrix enzyme involved in the oxidation of acetate. *The Journal of Biological Chemistry, 276*(14), 11420-11426.

Fukushima, N., Koopmann, J., Sato, N., Prasad, N., Carvalho, R., Leach, S. D., et al. (2005). Gene expression alterations in the non-neoplastic parenchyma adjacent to infiltrating pancreatic ductal adenocarcinoma. *Modern Pathology : An Official Journal of the United States and Canadian Academy of Pathology, Inc, 18*(6), 779-787.

Giannakou, M. E., & Partridge, L. (2004). The interaction between FOXO and SIRT1: Tipping the balance towards survival. *Trends in Cell Biology, 14*(8), 408-412.

Glozak, M. A., Sengupta, N., Zhang, X., & Seto, E. (2005). Acetylation and deacetylation of non-histone proteins. *Gene, 363*, 15-23.

Gogvadze, V., Orrenius, S., & Zhivotovsky, B. (2008). Mitochondria in cancer cells: What is so special about them? *Trends in Cell Biology, 18*(4), 165-173.

Gottlieb, S., & Esposito, R. E. (1989). A new role for a yeast transcriptional silencer gene, SIR2, in regulation of recombination in ribosomal DNA. *Cell, 56*(5), 771-776.

Guarente, L. (2007). Sirtuins in aging and disease. *Cold Spring Harbor Symposia on Quantitative Biology, 72*, 483-488.

Hafner, A. V., Dai, J., Gomes, A. P., Xiao, C. Y., Palmeira, C. M., Rosenzweig, A., et al. (2010). Regulation of the mPTP by SIRT3-mediated deacetylation of CypD at lysine 166 suppresses age-related cardiac hypertrophy. *Aging, 2*(12), 914-923.

Hagopian, K., Harper, M. E., Ram, J. J., Humble, S. J., Weindruch, R., & Ramsey, J. J. (2005). Long-term calorie restriction reduces proton leak and hydrogen peroxide production in liver mitochondria. *American Journal of Physiology.Endocrinology and Metabolism, 288*(4), E674-84.

Hagopian, K., Ramsey, J. J., & Weindruch, R. (2003). Caloric restriction increases gluconeogenic and transaminase enzyme activities in mouse liver. *Experimental Gerontology, 38*(3), 267-278.

Haigis, M. C., & Guarente, L. P. (2006). Mammalian sirtuins--emerging roles in physiology, aging, and calorie restriction. *Genes & Development, 20*(21), 2913-2921.

Haigis, M. C., Mostoslavsky, R., Haigis, K. M., Fahie, K., Christodoulou, D. C., Murphy, A. J., et al. (2006). SIRT4 inhibits glutamate dehydrogenase and opposes the effects of calorie restriction in pancreatic beta cells. *Cell, 126*(5), 941-954.

Haigis, M. C., & Sinclair, D. A. (2010). Mammalian sirtuins: Biological insights and disease relevance. *Annual Review of Pathology, 5*, 253-295.

Halliwell, B. (2007). Biochemistry of oxidative stress. *Biochemical Society Transactions, 35*(Pt 5), 1147-1150.

Hallows, W. C., Albaugh, B. N., & Denu, J. M. (2008). Where in the cell is SIRT3?--functional localization of an NAD+-dependent protein deacetylase. *The Biochemical Journal, 411*(2), e11-3.

Hallows, W. C., Lee, S., & Denu, J. M. (2006). Sirtuins deacetylate and activate mammalian acetyl-CoA synthetases. *Proceedings of the National Academy of Sciences of the United States of America, 103*(27), 10230-10235.

Hasegawa, K., Wakino, S., Yoshioka, K., Tatematsu, S., Hara, Y., Minakuchi, H., et al. (2008). Sirt1 protects against oxidative stress-induced renal tubular cell apoptosis by the bidirectional regulation of catalase expression. *Biochemical and Biophysical Research Communications, 372*(1), 51-56.

Hassa, P. O., Haenni, S. S., Elser, M., & Hottiger, M. O. (2006). Nuclear ADP-ribosylation reactions in mammalian cells: Where are we today and where are we going? *Microbiology and Molecular Biology Reviews : MMBR, 70*(3), 789-829.

Hirschey, M. D., Shimazu, T., Goetzman, E., Jing, E., Schwer, B., Lombard, D. B., et al. (2010). SIRT3 regulates mitochondrial fatty-acid oxidation by reversible enzyme deacetylation. *Nature, 464*(7285), 121-125.

Huang, J. Y., Hirschey, M. D., Shimazu, T., Ho, L., & Verdin, E. (2010). Mitochondrial sirtuins. *Biochimica Et Biophysica Acta, 1804*(8), 1645-1651.

Ishii, N. (2007). Role of oxidative stress from mitochondria on aging and cancer. *Cornea, 26*(9 Suppl 1), S3-9.

Iverson, S. L., & Orrenius, S. (2004). The cardiolipin-cytochrome c interaction and the mitochondrial regulation of apoptosis. *Archives of Biochemistry and Biophysics, 423*(1), 37-46.

Ivy, J. M., Klar, A. J., & Hicks, J. B. (1986). Cloning and characterization of four SIR genes of saccharomyces cerevisiae. *Molecular and Cellular Biology, 6*(2), 688-702.

Iwata-Ichikawa, E., Kondo, Y., Miyazaki, I., Asanuma, M., & Ogawa, N. (1999). Glial cells protect neurons against oxidative stress via transcriptional up-regulation of the glutathione synthesis. *Journal of Neurochemistry, 72*(6), 2334-2344.

Jacobs, K. M., Pennington, J. D., Bisht, K. S., Aykin-Burns, N., Kim, H. S., Mishra, M., et al. (2008). SIRT3 interacts with the daf-16 homolog FOXO3a in the mitochondria, as well as increases FOXO3a dependent gene expression. *International Journal of Biological Sciences, 4*(5), 291-299.

Jacobsson, A., Stadler, U., Glotzer, M. A., & Kozak, L. P. (1985). Mitochondrial uncoupling protein from mouse brown fat. molecular cloning, genetic mapping, and mRNA expression. *The Journal of Biological Chemistry, 260*(30), 16250-16254.

Jin, L., Galonek, H., Israelian, K., Choy, W., Morrison, M., Xia, Y., et al. (2009). Biochemical characterization, localization, and tissue distribution of the longer form of mouse SIRT3. *Protein Science : A Publication of the Protein Society, 18*(3), 514-525.

Jin, Q., Yan, T., Ge, X., Sun, C., Shi, X., & Zhai, Q. (2007). Cytoplasm-localized SIRT1 enhances apoptosis. *Journal of Cellular Physiology, 213*(1), 88-97.

Kaeberlein, M., McVey, M., & Guarente, L. (1999). The SIR2/3/4 complex and SIR2 alone promote longevity in saccharomyces cerevisiae by two different mechanisms. *Genes & Development, 13*(19), 2570-2580.

Kawahara, T. L., Michishita, E., Adler, A. S., Damian, M., Berber, E., Lin, M., et al. (2009). SIRT6 links histone H3 lysine 9 deacetylation to NF-kappaB-dependent gene expression and organismal life span. *Cell, 136*(1), 62-74.

Kawamura, Y., Uchijima, Y., Horike, N., Tonami, K., Nishiyama, K., Amano, T., et al. (2010). Sirt3 protects in vitro-fertilized mouse preimplantation embryos against oxidative stress-induced p53-mediated developmental arrest. *The Journal of Clinical Investigation, 120*(8), 2817-2828.

Kelly, G. (2010). A review of the sirtuin system, its clinical implications, and the potential role of dietary activators like resveratrol: Part 1. *Alternative Medicine Review : A Journal of Clinical Therapeutic, 15*(3), 245-263.

Kim, D., Nguyen, M. D., Dobbin, M. M., Fischer, A., Sananbenesi, F., Rodgers, J. T., et al. (2007). SIRT1 deacetylase protects against neurodegeneration in models for alzheimer's disease and amyotrophic lateral sclerosis. *The EMBO Journal, 26*(13), 3169-3179.

Kim, H. S., Patel, K., Muldoon-Jacobs, K., Bisht, K. S., Aykin-Burns, N., Pennington, J. D., et al. (2010). SIRT3 is a mitochondria-localized tumor suppressor required for maintenance of mitochondrial integrity and metabolism during stress. *Cancer Cell, 17*(1), 41-52.

Kim, S. C., Sprung, R., Chen, Y., Xu, Y., Ball, H., Pei, J., et al. (2006). Substrate and functional diversity of lysine acetylation revealed by a proteomics survey. *Molecular Cell, 23*(4), 607-618.

Kim, S. H., Lu, H. F., & Alano, C. C. (2011). Neuronal Sirt3 protects against excitotoxic injury in mouse cortical neuron culture. *PloS One, 6*(3), e14731.

Kong, X., Fan, H., Liu, X., Wang, R., Liang, J., Gupta, N., et al. (2009). Peroxisome proliferator-activated receptor gamma coactivator-1alpha enhances antiproliferative activity of 5'-deoxy-5-fluorouridine in cancer cells through induction of uridine phosphorylase. *Molecular Pharmacology, 76*(4), 854-860.

Kong, X., Wang, R., Xue, Y., Liu, X., Zhang, H., Chen, Y., et al. (2010). Sirtuin 3, a new target of PGC-1alpha, plays an important role in the suppression of ROS and mitochondrial biogenesis. *PloS One, 5*(7), e11707.

Koubova, J., & Guarente, L. (2003). How does calorie restriction work? *Genes & Development, 17*(3), 313-321.

Kowaltowski, A. J., de Souza-Pinto, N. C., Castilho, R. F., & Vercesi, A. E. (2009). Mitochondria and reactive oxygen species. *Free Radical Biology & Medicine, 47*(4), 333-343.

Kregel, K. C., & Zhang, H. J. (2007). An integrated view of oxidative stress in aging: Basic mechanisms, functional effects, and pathological considerations. *American Journal of Physiology.Regulatory, Integrative and Comparative Physiology, 292*(1), R18-36.

Kroemer, G., Galluzzi, L., & Brenner, C. (2007). Mitochondrial membrane permeabilization in cell death. *Physiological Reviews, 87*(1), 99-163.

Langley, E., Pearson, M., Faretta, M., Bauer, U. M., Frye, R. A., Minucci, S., et al. (2002). Human SIR2 deacetylates p53 and antagonizes PML/p53-induced cellular senescence. *The EMBO Journal, 21*(10), 2383-2396.

Larsson, N. G. (2010). Somatic mitochondrial DNA mutations in mammalian aging. *Annual Review of Biochemistry, 79*, 683-706.

Law, I. K., Liu, L., Xu, A., Lam, K. S., Vanhoutte, P. M., Che, C. M., et al. (2009). Identification and characterization of proteins interacting with SIRT1 and SIRT3: Implications in the anti-aging and metabolic effects of sirtuins. *Proteomics, 9*(9), 2444-2456.

Li, S., Banck, M., Mujtaba, S., Zhou, M. M., Sugrue, M. M., & Walsh, M. J. (2010). p53-induced growth arrest is regulated by the mitochondrial SirT3 deacetylase. *PloS One, 5*(5), e10486.

Lin, J. D. (2009). Minireview: The PGC-1 coactivator networks: Chromatin-remodeling and mitochondrial energy metabolism. *Molecular Endocrinology (Baltimore, Md.), 23*(1), 2-10.

Lin, M. T., & Beal, M. F. (2006). Mitochondrial dysfunction and oxidative stress in neurodegenerative diseases. *Nature, 443*(7113), 787-795.

Lin, S. J., Defossez, P. A., & Guarente, L. (2000). Requirement of NAD and SIR2 for life-span extension by calorie restriction in saccharomyces cerevisiae. *Science (New York, N.Y.), 289*(5487), 2126-2128.

Liszt, G., Ford, E., Kurtev, M., & Guarente, L. (2005). Mouse Sir2 homolog SIRT6 is a nuclear ADP-ribosyltransferase. *The Journal of Biological Chemistry, 280*(22), 21313-21320.

Liu, C. Y., Lee, C. F., & Wei, Y. H. (2009). Role of reactive oxygen species-elicited apoptosis in the pathophysiology of mitochondrial and neurodegenerative diseases associated with mitochondrial DNA mutations. *Journal of the Formosan Medical Association = Taiwan Yi Zhi, 108*(8), 599-611.

Lombard, D. B., Alt, F. W., Cheng, H. L., Bunkenborg, J., Streeper, R. S., Mostoslavsky, R., et al. (2007). Mammalian Sir2 homolog SIRT3 regulates global mitochondrial lysine acetylation. *Molecular and Cellular Biology, 27*(24), 8807-8814.

Longo, V. D., & Kennedy, B. K. (2006). Sirtuins in aging and age-related disease. *Cell, 126*(2), 257-268.

Luong, A., Hannah, V. C., Brown, M. S., & Goldstein, J. L. (2000). Molecular characterization of human acetyl-CoA synthetase, an enzyme regulated by sterol regulatory element-binding proteins. *The Journal of Biological Chemistry, 275*(34), 26458-26466.

Ma, Y. S., Wu, S. B., Lee, W. Y., Cheng, J. S., & Wei, Y. H. (2009). Response to the increase of oxidative stress and mutation of mitochondrial DNA in aging. *Biochimica Et Biophysica Acta, 1790*(10), 1021-1029.

Makar, T. K., Nedergaard, M., Preuss, A., Gelbard, A. S., Perumal, A. S., & Cooper, A. J. (1994). Vitamin E, ascorbate, glutathione, glutathione disulfide, and enzymes of glutathione metabolism in cultures of chick astrocytes and neurons: Evidence that astrocytes play an important role in antioxidative processes in the brain. *Journal of Neurochemistry, 62*(1), 45-53.

Mari, M., Morales, A., Colell, A., Garcia-Ruiz, C., & Fernandez-Checa, J. C. (2009). Mitochondrial glutathione, a key survival antioxidant. *Antioxidants & Redox Signaling, 11*(11), 2685-2700.

Marmorstein, R. (2004). Structure and chemistry of the Sir2 family of NAD+-dependent histone/protein deactylases. *Biochemical Society Transactions, 32*(Pt 6), 904-909.

Martin-Montalvo, A., Villalba, J. M., Navas, P., & de Cabo, R. (2011). NRF2, cancer and calorie restriction. *Oncogene, 30*(5), 505-520.

Matus, A. (1988). Microtubule-associated proteins: Their potential role in determining neuronal morphology. *Annual Review of Neuroscience, 11*, 29-44.

McCabe, E. R. (1992). Role of mitochondria in oncogenesis. *Biochemical Medicine and Metabolic Biology, 47*(2), 105-107.

McGarry, J. D., & Foster, D. W. (1980). Regulation of hepatic fatty acid oxidation and ketone body production. *Annual Review of Biochemistry, 49*, 395-420.

Michan, S., Li, Y., Chou, M. M., Parrella, E., Ge, H., Long, J. M., et al. (2010). SIRT1 is essential for normal cognitive function and synaptic plasticity. *The Journal of Neuroscience : The Official Journal of the Society for Neuroscience, 30*(29), 9695-9707.

Michishita, E., McCord, R. A., Berber, E., Kioi, M., Padilla-Nash, H., Damian, M., et al. (2008). SIRT6 is a histone H3 lysine 9 deacetylase that modulates telomeric chromatin. *Nature, 452*(7186), 492-496.

Michishita, E., Park, J. Y., Burneskis, J. M., Barrett, J. C., & Horikawa, I. (2005). Evolutionarily conserved and nonconserved cellular localizations and functions of human SIRT proteins. *Molecular Biology of the Cell, 16*(10), 4623-4635.

Milner, J. (2009). Cellular regulation of SIRT1. *Current Pharmaceutical Design, 15*(1), 39-44.

Min, J., Landry, J., Sternglanz, R., & Xu, R. M. (2001). Crystal structure of a SIR2 homolog-NAD complex. *Cell, 105*(2), 269-279.

Moldovan, L., & Moldovan, N. I. (2004). Oxygen free radicals and redox biology of organelles. *Histochemistry and Cell Biology, 122*(4), 395-412.

Mostoslavsky, R., Chua, K. F., Lombard, D. B., Pang, W. W., Fischer, M. R., Gellon, L., et al. (2006). Genomic instability and aging-like phenotype in the absence of mammalian SIRT6. *Cell, 124*(2), 315-329.

Nakagawa, T., Lomb, D. J., Haigis, M. C., & Guarente, L. (2009). SIRT5 deacetylates carbamoyl phosphate synthetase 1 and regulates the urea cycle. *Cell, 137*(3), 560-570.

Nakamura, Y., Ogura, M., Tanaka, D., & Inagaki, N. (2008). Localization of mouse mitochondrial SIRT proteins: Shift of SIRT3 to nucleus by co-expression with SIRT5. *Biochemical and Biophysical Research Communications, 366*(1), 174-179.

Nasrin, N., Wu, X., Fortier, E., Feng, Y., Bare', O. C., Chen, S., et al. (2010). SIRT4 regulates fatty acid oxidation and mitochondrial gene expression in liver and muscle cells. *The Journal of Biological Chemistry, 285*(42), 31995-32002.

Nemoto, S., Fergusson, M. M., & Finkel, T. (2005). SIRT1 functionally interacts with the metabolic regulator and transcriptional coactivator PGC-1{alpha}. *The Journal of Biological Chemistry, 280*(16), 16456-16460.

Neupert, W. (1997). Protein import into mitochondria. *Annual Review of Biochemistry, 66*, 863-917.

Niki, E. (2009). Lipid peroxidation: Physiological levels and dual biological effects. *Free Radical Biology & Medicine, 47*(5), 469-484.

North, B. J., Marshall, B. L., Borra, M. T., Denu, J. M., & Verdin, E. (2003). The human Sir2 ortholog, SIRT2, is an NAD+-dependent tubulin deacetylase. *Molecular Cell, 11*(2), 437-444.

North, B. J., & Verdin, E. (2004). Sirtuins: Sir2-related NAD-dependent protein deacetylases. *Genome Biology, 5*(5), 224.

Olmos, Y., Valle, I., Borniquel, S., Tierrez, A., Soria, E., Lamas, S., et al. (2009). Mutual dependence of Foxo3a and PGC-1alpha in the induction of oxidative stress genes. *The Journal of Biological Chemistry, 284*(21), 14476-14484.

Onyango, P., Celic, I., McCaffery, J. M., Boeke, J. D., & Feinberg, A. P. (2002). SIRT3, a human SIR2 homologue, is an NAD-dependent deacetylase localized to mitochondria. *Proceedings of the National Academy of Sciences of the United States of America, 99*(21), 13653-13658.

Palacios, O. M., Carmona, J. J., Michan, S., Chen, K. Y., Manabe, Y., Ward, J. L.,3rd, et al. (2009). Diet and exercise signals regulate SIRT3 and activate AMPK and PGC-1alpha in skeletal muscle. *Aging, 1*(9), 771-783.

Pardridge, W. M. (1991). Blood-brain barrier transport of glucose, free fatty acids, and ketone bodies. *Advances in Experimental Medicine and Biology, 291*, 43-53.

Pecqueur, C., Alves-Guerra, C., Ricquier, D., & Bouillaud, F. (2009). UCP2, a metabolic sensor coupling glucose oxidation to mitochondrial metabolism? *IUBMB Life, 61*(7), 762-767.

Pecqueur, C., Bui, T., Gelly, C., Hauchard, J., Barbot, C., Bouillaud, F., et al. (2008). Uncoupling protein-2 controls proliferation by promoting fatty acid oxidation and limiting glycolysis-derived pyruvate utilization. *The FASEB Journal : Official Publication of the Federation of American Societies for Experimental Biology, 22*(1), 9-18.

Perry, S. W., Norman, J. P., Barbieri, J., Brown, E. B., & Gelbard, H. A. (2011). Mitochondrial membrane potential probes and the proton gradient: A practical usage guide. *BioTechniques, 50*(2), 98-115.

Pfeiffer, T., Schuster, S., & Bonhoeffer, S. (2001). Cooperation and competition in the evolution of ATP-producing pathways. *Science (New York, N.Y.), 292*(5516), 504-507.

Pfister, J. A., Ma, C., Morrison, B. E., & D'Mello, S. R. (2008). Opposing effects of sirtuins on neuronal survival: SIRT1-mediated neuroprotection is independent of its deacetylase activity. *PloS One, 3*(12), e4090.

Pillai, V. B., Sundaresan, N. R., Jeevanandam, V., & Gupta, M. P. (2010). Mitochondrial SIRT3 and heart disease. *Cardiovascular Research, 88*(2), 250-256.

Puigserver, P., & Spiegelman, B. M. (2003). Peroxisome proliferator-activated receptor-gamma coactivator 1 alpha (PGC-1 alpha): Transcriptional coactivator and metabolic regulator. *Endocrine Reviews, 24*(1), 78-90.

Rodgers, J. T., Lerin, C., Haas, W., Gygi, S. P., Spiegelman, B. M., & Puigserver, P. (2005). Nutrient control of glucose homeostasis through a complex of PGC-1alpha and SIRT1. *Nature, 434*(7029), 113-118.

Saha, R. N., & Pahan, K. (2006). HATs and HDACs in neurodegeneration: A tale of disconcerted acetylation homeostasis. *Cell Death and Differentiation, 13*(4), 539-550.

Sanz, A., Pamplona, R., & Barja, G. (2006). Is the mitochondrial free radical theory of aging intact? *Antioxidants & Redox Signaling, 8*(3-4), 582-599.

Scher, M. B., Vaquero, A., & Reinberg, D. (2007). SirT3 is a nuclear NAD+-dependent histone deacetylase that translocates to the mitochondria upon cellular stress. *Genes & Development, 21*(8), 920-928.

Schlicker, C., Gertz, M., Papatheodorou, P., Kachholz, B., Becker, C. F., & Steegborn, C. (2008). Substrates and regulation mechanisms for the human mitochondrial sirtuins Sirt3 and Sirt5. *Journal of Molecular Biology, 382*(3), 790-801.

Schwer, B., Bunkenborg, J., Verdin, R. O., Andersen, J. S., & Verdin, E. (2006). Reversible lysine acetylation controls the activity of the mitochondrial enzyme acetyl-CoA synthetase 2. *Proceedings of the National Academy of Sciences of the United States of America, 103*(27), 10224-10229.

Schwer, B., North, B. J., Frye, R. A., Ott, M., & Verdin, E. (2002). The human silent information regulator (sir)2 homologue hSIRT3 is a mitochondrial nicotinamide adenine dinucleotide-dependent deacetylase. *The Journal of Cell Biology, 158*(4), 647-657.

Schwer, B., & Verdin, E. (2008). Conserved metabolic regulatory functions of sirtuins. *Cell Metabolism, 7*(2), 104-112.

Shi, T., Wang, F., Stieren, E., & Tong, Q. (2005). SIRT3, a mitochondrial sirtuin deacetylase, regulates mitochondrial function and thermogenesis in brown adipocytes. *The Journal of Biological Chemistry, 280*(14), 13560-13567.

Shimazu, T., Hirschey, M. D., Hua, L., Dittenhafer-Reed, K. E., Schwer, B., Lombard, D. B., et al. (2010). SIRT3 deacetylates mitochondrial 3-hydroxy-3-methylglutaryl CoA synthase 2 and regulates ketone body production. *Cell Metabolism, 12*(6), 654-661.

Shoba, B., Lwin, Z. M., Ling, L. S., Bay, B. H., Yip, G. W., & Kumar, S. D. (2009). Function of sirtuins in biological tissues. *Anatomical Record (Hoboken, N.J.: 2007), 292*(4), 536-543.

Sinclair, D. A., & Oberdoerffer, P. (2009). The ageing epigenome: Damaged beyond repair? *Ageing Research Reviews, 8*(3), 189-198.

Sirk, D. P., Zhu, Z., Wadia, J. S., & Mills, L. R. (2003). Flow cytometry and GFP: A novel assay for measuring the import and turnover of nuclear-encoded mitochondrial proteins in live PC12 cells. *Cytometry.Part A : The Journal of the International Society for Analytical Cytology, 56*(1), 15-22.

Solaini, G., Sgarbi, G., Lenaz, G., & Baracca, A. (2007). Evaluating mitochondrial membrane potential in cells. *Bioscience Reports, 27*(1-3), 11-21.

Someya, S., Yu, W., Hallows, W. C., Xu, J., Vann, J. M., Leeuwenburgh, C., et al. (2010). Sirt3 mediates reduction of oxidative damage and prevention of age-related hearing loss under caloric restriction. *Cell, 143*(5), 802-812.

Spitz, D. R., Sim, J. E., Ridnour, L. A., Galoforo, S. S., & Lee, Y. J. (2000). Glucose deprivation-induced oxidative stress in human tumor cells. A fundamental defect in metabolism? *Annals of the New York Academy of Sciences, 899*, 349-362.

Stout, J. T., & Caskey, C. T. (1985). HPRT: Gene structure, expression, and mutation. *Annual Review of Genetics, 19*, 127-148.

Suh, S. W., Gum, E. T., Hamby, A. M., Chan, P. H., & Swanson, R. A. (2007). Hypoglycemic neuronal death is triggered by glucose reperfusion and activation of neuronal NADPH oxidase. *The Journal of Clinical Investigation, 117*(4), 910-918.

Sundaresan, N. R., Gupta, M., Kim, G., Rajamohan, S. B., Isbatan, A., & Gupta, M. P. (2009). Sirt3 blocks the cardiac hypertrophic response by augmenting Foxo3a-dependent antioxidant defense mechanisms in mice. *The Journal of Clinical Investigation, 119*(9), 2758-2771.

Sundaresan, N. R., Samant, S. A., Pillai, V. B., Rajamohan, S. B., & Gupta, M. P. (2008). SIRT3 is a stress-responsive deacetylase in cardiomyocytes that protects cells from stress-mediated cell death by deacetylation of Ku70. *Molecular and Cellular Biology, 28*(20), 6384-6401.

Tanno, M., Sakamoto, J., Miura, T., Shimamoto, K., & Horio, Y. (2007). Nucleocytoplasmic shuttling of the NAD+-dependent histone deacetylase SIRT1. *The Journal of Biological Chemistry, 282*(9), 6823-6832.

Tao, R., Coleman, M. C., Pennington, J. D., Ozden, O., Park, S. H., Jiang, H., et al. (2010). Sirt3-mediated deacetylation of evolutionarily conserved lysine 122 regulates MnSOD activity in response to stress. *Molecular Cell, 40*(6), 893-904.

Tissenbaum, H. A., & Guarente, L. (2001). Increased dosage of a sir-2 gene extends lifespan in caenorhabditis elegans. *Nature, 410*(6825), 227-230.

Trentesaux, C., & Riou, J. F. (2010). Senescence and cellular immortality. Senescence et immortalite cellulaire *Bulletin Du Cancer, 97*(11), 1275-1283.

Turrens, J. F. (2003). Mitochondrial formation of reactive oxygen species. *The Journal of Physiology, 552*(Pt 2), 335-344.

Vakhrusheva, O., Smolka, C., Gajawada, P., Kostin, S., Boettger, T., Kubin, T., et al. (2008). Sirt7 increases stress resistance of cardiomyocytes and prevents apoptosis and inflammatory cardiomyopathy in mice. *Circulation Research, 102*(6), 703-710.

Vaquero, A., Scher, M. B., Lee, D. H., Sutton, A., Cheng, H. L., Alt, F. W., et al. (2006). SirT2 is a histone deacetylase with preference for histone H4 lys 16 during mitosis. *Genes & Development, 20*(10), 1256-1261.

Wai, L. K. (2004). Telomeres, telomerase, and tumorigenesis--a review. *MedGenMed : Medscape General Medicine, 6*(3), 19.

Wang, F., Nguyen, M., Qin, F. X., & Tong, Q. (2007). SIRT2 deacetylates FOXO3a in response to oxidative stress and caloric restriction. *Aging Cell, 6*(4), 505-514.

Wilson, J. X. (1997). Antioxidant defense of the brain: A role for astrocytes. *Canadian Journal of Physiology and Pharmacology, 75*(10-11), 1149-1163.

Wong, M. L., & Medrano, J. F. (2005). Real-time PCR for mRNA quantitation. *BioTechniques, 39*(1), 75-85.

Wu, Z., Puigserver, P., Andersson, U., Zhang, C., Adelmant, G., Mootha, V., et al. (1999). Mechanisms controlling mitochondrial biogenesis and respiration through the thermogenic coactivator PGC-1. *Cell, 98*(1), 115-124.

Yamamoto, H., Schoonjans, K., & Auwerx, J. (2007). Sirtuin functions in health and disease. *Molecular Endocrinology (Baltimore, Md.), 21*(8), 1745-1755.

Yang, H., Yang, T., Baur, J. A., Perez, E., Matsui, T., Carmona, J. J., et al. (2007). Nutrient-sensitive mitochondrial NAD+ levels dictate cell survival. *Cell, 130*(6), 1095-1107.

Yang, Y. H., Chen, Y. H., Zhang, C. Y., Nimmakayalu, M. A., Ward, D. C., & Weissman, S. (2000). Cloning and characterization of two mouse genes with homology to the yeast Sir2 gene. *Genomics, 69*(3), 355-369.

Yonezawa, T., Kurata, R., Hosomichi, K., Kono, A., Kimura, M., & Inoko, H. (2009). Nutritional and hormonal regulation of uncoupling protein 2. *IUBMB Life, 61*(12), 1123-1131.

Yu, J., & Auwerx, J. (2009). The role of sirtuins in the control of metabolic homeostasis. *Annals of the New York Academy of Sciences, 1173 Suppl 1*, E10-9.

Yu, W., Fu, Y. C., Zhou, X. H., Chen, C. J., Wang, X., Lin, R. B., et al. (2009). Effects of resveratrol on H(2)O(2)-induced apoptosis and expression of SIRTs in H9c2 cells. *Journal of Cellular Biochemistry, 107*(4), 741-747.

Zhang, J., Sprung, R., Pei, J., Tan, X., Kim, S., Zhu, H., et al. (2009). Lysine acetylation is a highly abundant and evolutionarily conserved modification in escherichia coli. *Molecular & Cellular Proteomics : MCP, 8*(2), 215-225.

Zhang, S. C. (2001). Defining glial cells during CNS development. *Nature Reviews.Neuroscience, 2*(11), 840-843.

Zuin, A., Gabrielli, N., Calvo, I. A., Garcia-Santamarina, S., Hoe, K. L., Kim, D. U., et al. (2008). Mitochondrial dysfunction increases oxidative stress and decreases chronological life span in fission yeast. *PloS One, 3*(7), e2842.